

*Republic of Iraq
Ministry of Higher Education and
Scientific Research
University of Baghdad
College of Education for Pure Science
Ibn-AL-Haitham*



Theoretical Study Of Low Lying Spectrum For Light Nuclei By Using Nuclear Shell Model



A Thesis

*Submitted to University of Baghdad/College of Education for Pure
Science(Ibn-AL-Haitham) Fulfillment of the Requirement for the
Degree of Master of Science
In Physics*

By

Hoda Butris Bahnam

B.Sc. 1994

Supervisors

Asst. Prof. Dr. Hadi J. Al-Agealy

2015

المجد لله في الاعالي وعلى
الارض السلام وبالناس
المسرة

(لوقا 2:14)

DEDICATION

To my Lovely Parents

My beloved sisters

Fatin, Abeer, Rasha

And especially, To my son

Yousif and my Daughter Sally

my life would feel empty without them.

ACKNOWLEDGEMENT

All thanks to my GOD for the good health and ability, I have enjoyed throughout the duration of the project.

Also, I would like to thank my supervisor: Dr. Hadi J. Al-Agealy who knows how to teach and lead me to the understanding of physics.

I also wish to thank the Dean of College of Education Ibn-AL-Haitham for Pure Science and the head of the Physics Department in Baghdad University for their continuous help and assistance during the work .

I would like to thank Dr.Khalid Hadi Mahdi who taught me the basic theoretical tools in nuclear physics and Special thanks to professo :Dr. Samir Atta for support.

I wish to express my gratitude to person for their contributions towards this dissertation Dr.Mustafa Kamel

Many thanks should also go to:

- My big family; parents, husband, kids , brothers, and sisters because without their help this work would have never been done*
- My close friends; and others sorry to those I have not mentioned, for their great continuous help, encourage and support.*

Supervisor's certification

I certify that this thesis was prepared under my supervision at the University of Baghdad \College of Education for Pure Science Ibn-AL-Haitham \Department of physics in partial fulfillment of the requirements for the degree of Master of Science in physics.

Signature:

Name: Dr.Hadi.J.Mujbil Al-Agealy

Title: Asst .Proff.

Department of physics

College of Education for Pure Science Ibn-AL-Haitham

University of Baghdad

The Council of the Department of physics has approved the examining committee

Signature:

Name: Dr.Mohammed Abdul-Nabi Thejeel

Titel:Asst.of Proff

Department of physics

College of Education for Pure Ibn-AL-Haitham

University of Baghdad

Date:

Summary

Binding and excitation energies have been calculated at low lying levels for $^{18}_8\text{Ne}_{10}$, $^{30}_{16}\text{S}_{14}$ and $^{30}_{14}\text{Si}_{16}$ nuclei using shell-model calculation with two protons in the S-d shell for $^{18}_8\text{Ne}_{10}$, and $^{30}_{16}\text{S}_{14}$ while two neutrons for $^{30}_{14}\text{Si}_{16}$ in orbits outside the closed core. The effective two-body matrix elements are obtained from the USDA, USDB and (USD) potential interaction. Results of calculated binding and excitation energies are show a good agreement with experimental data with calculated by using theoretical matrix elements .

The shell model calculation is used to investigate properties of levels at low lying in the mass number of nuclei $A = 18$ and 30 . An inert core with a residual two-particle interaction between the outer nucleons of $^{16}_8\text{O}_8$, and $^{28}_{14}\text{Si}_{14}$ as summed. For the positive parity states all configurations in the s-d shell are taken into account are described by a closed shell, two nucleons in the S-d shell .

The effective two-particle interaction is chosen to be a described by the USD,USDA ,and USDB potential. Good agreement with experiment is obtained for the binding and excitation energies. It is considered USDA , USDB and USD potential for two-body matrix element interaction as the most input parameters to the calculation is the nuclear energies, which contains realistic two (N-N) interactions. Provided the calculation is performed in a large enough basis space, the ground-state energy will converge.

Content

Title	Page
Chapter One (General Introduction)	
(1-1)Introduction	1
(1-2)Previous Studies	3
(1-3)Aims and Outline of Thesis	11
Chapter Two (<i>Background Theory And Nuclear Shell-Model</i>)	
(2-1) Introduction	12
(2-2) The Liquid-Drop Model	12
(2-3)The Semi Empirical Liquid Drop Model	15
(2-4)The Fermi Gas Model	17
(2-5)The Collective Model	20
(2-6)The optical model	23
(2-7)Cluster Model	24
(2-8) Shell Model	26
(2-9) Nuclear Shell Model	26
(2-10) Quantum Consideration of the Shell Model	27
(2-11) Magic Numbers in Nuclei	30
(2-12) The Independent-Particle Model	34

(2-13)The Spin-Orbit Coupling Interaction	37
(2-14)Nuclear Energy Levels	39
(2-15)Single particle energies	42
(2-16)Binding and Excitation energies	42
(2-17) Isospin and Isobaric Analogue States	45
Chapter Three (The Mathematical Model)	
(3-1)Binding and Excitation Energies	47
(3-2)Addition of two Angular Momentums	53
(3-3)Addition of many Angular Momentums	55
Chapter four (Results and Discussion)	
(4-1) Introduction	58
(4-2) Closed-Shell Cores	58
(4-3) Calculation of The Single Particle Energy	60
(4-3-1) Calculation of The Single Particle Energies for ${}^8_{18}\text{Ne}_{10}$ Nuclei	61
(4-3-2)Calculation of The Single Particle Energies for ${}^{30}\text{S}$ and ${}^{30}\text{Si}$ Nuclei	65
(4-4)Calculation of the Binding Energy	67
(4-4-1)Calculation of the Binding Energy for ${}^{18}\text{Ne}$ Nuclei	68

(4-4-2)Calculation of the Binding Energy for ^{30}S Nuclei	75
(4-4-3)Calculation of the Binding Energy for ^{30}Si Nuclei	77
(4-5) Calculation of Excitation Energies for $^{18}_8\text{Ne}_{10}$, $^{30}_{16}\text{S}_{14}$, and $^{30}_{14}\text{Si}_{16}$ Nucleus	80
(4-6)Discussion	85
(4-6-2) Theoretical of shell model calculation	86
(4-6-3)The Energy Level of ^{18}Ne Nuclei	88
(4-6-4)Energy Levels of ^{30}S Nuclei	91
(4-6-5)Energy Levels of ^{30}Si Nuclei	94
(5-1) Conclusions	98
(5-2) Suggested Future work	99

List of figurations

Figure	Page
Figure (2-1): Binding energy per nucleon as a function of mass number A.	13
Figure (2-2): Surface layer and core of nucleus in the liquid drop model .	14
Figure (2-3): Relative contributions to the binding energy per nucleon showing the importance of the various terms in the semi-empirical Weizsäcker formula.	15
Figure (2-4): Ground-state energy levels for neutrons and protons in nuclei .	18
Figure (2-5): Schematic of the coupling of the collective angular momentum.	22
Figure (2-6): Shell and Cluster model pictures of ${}^7\text{Li}$.	25
Figure(2-7): Energy levels depending on the harmonic potential.	29
Figure (2-8): The nuclide chart from the Atomic-Mass Evaluation (AME) .	31
Figure (2-9): Neutron separation energy.	32
Figure(2-10):Cross section due to Neutron number .	32
Figure(2-11):Excited energy state for magic nuclei.	33
Figure (2-12): Neutron single-particle states in with three different potential for nuclear: harmonic oscillator (left), Woods-Saxon (centre) and Woods-Saxon plus spin-orbit interaction	35

(right)	
Figure(2-13): A Schematic diagram presenting the differences in the Shapes of three nuclear potentials.(Red) harmonic oscillator,(black)the finite square well and (blue) the Woods-Saxon potential.	36
Figure (3-1): (a) The two-body interaction $V_{ik}(r_i - r_k)$ in a nucleus, is repulsive (attractive) at short (long) distances between the nucleons. (b) The average one body potential $U_i(r)$ is used to approximate of the two body interaction	47
Figure (4-1): The neutron and proton particle configurations for the doubly-magic nucleus $^{16}_8\text{O}_8$ and $^{28}_{14}\text{Si}_{14}$	59
Figure (4-2): Energy levels for doubly-magic oxygen-16	61
Figure (4-3): Within the shell model the first several excited states in $^{17}_8\text{O}_9$ are explained by the valence neutron configurations	62
Figure (4-4) : Energy levels for doubly-magic oxygen- $^{16}_8\text{O}_8$ and oxygen- $^{17}_8\text{O}_9$	64
Figure (4-5): Energy levels for doubly-magic $^{28}_{14}\text{Si}_{14}$.	65
Figure (4-6):The effective single energies for $^{30}_{14}\text{Si}_{16}$	66

<p>figure(4-7):Our theoretical data of level energy for $^{18}_8\text{Ne}_{10}$ using USD, USDA, and USDB potential compare with the experimental data.</p>	<p>89</p>
<p>Figure (4-8): our theoretical data of level energy for $^{30}_{16}\text{S}_{14}$ using USD,USDA and USDB potential compare with experiment data</p>	<p>92</p>
<p>Figure (4-9): our theoretical data of level energy for $^{30}_{14}\text{Si}_{16}$ using USD,USDA and USDB potential compare with experiment data</p>	<p>94</p>

List of Tables

Table	Page
Table (4-1):The two body matrix element interactions by using USD, USDA and USDB potential (are given in MeV) . The shell-model orbits are labeled $1 \cong 1 d_{\frac{3}{2}}$, $2 \cong 1 d_{\frac{5}{2}}$ and $3 \cong 2 s_{\frac{1}{2}}$.	69-71
Table(4-2):Results of our calculation of the two body matrix element for $^{18}_8\text{Ne}_{10}$ using USD,USDA and USDB interaction.	72-73
Table(4-3):Results of the binding energy B.E(MeV) for $^{18}_8\text{Ne}_{10}$ that calculated with USD,USDA,and USDB potential .	74-75
Table(4-4):Results of our calculation of the matrix element for $^{30}_{16}\text{S}_{14}$ using USD,USDA,and USDB interaction.	76
Table(4-5):Results of the binding energy B.E(MeV) for $^{30}_{16}\text{S}_{14}$ that calculated with USD,USDA,and USDB.	77
Table(4-6):Results of our calculation of the matrix element for $^{30}_{14}\text{Si}_{16}$ using USD,USDA,and USDB interaction.	79
Table(4-7):Results of the binding energy B.E(MeV) for $^{30}_{14}\text{Si}_{16}$ that calculated with USD,USDA,and USDB.	80
Table(4-8):Results of the excitation energy (MeV) for $^{18}_8\text{Ne}_{10}$ that calculated with USD,USDA,and USDB.	81-82
Table(4-9):Results of the excitation energy (MeV) for $^{30}_{16}\text{S}_{14}$ that calculated with USD,USDA,and USDB.	83
Table(4-10):Results of the excitation energies (MeV) for $^{30}_{14}\text{Si}_{16}$ that calculated with USD,USDA,and USDB interaction.	84
Table(4-11):Compared results data of the excitation energy	90-91

B.E(MeV) for $^{18}_8\text{Ne}_{10}$ that calculated with USD,USDA,and USDB with expermental and other theory .	
Table(4-12):Results of the excitation energy Ex_1 (MeV) for $^{30}_{16}\text{S}_{14}$ that calculated with USD,USDA,and USDB.	93
Table(4-13):Compared our results of the binding and excitation energies (MeV) for $^{30}_{14}\text{Si}_{16}$ that calculated with Wildenthal ,USDA,and USDB with expermental data.	96

Abbreviations and Symbols

USDA	The universal potential energies A
USDB	The universal potential energies B
USD	The universal potential
SU(3)	Radical anion
NN	Nucleon–nucleon
C.G.	Clebsch-Gordan coefficient values
MSDI	Modified Surface Delta Interaction
(M3Y)	Michigan three-rang Yakawa
(Z)	Protons
(N)	Neutrons
A	Mass number
p_F	Fermi momentum
E_F	Fermi level energy
n_F	Concentration of nucleon
\hat{R}	The collective angular momentum
\hat{J}	The angular momentum
\hat{I}	The inertia momentum
(C M)	Collective Model

\hat{H}_0	The Hamiltonian
ω	The rotational frequency
\hat{J}_x	The total angular momentum projection operator
(DWBA) ,	The distorted wave Born approximation
π	The parity
R	The radius
$V(r)$	The realistic nuclear potential
j	The total angular momentum, and intrinsic
l	The orbital angular momentum
s	Spin
V_{ls}	Woods-Saxon strength constant.
V	The residual interaction
H_i	The independent-particle Hamiltonian
$\psi(r)$	The total wave function
$\phi(r)$	The eigenfunctions
$U_i(r)$	The average potential
e_{nlj}	The single-particle energies
E_B	Binding energies

E_{Ex}	Excitation energies
t	Isospin
T_z	The projection of the total isospin
V_{ik}	Two -body interaction
$V_{ik}(r_i - r_k)$	The two-body interaction
$U_i(r_i - r_k)$	The mean field potential
$\hat{H}^{(0)}$	The Hamiltonian of one body potential
$\hat{H}_{res}^{(1)}$	The residual interaction
$W(i, j)$	The potential is repulsive
E_{JT}	The energy of the residual interaction
$V_{JT}(ab; cd)$	The two-body matrix element
Q	Values reaction and decays

CHAPTER

One

General

Introduction

(1-1)Introduction

For more than a century, the development of modern physics has brought human beings the deepest understanding of nature in terms of the building blocks of matter and their interactions. In particular, it has been established that all matter consists of a number of particles more fundamental than previously thought from the 6th century [1]. Towards the end of the nineteenth century, it was believed that each element in nature consisted of atoms, named after the Greek word “atomos” In 1897 J. J. Thomson discovered the electron ,which weighed much less than the lightest atom and was believed to be a constituent of atoms. In 1911 the discovery of nucleus in atoms by E. Rutherford established the nuclear structure of atoms[2].

In modern science, the idea of indivisible building blocks goes back to 1803 with atom of Dalton how introduced in 19th century. At that time, the atom was regarded as the elementary particle of the matter. In the early part of the 20th century, discoveries revealed that the atom is not an elementary particle after all, but consists of a positively charged nucleus and negatively charged electrons orbiting the nucleus. The nucleus itself was later found to be composed of protons and neutrons [3].

In 1932, the positron was discovered, i.e., the positively charged antiparticle of the electron had actually been predicted a few years earlier by Dirac based on theoretical considerations. The neutrino was predicted by Pauli in 1930 but proved very elusive. It was finally discovered in 1956 · In 1933 it was discovered that the magnetic moment of the proton was 2.5 times larger than expected from the Dirac theory. The assumption of substructure in the nucleon was born. Also new particles were discovered: a second nucleon called the neutron (found in 1932); mesons like the pion (predicted in 1934 and found in 1937) and new strange particles, some

again mesons like the K^0 , others, baryons like the Λ . Thus a new field of strong interaction physics and its experimental investigation was opened[4].

The development of science and technology gives us much more detailed information of the matter. The elementary particle was regarded as "unbreakable" constituent consists of smaller particles. Such a change of picture of the elementary particle was repeated in the history of science[5]. Elementary particles might be composite particles. From the middle of the 1940s, many new sub-atomic particles were discovered by studying collisions between known particles at high energy. The new particles were found to be very unstable with short lifetimes. Until the 1960s, physicists were confused by the large number and variety of subatomic particles being discovered. They were trying to find a pattern that would provide a better understanding of the variety of particles[6].

Today there are a number of models which have their specific domains where they can explain a limited number of experimentally observed phenomena, but no universal nuclear model exists. A goal of experimental nuclear structure physics is to provide stringent tests of nuclear models so that theory can advance towards a more fundamental understanding of nuclei[7].

Many theoretical models have been introduced for this purpose such that ; The Liquid-Drop Model ,the Fermi Gas Model ,the Collective Model ,optical model Statistical model Cluster Model, and shell-model . Shell-model is one of them and it leads to a very successful description. The nuclear shell model was one of the first models that was created to describe the structure of nuclei. It has proved to be very successful to describe nuclei near closed shells. The shell model is one of fundamental tools to describing properties of atomic nuclei. It considers the nucleons to be independent no interacting particles moving inside an external potential well. The "external" potential is however a ~~field~~ ~~field~~ created by the

mutual interaction of nucleons. The fact that the nucleus may be viewed as a potential well containing no interacting particles is surprising and is caused by specific properties of inter nucleon interaction [8].

In principle, the nuclear shell model represents the ideal theoretical microscopic tool to attack the problem of understanding the evolution of collective nuclear structure. However, the description of collective excitations often requires a very large configuration space and, hence model calculations must be truncated to appropriate valence spaces leading to necessary readjustments for the parameters of the effective residual interactions and single-particle energies. These effective model parameters must be obtained from experiment [9]. Traditional shell-model studies have recently received a renewed interest through large scale shell-model calculations in both no-core calculations for light nuclei, the $1s0d$ shell, the $1p0f$ shell and the $2s1d0g7/2$ shell with the inclusion of the $0h11/2$ intruder state as well. It is now therefore fully possible to perform large-scale shell-model investigations and study the excitation spectra for systems with many basis states [10]. In this thesis the sd-nuclear shell model is considered to investigation and studied the nuclear structure for some nucleus depending on calculation the binding and excitation energies. We have applied the USD,USDA,and USDB potential for two body matrix element in $2S\ 1d$ configuration interaction to study the nuclear level structure of even-even $^{18}_8\text{Ne}_{10}$, $^{30}_{16}\text{S}_{14}$, $^{30}_{14}\text{Si}_{16}$ isotopes respectively.

(1-2)Previous Studies

The most fundamental forms of matter have been the interest of scholars as long ago as the Greek philosophers, when in the 4th century BC, Democritus postulated the existence of atomos: elementary blocks of indivisible substance. The word atomos in Greek is in fact the very translation of indivisible. Retrospectively, the

foresight of Democritus was indeed remarkable, especially, since over two millennia later, the elucidation of the atomic enigma was no closer. It was the work of experimental physicists and chemists in the early 19th century, such as Dalton, Avogadro and Faraday, that initiated the contemporary understanding of atoms. In the time since, many of the most famous physicists have contributed to the subject of atomic and nuclear physics, including, for example, Einstein , Rutherford , Fermi and Bohr . Democritus could probably be forgiven for postulating that atoms are indivisible matter; it is perhaps ironic that dividing the indivisible has since moulded our world so profoundly. Nuclear physics has played a very prominent role in twentieth century science, so that today, there exists a refined understanding of microscopic phenomena that occur in atomic nuclei[11].

Many researcher had been studied the nuclear structure depending on shell model such that :

Sharda H. R. K. and etal in 1998 studied and extracted the average effective of two-body interaction matrix elements in the s-d shell model. Dependent on data from experimentally measured isospin centroids. On the other hand they made combining the recently derived new sum rule equations for pick-up reactions with similar known equations for strip-ping reactions performed on general multi shell target states. Under using this combination of stripping equations, the average effective matrix elements for the, $1d_{3/2}$ $2S_{1/2}$ and $1d_{5/2}$ levels shells respectively have been obtained[12].

Liuy Xu. YB . And etal in 1999 using Modifid Surface Delta Interaction MSDI to studied and calculated the energy levels for allowable total angular momentum and the parity by shell model application for different nuclei Ca^{42} , Sc^{42} and Ti^{42} equivalent in mass number (Isobars) and contain two nucleons outside the close core (Ca^{40}) . In this study, a computer programmes were take up to

calculate the Clebsch- Gordan Coefficients and Matrix Elements $\langle j_2 | V^{\text{MSDI}} | j_2 \rangle$ which use to calculate the energy levels[13] .

Taqi A H in 2000 has been studied the effect of expand the space configuration of wave function on the spectra by modified the Hamiltonian operator to diagonal matrix element with modified surface delta potential interaction using the nuclear shell model calculation .That lead to agreement the theoretical calculation with experimental above 70% [14].

Ali K Hassan in 2001 been calculation the half life ^{42}Ca nuclei by applied the nuclear calculation with assume configuration model space . The nucleon assume is moving in space configuration spd and calculated the half life by using a program was proved to this. Result was agreement with experimental in 60% [15].

Vesselin Gueorguiev calculated in 2002 all eigen values for larger model spaces configuration to the nuclear shell model by using the advances in computer technologies.He used the Lanczos method for diagonalization of large matrices, and the Cholesky algorithm to solving generalized eigen value problems, the method is applied to ^{24}Mg and ^{44}Ti nuclei. Results for ^{24}Mg , obtained using the USD interaction in a space that spans less than 10% of the full-space, reproduce the binding energy within 2% as well as an accurate reproduction of the low-energy spectrum and the structure of the states 90% overlap with the exact eigen states. On the other hand the calculations for ^{44}Ti was supported using the mixed-mode scheme of the pure SU(3) calculations . The results suggest that a mixed-mode for shell-model theory may be useful in situations where competing degrees of freedom dominate the dynamics, and full-space calculations are not feasible[16].

Jennifer Anne in 2003 has been studied some of light nuclei N=20 using shell model calculation with assume $1d_{3/2}$ and $f_{7/2}$.This model based on the valance

space expand from sd to pf Monte Carlo shell model to calculate Gamma transition probability. All excited states are calculated theoretically and compared with a result measurement for transition by Coulomb excitation. All electric and magnetic transitions are calculated according to the QXBASH shell model [17].

Deana D.J., et al. in 2004 derived the interactions between effective particles in various many-body approaches and spectroscopic data extracted depending on large scale shell-model studies. To achieve this, many-body scheme starts with the free nucleon–nucleon (NN) interaction, typically modeled on various meson exchanges. The NN interaction is in turn renormalized in order to derive an effective medium dependent interaction. The latter is in turn used in shell-model calculations of selected nuclei. Also describe how to sum up the parquet class of diagrams and present initial uses of the effective interactions in coupled cluster many-body theory. A result applied on ^{40}Ca , ^{48}Ca or the excitation spectra of ^{47}Ca and ^{49}Ca . Eventual discrepancies with experiment such as the missing reproduction of e.g., the first excited 2^+ state in a pf calculation of ^{48}Ca , can then be ascribed to eventual missing three-body forces, as indicated by the studies for light nuclei [18].

Samah A.H. Al Ramahy in 2005 applied the nuclear shell model on the isotones ^{50}Ti , ^{51}V and ^{52}Cr that contain two, three and four protons respectively and with the use Modified Surface Delta Interaction MSDI and a computer program for calculation the Clebsch-Gordan coefficient values C.G. and matrix elements values. The energy levels, angular momenta and parity are calculated for each of the previously mentioned nuclei. Energy levels values that were not confirmed experimentally are confirmed in the present study, where angular momentum and parity values are respectively. With application of many tests on the correction

parameters used in calculation Modified Surface Delta Interaction MSDI , the range of these parameters is determined for each of the studied nuclei [19] .

Praha Listopad in 2006 were used the shell model one-body densities and the effective interaction to generate the optical model potentials and the form factors for inelastic scattering. You have measured for the first time the angular distribution of the quasielastic scattering of proton in nuclei ${}^7\text{Be}$ and ${}^8\text{B}$ on the ${}^{12}\text{C}$ target. The calculation of quasielastic scattering accounts well for ${}^7\text{Be}$ while for ${}^8\text{B}$ the agreement is not sufficient. Monte Carlo simulation was performed in order to carefully evaluate the efficiency of the detector setup and to estimate the experimental error bars. They were summarize main results for your experiment using fragmentation of the neutron-rich projectile ${}^{36}\text{S}$ and the spectrometer have been found the particle stability and structure of nuclei near the neutron drip line:- In the neutron-rich region, no standard doubly-magic nuclei, therefore, in the next period we concentrated to mass measurement of very neutron rich nuclei to determine their binding energy and two-neutron separation energy which are the leading quantities to establish clear signature of nuclear shells [20] .

Ali H. T., and Ra'ad. A. R. in 2007 were studied the Random Phase Approximation RPA for ${}^{16}\text{O}$, ${}^{12}\text{C}$ and ${}^{40}\text{Ca}$ using the longitudinal form factors of the low-lying $T = 0$ for particle states by shell model calculation . The basis of single particle states is considered to include $0s$, $0p$, $1s-0d$ and $0f-1p$. The Hamiltonion was diagonalized in the presence of Michigan three-rang Yakawa (M3Y) interaction and compared with our previous results depend on Modi Surface Delta MSDI interaction. Admixture of higher cofiguration up to $2p-1f$ is considered for the ground state. Effective charges are used to account for the core polarization effect. Comparisons were made to experimental data where available and the theoretical significance of the calculation and its results is discussed [21].

Nicholas J. Thompson in 2008 has been study the transition and the binding and excitation energies $^{91,92}\text{Zr}$ isotopes for reactions $^{82}\text{Se}(^{13}\text{C},\text{xn})^{96}\text{xZr}$ at an incident beam energy of 50 MeV . Angular correlation and linear polarisation analyses were performed on these transitions. A modified effective interaction has been produced for the shell model code OXBASH which embeds the empirical matrix elements of the Ji-Wildenthal interaction into a new interaction developed by Hjorth-Jenson for N=50 nuclei. This interaction together with newly derived single particle energies allows calculations in the basis $[1f_{\frac{5}{2}}\ 5/2; 2p_{3/2} ; 2p_{1/2}; (1g_{9/2})]; [2p_{1/2}; 1g_{9/2} ; 2d_{5/2} ; 3s_{1/2} ; 1g_{7/2} ; 2d_{3/2}; 1h_{1/2}]$ [22] .

Bertsch G. F. and C. W. Johnson carry out in 2009 an interacting shell-model study of binding energies and spectra in the sd-shell nuclei to examine the effect of truncation of the shell-model spaces. Starting with a Hamiltonian ~~file~~ in a larger space and truncating to the sd shell, the binding energies are strongly affected by the truncation, but the effect on the excitation energies is an order of magnitude smaller. We then ~~fit~~ the matrix elements of the two -particle interaction to compensate for the space truncation and find that it is easy to capture 90% of the binding energy shifts by ~~fitting~~ fitting a few parameters. With the full parameter space of the two-particle Hamiltonian, they found that both the binding energies and the excitation energy can be fitted with remaining residual error about 5% of the average error from the truncation. Numerically, the rms initial error associated with our Hamiltonian is 3.4 MeV and the remaining residual error is 0.16 MeV. This is comparable to the empirical error found in sd-shell interacting shell-model fits to experimental data [23].

Simon Mark Brown in 2010 was investigated the N=20 shell gap in neutron-rich nuclei by studying the single-particle structure of ^{27}Ne via neutron transfer

onto a ^{26}Ne beam. The observation of low-lying negative parity states in ^{27}Ne above the $3/2^+$ ground state is further evidence of the raising of the $d_{3/2}$ orbital that is seen in other neutron-rich nuclei in the $N=20$ region. The previously unseen $7/2^-$ state has been identified as unbound by 331 keV and lies above the already known $3/2^-$ level. Monte-Carlo Shell Model predictions, had been used to the measurement of data. The calculations of the single-particle energies of the pf shell are artificially lowered by 1 MeV. This modification was made to mimic the closing of the $N = 20$ shell gap in neutron-rich nuclei. The calculations show that core-excited configurations play a significant role in both the $3/2^+$ ground state and the $7/2^-$ intruder state in ^{27}Ne [24].

LEI Yang and etal in 2010 had been studied the structure coefficients of collective nucleon pairs with spin zero and spin two are further simplified to sd shell model to bosons, and widely applied to study low-lying states of atomic nuclei in the nucleon pair approximation of the shell model. They investigated the effect of the shell structure coefficients with respect to different configurations and the evolution of SD-pair structure coefficients with valence nucleon number. They showed that more sophisticated configurations affect the pair structures of S and D pairs very slightly. Second, they studied the evolution of collective SD-pair structure coefficients. Results calculated D-pair structure coefficients change quickly with nucleon pair number N . The small variations of energies for the isotopes does not necessarily lead to small variations of pair structure coefficients of SD pairs[25].

Angelo Signoracci in 2011 using new technique methods to study SD region, which combine configuration interaction theory and energy density functional methods in order to exploit their finite properties, are currently under investigation for improved theoretical capabilities. A new technique to produce

nuclear Hamiltonians has been developed, implementing renormalization group methods, many-body perturbative techniques, and energy density functional methods. Connection to the underlying physics is a primary focus, limiting the number of free parameters necessary in the procedure. The main ~~benefit~~ of this approach is the improvement in the quality of effective interactions outside of standard model spaces region . An SD shell interaction is produced for a proof of principle, and extensive results are obtained in the inversion region and for ^{42}Si . One hundred nuclei are calculated near the island of inversion region of the nuclear chart. Binding energies and low-lying excitations agree well with available experimental data. Many-body perturbative techniques, in the form of Rayleigh- and Schrödinger theory, implement the realistic basis to convert the low-momentum interaction into a model space of interest[26].

Fiase J. O. and Gbaorunin F. in 2012 studied the effects of correlations on the positive parity states of ^{20}Ne nucleus depending on sd shell model . Two-body nuclear matrix elements were obtained by the lowest order constrained variational technique with and without correlations. The matrix elements calculated are used as input into the NUSHELL shell model code to calculate the energy spectrum of ^{20}Ne nucleus . He had found that the effects of correlations is to open up the calculated energy spectrum and provide reasonable agreement with experiment, whereas the energy spectrum calculated without correlations is compressed and provides significant disagreement with experimental data. This feature is consistent with our observations for nuclei in the range $18 \ll A \ll 40$. The results presented the strong evidence found in nuclear structure calculations that tensor correlations are very important in nuclei and their presence cannot be ignored[27].

Khalid S. Jassim, and Hassan A₁ K₁ in 2013 had been calculated factors of inelastic scattering in some odd nuclei (¹⁷O, ²⁷Al and ³⁹K) using Sd-shell model calculation according to Pauli exclusion principle by taking into account higher energy configurations outside sd-shell model space. It's used the two-body Wildenthal interaction for the sd-shell model space and the two-body Michigan three Yukawas (M3Y) interactions are used for the core- matrix elements. This interaction was given in LS-coupling to get the relation between the two-body shell model matrix elements and the relative and center of mass coordinates using the harmonic oscillator radial wave functions with Talmi-Moshinsky transformation. The sd-shell model calculations succeed to describe the experimental data very well in both the absolute strength and the momentum transfer dependence[28].

(1-3) Aims and Outline of The Thesis

The first aim of this thesis derive mathematical equation for calculation the binding and excitation energies depending on a quantum theory consideration and the perturbation theory to gate relationship enables us to study the nuclear structure. This would be applicable to evaluate the binding and excitation energies amount of nucleus . .

The second aim of this study is to investigate and understand the levels spectra of three nuclei for depending on our theoretical expression. In particular, how the different configuration space in nucleus systems and the two body matrix element potential strength, single particle energy and the binding energy of core can effect on the spectrum of nucleus.

CHAPTER

Two

Background Theory

And Nuclear Shell

Model

(2-1) Introduction

One of the major aims in nuclear physics is to produce a better understanding of the internal structure of atomic nuclei. The atomic nucleus is a quantum system in dimension about 10^{-14} m to 10^{-15} m. Each nucleus is comprised of number of protons(Z) and neutrons(N) which interact strongly with each other, and is an excellent environment for studying a many-body quantum system with a finite (non-statistical) number of particles. These nucleons are quantum mechanical particles and thus the nucleus itself is a quantum mechanical many body system[17]. Theoretical solutions to the nuclear many-body problem are partly phenomenological, and thus theory and experiment are closely tied together. Theory takes its inspiration from experiment in guiding the structure of the models and their parameters [28]. Early in the development of the theory of the nucleus there arose several empirical models have been formulated over the last 70 years in an attempt to describe observed nuclear-structure characteristics such that : the liquid-drop model , the Fermi gas model , the collective model, statistical model, cluster model, and the shell model . There are two basic types of models used:

1. Those which describe the nucleus as individual nucleons that interact with each other, and give rise to the observed structure (microscopic models).
2. Those that attempt to describe nuclear structure by considering the motion of many nucleons simultaneously (collective models)[29].

The liquid drop model of Neils Bohr took a very classical view of the nucleus as a drop of some nuclear liquid, and through the use of hydrodynamics with some quantum corrections, while the shell model took quantum theory. In the following sections, a most of the nuclear models are explain and discussed.

(2-2) The Liquid-Drop Model

The liquid-drop model is a model that describes the nucleus as a drop of incompressible nuclear fluid. The model is able to account for “macroscopic” properties of the nuclei that can not yet be described accurately by pure quantum

models like the shell model. The liquid drop model first proposed by George Gamow in 1928[7].

The liquid drop model is one of the first models which could describe very well the behavior of the nuclear binding energies and therefore of nuclear masses was the mass formula of von Weizsäcker published in 1935. This microscopic model is based on several assumptions like a constant mass density inside the nuclei or a saturation of a charge independent nuclear force. The nuclear binding energy based on the liquid drop model as a function of mass number A , that's shown in figure (2-1). As we have already discussed, experiments revealed that nuclei were essentially spherical objects, with sizes that could be characterized by radii proportional to mass numbers A s, which suggested that nuclear densities were almost independent of nucleon number[30].

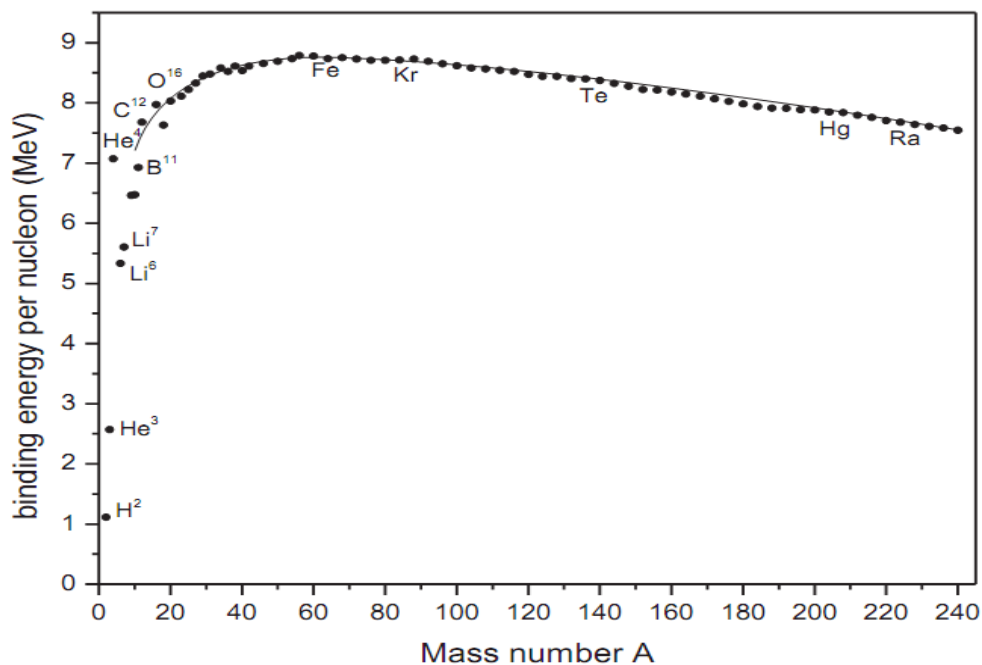


Figure (2-1): Binding energy per nucleon as a function of mass number A [30].

As in the case of a liquid drop, the nucleus is imagined as composed of a stable central core of nucleons for which the nuclear force is completely saturated and a surface layer of nucleons that is not bound as tightly (forces not saturated). This weaker binding at the surface decreases the effective binding energy per nucleon $\left(\frac{B}{A}\right)$, and provides a "surface tension" or an attraction of the surface nucleons towards the center (see Fig (2-2))[31].

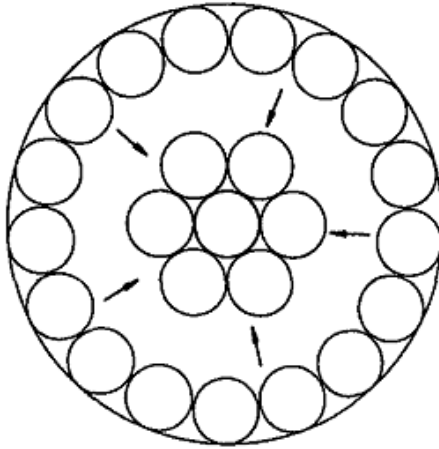


Figure (2-2): Surface layer and core of nucleus in the liquid drop model[31].

The Weizsacker binding energy is an empirically refined form of the liquid drop model and is given by[32]:

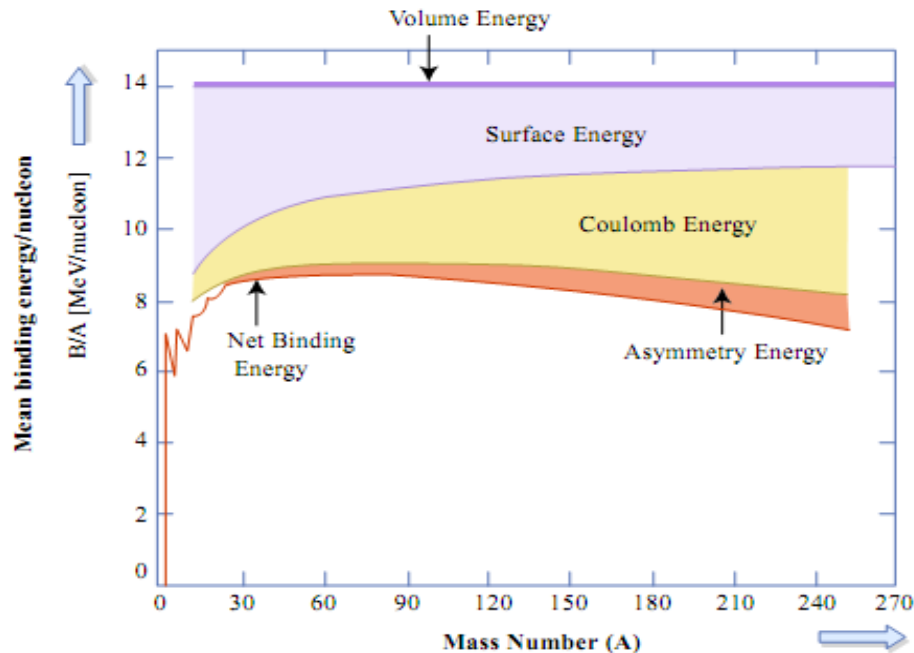
$$B(A, Z) = E_V + E_S^0 + E_C^0 + E_{Sym} + E_{Pair} \dots\dots\dots(2-1)$$

That's means the binding energies may be written by[32]

$$B(A, Z) = a_{vol}A - a_{sur}A^{2/3} - a_c Z(Z - 1)A^{-1/3} - a_{sym} \frac{(A-2Z)^2}{A} + \delta \dots\dots(2-2)$$

Where δ is the pair energy and five terms are illustrated in figure (2-3) give the volume binding energy, surface binding energy, Coulomb repulsion energy, symmetry energy, and the pair energy were first proposed by von Weizsäcker in

1935. The magnitudes of the various contributions to the binding energy curve are depicted in figure (2-3).



Figure(2-3): Relative contributions to the binding energy per nucleon showing the importance of the various terms in the semi-empirical Weizsäcker formula[33].

The binding energy is proportional to the volume of the nucleus or the mass number A . This assumes every nucleon is like every other nucleon. It is quite understandable that the surface term should vary with $A^{2/3}$ or R^2 [34]. The Coulomb repulsion and the surface binding energy are shape dependent; therefore in order to apply the liquid drop model to deformed nuclei some modification is needed[35].

(2-3)The Semi Empirical Liquid Drop Model

In the semi-empirical liquid drop formula, the binding energy of the nucleus in Eq.(2-3) is parameterized as follows (in a slightly generalized form of the original von Weizsäcker formula):[36].

$$B(A, Z) = a_v A \left[1 - \kappa_v \left(\frac{N-Z}{A} \right)^2 \right] - a_s A^{2/3} \left[1 - \kappa_s \left(\frac{N-Z}{A} \right)^2 \right] - \frac{3}{5} \frac{Z(Z-1)e^2}{4\pi\epsilon_0 R_c} + E_{Pair} . \quad (2-3)$$

where κ_v is the correlation factor of volume term and κ_s is the correlation of surface term. The first two terms are the volume and surface energy, respectively. The isospin dependence is discussed by Myers and Swiatecki and favours $N=Z$, limiting the effects of the Pauli principle. Coulomb term is also quite self-evident considering that $Z(Z-1)$ is the number of pairs that one can form from Z protons and the $A^{-1/3}$ factor comes from the $1/R$. This effect is counter balanced by the Coulomb repulsion between the protons, the third term of the expression (2-3), which favours a neutron excess. The observed odd-even effect in the nuclear masses leads to the addition of a pairing energy term $E_{Pair} = (-\Delta, 0, \Delta)$ with $\Delta \approx 12/\sqrt{A}$ MeV for odd-odd, odd-even and even-even nuclei, respectively [36].

The comparison between semi-empirical and measured nuclear masses showed clear deviations around the closed proton and neutron shells as well as at mid-shell and provided evidence for the need for shell corrections. It is introduced by Myers and further refined in the Strutinsky theorem [37], these corrections account for the non-uniform level density. This term is not only important for reproducing the nuclear masses of nuclei near closed shells but it also generates non-spherical nuclear shapes. Meanwhile many refinements have been added to the liquid drop model, also with respect to the calculation of nuclear radii. In the droplet-model deviations from the spherical nuclear shape are included. The redistribution of the proton and neutron distribution increases all radial distributions and quadrupole moments [36].

(2-4)The Fermi Gas Model

The Fermi-gas model was one of the earliest attempts to incorporate quantum mechanical effects into the discussion of nuclear structure. It assumes that a nucleus can be regarded as a gas of free protons and neutrons confined to a very small region of space, namely to the nuclear volume. Under such conditions the nucleons would be expected to populate discrete (quantized) energy levels within the nucleus. The protons and neutrons as moving inside a spherically symmetric well whose range is given by the radius of the nucleus and whose depth can be adjusted obtain the correct binding energy. Because protons carry electric charge they sense a potential that differs from that sensed by neutrons. The observed energy levels for neutrons and protons will therefore differ somewhat depending on the specific range and depth of the individual potentials[31]. On the other hand the all elementary particle physics is a domain of physics that uses the scientific method to describe the fundamental building blocks of matter and the elementary interactions between them[38] can be classified as either bosons or fermions and that protons and neutrons being fermions obey Fermi-Dirac statistics [39]. In the Fermi gas model the nucleus is considered a collection of confined non interacting fermions. The nucleon wave functions are approximated by plane waves that satisfy the periodic boundary conditions imposed by the confinement volume. The gas of fermions is taken to be at absolute zero temperature, i.e., degenerate so that all the available low lying single particle state are filled[40]. The energy levels of protons and neutrons are alike but not identical because of a Coulomb force that affects only protons. Both protons and neutrons obey the exclusion principle so that filling of the lowest and subsequent pairs of energy levels. The Fermi gas model defines properties of a system of non-interacting Fermions in an infinite potential well that shown in figure(2-4).

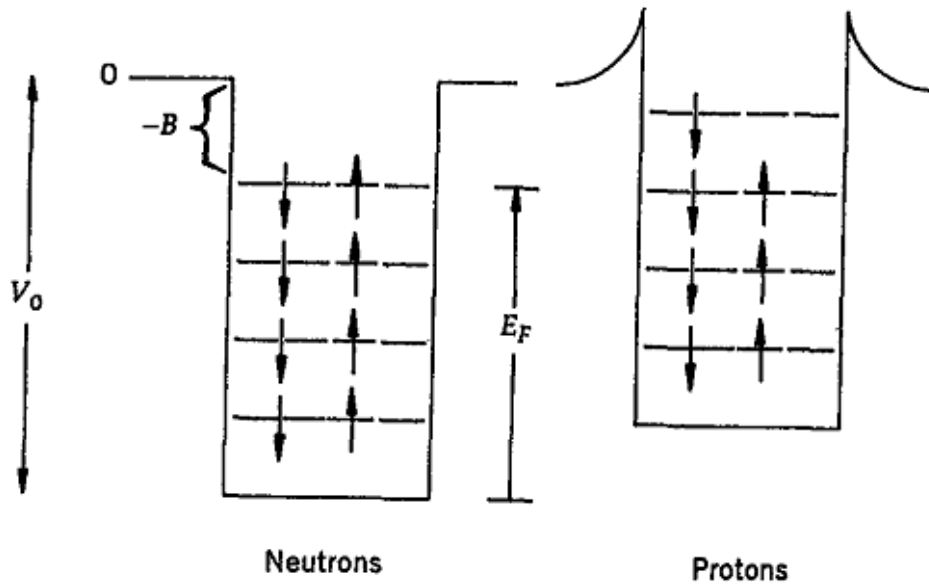


Figure (2-4): Ground-state energy levels for neutrons and protons in nuclei [31].

The model assumes that all fermions occupy the lowest energy states available to them up to the Fermi energy and that there is no excitations across the Fermi energy (i.e. zero temperature). In nuclei the model assumes that protons and neutrons are independent filling two separate potential wells. The model assumes however common Fermi energy for the protons and neutrons in stable nuclei.

In an ideal Fermi gas the number of states can be obtained by[41].

$$D(\epsilon) = \frac{2V}{4\pi^2} \left(\frac{2m}{\hbar^2}\right)^{3/2} \sqrt{\epsilon} \dots \dots \dots (2-4)$$

Where V is the volume, $\hbar = \frac{h}{2\pi}$, h is Planck's constant, m is the mass of a nucleon and ϵ is the energy of the states.

The Fermi distribution is given by[41].

$$f(\epsilon, T, \mu) = \frac{1}{e^{\frac{\epsilon - \mu}{k_B T}} + 1} \dots \dots \dots (2-5)$$

Where T is the absolute temperature and μ is the chemical potential .

The corresponding Fermi momentum p_F is associated with the Fermi level energy E_F through [42].

$$p_F = \sqrt{2mE_F} \dots \dots \dots (2-6)$$

Ignoring the presence of fermions beyond the fermi level, we can write the volume for states in momentum space as

$$V_{P_F} = \frac{4\pi}{3} \rho_F^3 \dots \dots \dots (2-7)$$

It follows therefore that the number of fermions that can fill states up to and including the fermi level is [42].

$$n_F = 2 \frac{V_{TOT}}{(2\pi\hbar)^3} = \frac{2}{(2\pi\hbar)^3} \left(\frac{4\pi}{3}\right)^2 r_o^3 \rho_F^3 A = \frac{4}{9\pi} \frac{r_o^3 \rho_F^3}{(\hbar)^3} A \dots \dots \dots (2-8)$$

where the factor of 2 arises because each state can be occupied by two fermions with opposite spins. For simplicity, let us now consider a nucleus with $N = Z = A/2$, and assume that all the states up to and including the fermi level are filled. In this case we have [42].

$$N = Z = \frac{A}{2} = \frac{4}{9\pi} \frac{r_o^3 \rho_F^3}{(\hbar)^3} A \dots \dots \dots (2-9)$$

Or

$$\rho_F = \frac{\hbar}{r_o} \left(\frac{9\pi}{8}\right)^{1/3} \dots \dots \dots (2-10)$$

In other words the fermi momentum for this case is a constant independent of the nucleon number. It follows that [42].

$$E_F = \frac{p_F^2}{2m} = \frac{1}{2m} \left(\frac{\hbar}{r_0}\right)^2 \left(\frac{9\pi}{8}\right)^{2/3} \approx \frac{2.32}{2mc^2} (\hbar c)^2 \approx 33 \text{ MeV} \dots\dots\dots(2-11)$$

Taking the average binding energy per nucleon of about (-8)MeV to represent the binding of the last nucleon it follows from our simple approximation that the depth of the potential well is about 40 MeV, namely[42].

$$V_0 = E_F + B \approx 40 \text{ MeV} \dots\dots\dots(2-12)$$

This result is consistent with the value of V_0 obtained through other considerations. The Fermi-gas model has been used to study excited states of complex nuclei, which can be accessed by "raising the temperature of the nucleon gas (i.e., by adding kinetic energy to the nucleus).

(2-5)The Collective Model

The Collective Model emphasizes the coherent behavior of all of the nucleons. In addition to the motion of the individual nucleus inside the nuclear potential the potential itself rotates and vibrates which is called collective motion[43].

The collective model was first described by Inglis D.R. in 1954 and was expanded by Frauendorf S. and Bengtsson R . in 1979[44]. Among the kinds of collective motion that can occur in nuclei are rotations or vibrations that involve the entire nucleus. The collective model provides a good starting point for the understanding the fission. In addition to fission the collective model has been very successful in describing a variety of nuclear properties especially energy levels in nuclei with an even number of protons and neutrons. These energy levels show the characteristics of rotating or vibrating systems expected from the laws of quantum mechanics. The shell model and the collective model represent the two extremes of the behavior of nucleons in the nucleus. More realistic models

known as unified models attempt to include both shell and collective behaviors. [43]. A nucleus can generate angular momentum in two different ways either collectively as rotations and vibrations of the droplet of the nuclear matter or by nucleon excitations in which a small number of unpaired nucleons rearrange to generate the angular momentum. In practice most nuclear states carrying large angular momentum are a mixture of these two modes.

The collective angular momentum \hat{R} represents the motion of the nucleus as a whole, i.e. the rotation of the droplet. This angular momentum coupling is shown schematically in figure (2-5). It is impossible to have collective rotation about an axis of symmetry since the different orientations are indistinguishable in the quantum mechanics. In the important case of an axially-symmetric nucleus the collective rotation must be about an axis perpendicular to the symmetry axis. The angular momentum \hat{J} of the nucleus generated by the rearrangement of the valence nucleons will be :[44].

$$\hat{I} = \hat{R} + \hat{J} \dots \dots \dots (2-13)$$

Where \hat{I} is the inertia momentum

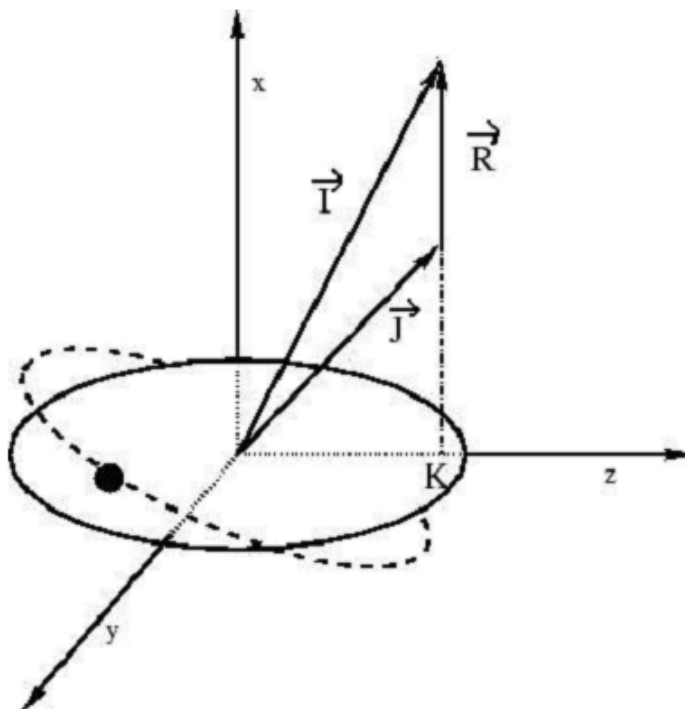


Figure (2-5): Schematic of the coupling of the collective angular momentum [44].

Nuclei can also generate collective angular momentum by vibrating. Vibration quanta are classical which are characterized the multipolarity of the distortion of the nucleus surface [45]. The single-particle motion was described by the collective model (C M) through the equation[44].

$$\hat{H} = \hat{H}_0 - \hbar w \hat{j}_x \dots \dots \dots (2-14)$$

where \hat{H}_0 is the Hamiltonian in the absence of rotation, w is the rotational frequency and \hat{j}_x is the total angular momentum projection operator onto the rotation axis. Rotation of spherical nuclear shapes are used to treat the excited states in this model. The center mass justifies the interaction between rotation and single particle excitation. Also it explains independent single particle motion in a potential like the spherical and deformed shell models. The rotation operator given by[44].

$$\hat{R}_x = e^{ij_x\omega t} \dots\dots\dots(2-15)$$

where j_x represents the projection of the total angular momentum on the x-axis, ω represents angular velocity and t represents the time of rotation. The expanding separation of orbitals with increasing rotation is referred to as signature splitting [46]. Collective motion induces oscillation/rotation of the potential. The fluctuation of the potential changes the nucleonic single-particle motion. Thus in these cases the motion of single nucleons must be correlated giving rise to a collective motion. Collective models contrary to single particle ones describe the motions exhibited by the nucleus as a whole not considering the behavior of individual nucleons[8].

(2-6)The Optical Model

The nuclear optical model has long been a fundamental tool of nuclear physics. It is used to describe elastic scattering of particles from nuclei. The basis of the optical model was established by Herman Feshbach and collaborators in 1953. An optical model which successfully describes elastic scattering is used to calculate distorted waves for use in the distorted wave Born approximation (DWBA) or as a potential to be modified for use in calculation. The optical potential can also be viewed as the one body approximation of the fundamental many body problem of nuclear scattering and thus as a testing ground for microscopic model of nuclear scattering[47]. The optical model has a significant impact on many branches of nuclear reaction physics. The central assumption of that model is that the complicated interaction between an incident particle and a nucleus can be represented by a complex mean-field potential which divides the reaction flux into a part covering shape elastic scattering and a part describing all competing non-elastic channels.

It seems that there are three methods commonly used to set the parameterization of the phenomenological optical model which vary in the amount and type of data used. They are :

- (1) A “best-fit” optical model representing a potential for one nucleus and one single incident energy
- (2) A local optical model representing a potential for one nucleus and an energy region and
- (3) A global optical model in which a potential is specified for both a mass region and an energy region.

In addition to this classification one can consider neutron and proton potentials separately or a more general isospin dependent nucleon potential and one can distinguish between the spherical and deformed optical model [48]. The nuclear optical model has been outstandingly successful in describing the elastic scattering of neutrons and other nuclear particles above the energy of perhaps 6 MeV. where compound elastic scattering processes are not important. Below these energies it is necessary to include some estimates of compound elastic scattering. At neutron energies below the first excited state of the target nucleus inelastic scattering is not possible[49].

(2-7) Cluster Model

Some nuclei particularly light one can be well described in terms of clustering. A ^8Be nucleus for example, can be described as two α -particles. ^7Li can be described as a triton particle above a closed α -closed. The cluster model picture is contrasted with the shell model in figure(3-6). In the Shell model description the unpaired proton determines the spin parity of the ^7Li nucleus. To describe ^7Li as an α -t cluster system, we must construct first the ground state with the correct spin and parity. The quantum numbers $(N; L)$ of the yield state can be with the help of the Talmi-Moshinsky transformation [50].

$$2(N - 1) + L = \sum_i (2(n_i - 1) + l_i) \dots \dots \dots (2-16)$$

where the sum i runs over all the nucleons in the cluster each with quantum numbers n_i, l_i . This quantum numbers of the state[50].

$$2N + L = 5 \dots \dots \dots (2-17)$$

We must recover the spin-parity of the ${}^7\text{Li}$ ground state such that $\frac{3}{2}^-$. The intrinsic spin of the triton is $\frac{1}{2}^+$, therefore the lowest angular momentum L that can couple to a value of $\frac{3}{2}$ is $= 1$. The parities combine correctly to equation (2-17) gives $N = 2$. The ground state of the triton in the cluster model is $2p_{\frac{3}{2}}^-$. The cluster description allows for calculations to be made for cluster-transfer reactions in an analogous way to how they are performed for single nucleon transfer reactions. It has been particularly useful in the description of breakup channels by treating breakup (emitting a cluster) as an excitation of a cluster to unbound continuum states. A general explanation of how such calculations are performed is given in the following section.

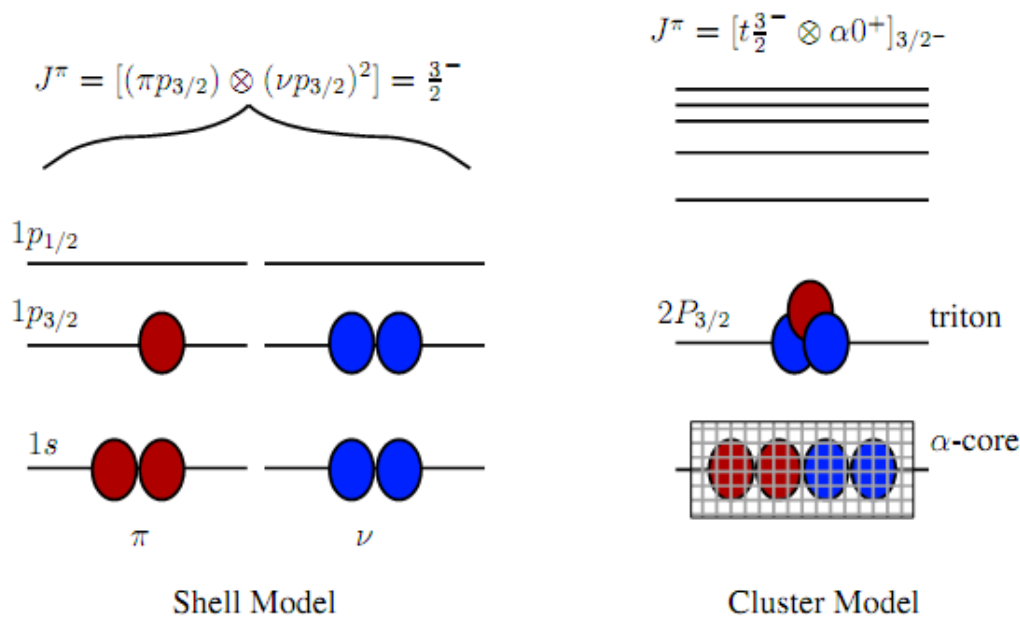


Figure (2-6): Shell and Cluster model pictures of ${}^7\text{Li}$ [51].

(2-8) Shell Model

The nuclear shell model is the first quantum mechanical model of the nucleus. Its name has come from the results of empirical correlation of certain nuclear data. A shell model in which the system is thought to consist of individual particles moving in bound orbits in response to the remainder of the system. Each orbital has a well designated energy angular momentum and parity associated with it [52]. The shell model is suggested in analogy with the electronic structure of the atom. This model is sensitive to nucleon angular momentum. It can predict total angular momentum and parity if valid. The nucleon shells are filled up according to the Pauli principle. This principle results in a finite number of such particles occupying a given energy level and thus leads the concept of closed (filled levels) shell [52]. When a shell is filled any additional particles of that type must be put in a different level (shell).

(2-9) Nuclear Shell Model

The shell model has been among the most successful and widely used microscopic models and as such forms the basis for the theoretical calculations[29]. In some sense the shell structure of nuclei is more complicated than the shell structure of atoms. The shell structure of atoms is due to the Coulomb force between the nucleus and the electrons. It may be a nice coincidence but it is a fact that the Coulomb potential problem in quantum mechanics is an exactly solvable problem [53]. In the case of nuclei the situation is more complicated. The reason is that there is no single source of a central potential. Instead all nucleons are considered to act together generating a mean field. Within this mean field the problem is more tractable [46]. The nuclear shell model has been the foundation upon which almost all of understanding of the structure of the atomic nucleus is based. In this model the nucleus is considered to be a collection of nucleons bound in a common one body potential well interact with each other with some weak effective interaction. This model is simple and very successful but its origin is still not fully understood[54]. This model was originally adopted when

an attempt to describe the nuclear system with the atomic shell structure proved to be successful. The model describes the shelling of the orbits and completing shell of nucleons with increasing energy within nuclear potential. Shell filled in a manner consistent with the Pauli exclusion principle. Each nucleon is treated individually as an independent orbiting particle in a central potential despite the existence of strong interaction between nucleons. The motion of each nucleon is therefore governed by this central potential which is designed to approximate the bulk of individual interactions between nucleons. Each nucleon retains however an individual set of quantum number and wave function[21].

(2-10) Quantum Consideration of the Shell Model

The shell model of the nucleus is based on its analog in atomic physics namely the orbital structure of electrons in complex atoms. The model can account for many crucial nuclear properties and we will therefore review several features of atomic structure before discussing the application to the nuclear domain. As we know the binding of electrons to a nucleus in a complex atom is attributed to the central Coulomb potential. Electron orbits and energy levels for such a quantum system can be obtained by solving the appropriate Schrodinger equation[31]. In general the magic numbers can be explained in terms of the shell model of the nucleus which considers each nucleon to be moving in some potential and classifies the energy levels in terms of quantum numbers nlj . For a central potential the wave function for any nucleon whose coordinates from the centre of the nucleus are given by the form:[31].

$$\Psi_{nlm} = R_{nl}(r)Y_l^m(\theta, \phi) \dots \dots \dots (2-18)$$

Where $R_{nl}(r)$, and $Y_l^m(\theta, \phi)$ are the radial and angular part wave function.

The energy eigen values will depend on the principle quantum number, n and the orbital angular momentum l but are degenerate in the magnetic quantum number m . These energy levels come in ‘bunches’ called “shells” with a large energy gap just above each shell. In their ground state the nucleons fill the available energy levels from the bottom upwards with two protons (neutrons) in each available proton (neutron) energy level. For a central potential the Schrodinger equation can be separated into a radial and an angular part which are

independent of each other. To solve the angular part the orbital angular quantum number, l is introduced through

$$\vec{l}^2 |\Psi_{nlm}\rangle = l(l+1)\hbar^2 |\Psi_{nlm}\rangle \dots \dots \dots (2-19)$$

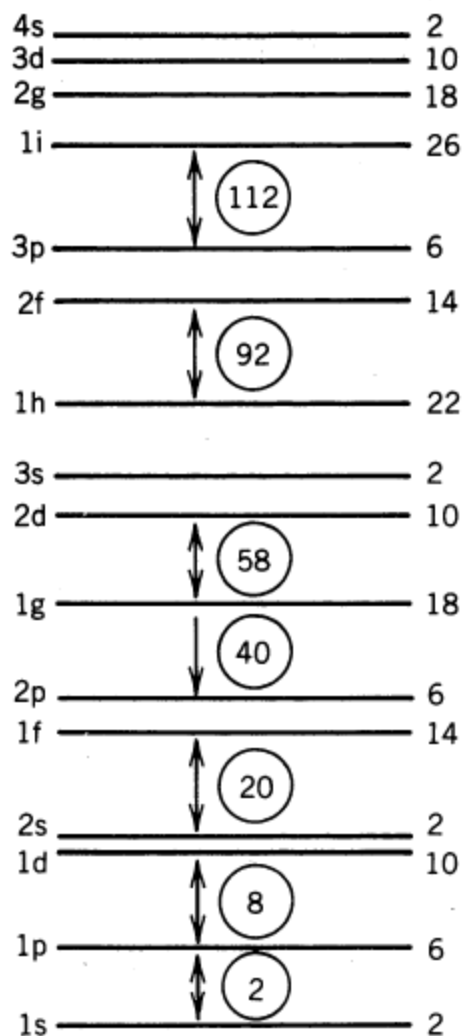
where $\hbar = \frac{h}{2\pi}$, h is the Planck's constant, l can only take integer values denoted s, p, d, etc. corresponding to $l = 0, 1, 2, \dots$ etc. Connected to the orbital angular momentum is the quantum number parity π . It gives the symmetry of a wave function if its space coordinates are changed from $r \rightarrow -r$. The parity is determined by [31].

$$\pi = (-1)^l \dots \dots \dots (2-20)$$

Hence orbitals with an even (odd) orbital angular quantum number have a positive (negative) parity. The orbital angular momentum vector has different orientations in space with respect to the quantisation axis z . The projection of l_z on the z -axis is given by: [31].

$$l_z |\Psi_{nlm}\rangle = m_l \hbar |\Psi_{nlm}\rangle \dots \dots \dots (2-21)$$

Where m_l takes integer values from $-l, \dots, \dots, l$. The protons and neutrons have an intrinsic spin \vec{S} of $\frac{1}{2}$. A simple harmonic potential (i.e. $V(r) \propto r^2$) would yield equally spaced energy levels in figure (2-7) and we would not see the shell structure and hence the magic numbers.



Figure(2-7): Energy levels depending on the harmonic potential [31].

For such a potential it turns out that the lowest level is 1s (i.e. $n = 1$, $l = 0$) which can contain up to 2 protons or neutrons. Then comes 1p which can contain up to a further 6 protons (neutrons). This explains the first 2 magic numbers (2 and 8). Then there is the level 1d, but this is quite close in energy to 2s so that they form the same shell. This allows a further 2+10 protons (neutrons) giving us the next magic number of 20. The next two levels are 1f and 2p which are also quite close together and allow a further 6+14 protons (neutrons). This would suggest that the next magic number was 40 – but experimentally it is known to be 50. The solution to this puzzle lies in the spin-orbit coupling. Spin-orbit coupling interaction between the orbital angular momentum and spin angular momentum. In atomic physics, the origin is magnetic and the effect is a small correction. In the

case of nuclear binding the effect is about 20 times larger and it comes from a term in the nuclear potential itself which is proportional to $L \cdot S$, i.e.

$$V(\vec{r}) \rightarrow V(r) + f(r)L \cdot S \dots \dots \dots (2-22)$$

Where $f(r)$ is the force that coupling of spin and angular momentum .

(2-11) Magic Numbers in Nuclei

The mass is one of the fundamental properties of nuclei and is unique for each of the nearly 3000 known isotopes in the nuclide chart in figure(2-8). More than 90 % of these nuclei are unstable and decay via particle emission. For light nuclei the stable isotopes are arranged near the $N = Z$ line whereas a preference for a neutron excess exists for heavier ones. In all techniques for measuring masses which are used today the achievable precision is directly connected to the observation time which is limited by the half-life of the nuclide of interest [55].

The characteristic gaps between certain numbers of neutrons and protons result

“magic numbers” that require a relatively large amount of energy to excite a nucleon into the next highest orbit. The binding energies predicted by the Binding Energy Model underestimate the actual binding energies of “magic nuclei” for which either the number of neutrons $N = (A - Z)$ or the number of protons, Z is equal to one of the following “magic numbers” as determined experimentally, agreement is only achieved for lighter nuclei as these magic numbers should be .

2, 8, 20, 28, 50, 82, 126.

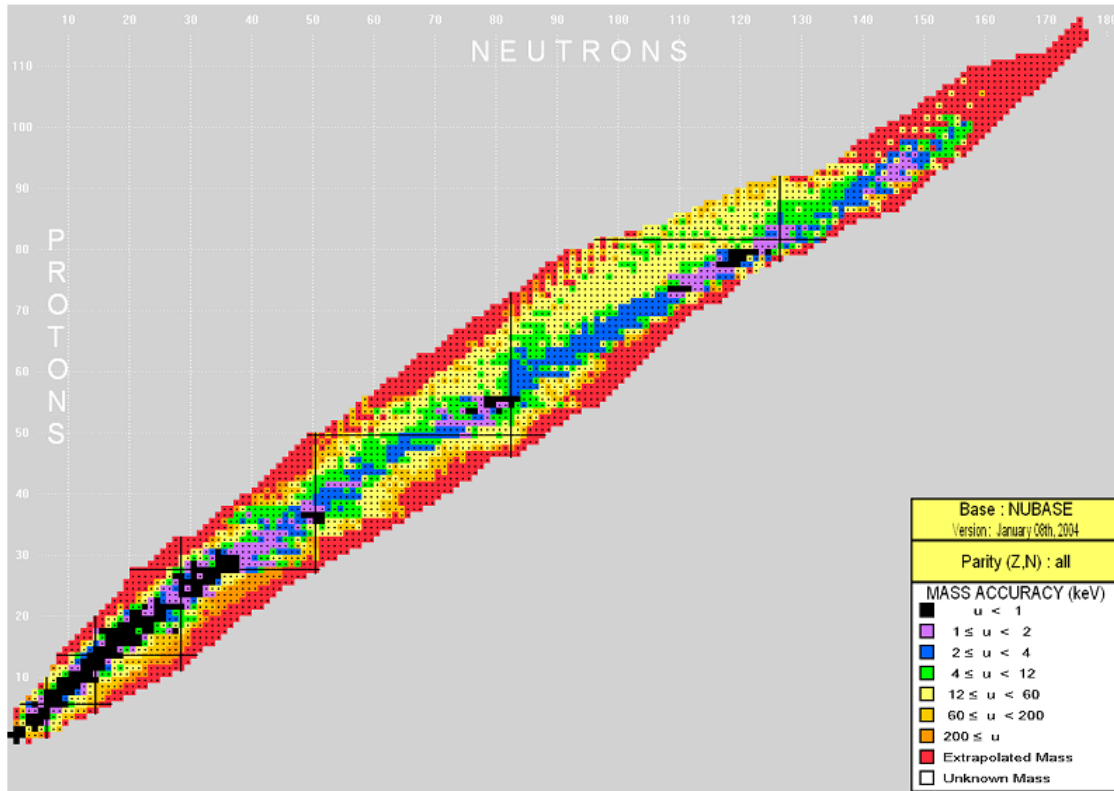


Figure (2-8): The nuclide chart from the Atomic-Mass Evaluation (AME 2003 [56]).

This is particularly the case for “doubly magic” nuclei in which both the number of neutrons and the number of protons are equal to magic numbers. For the harmonic oscillator potential restricting to one type of nucleon, the magic numbers are 2; 8; 20; 40; 70, and 112[57]. There are other special features of magic nuclei:

- 1- The neutron (proton) separation energies (the energy required to remove the last neutron (proton)) peaks if N (Z) is equal to a magic number that's shown in figure(2-9).

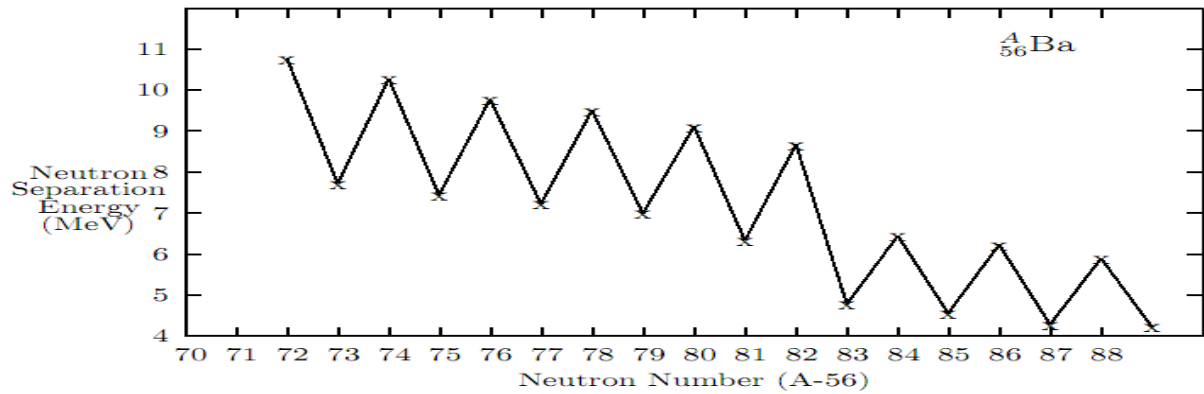
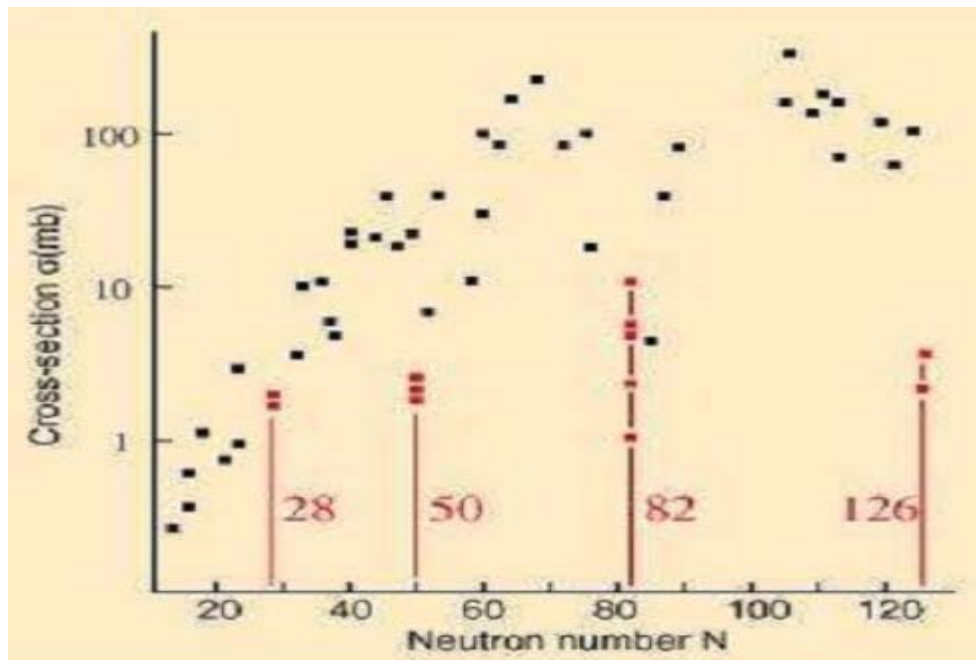


Figure (2-9): Neutron separation energy [57].

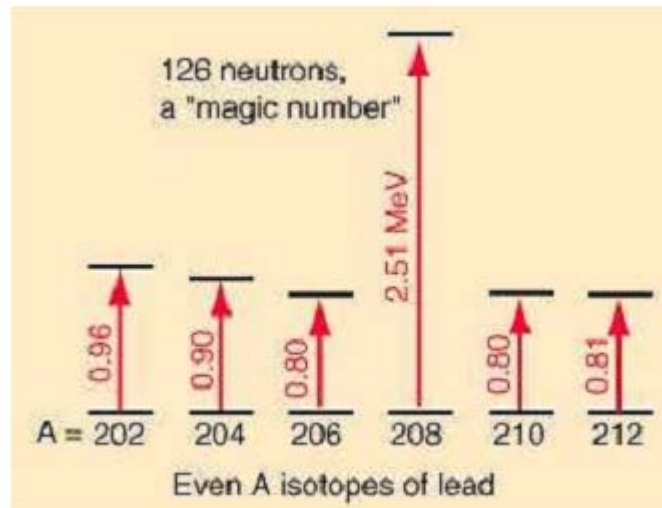
2- There are more stable isotopes if Z is a magic number and more stable isotones if N is a magic number.

3- If N is magic number then the cross-section for neutron absorption is much lower than for other nuclides such that show in figure(2-10).



Figure(2-10): Cross section due to Neutron number [57].

4- The energies of the excited states are much higher than the ground state if either N or Z or both are magic numbers.



Figure(2-11): Excited energy state for magic nuclei[58].

5- Elements with Z equal to a magic number have a larger natural abundance than those of nearby elements[58].

These magic numbers can be explained in terms of the shell model of the nucleus which considers each nucleon to be moving in some potential and classifies the energy levels in terms of quantum numbers .

Maria G. Mayer's discussion of the magic numbers in nuclei has clearly demonstrated the nuclear shell structure associated with the independent-particle model for nuclei [16]. In this model each closed-shell configuration provides a convenient first approximation. In this approximation one can assume that the system under consideration consists of a closed-shell core plus valence particles in a valence shell. This approach very successfully explains the ground state properties of nuclei [16].

(2-12) The Independent-Particle Model

The accumulation of empirical data over the last half century has provided remarkable evidence for the existence of a nuclear shell structure analogous to that observed in atomic shell structure. Systematic changes over proton and neutron numbers such as binding energy neutron and proton separation energies nuclear size, spin and level density indicate closed shells or magic numbers for 2, 8, 20, 28, 50, 82 and 126 neutrons or protons. The nuclear shell structure derives from forces between the neutrons and protons which can be simplified for many purposes in the form of a collectively generated potential. For simplicity let us consider a nucleus with Z protons and N neutrons that interact with two-body forces and obey the time-independent Schrodinger equation as in figure(2-12).

The single particle levels are calculated by solving the 3-D Schrodinger equation:

$$\left(\frac{-\hbar^2}{2m}\nabla^2 + V(r)\right)|\varphi\rangle = E|\varphi\rangle\dots\dots\dots(2-23)$$

where m is the mass of the nucleon, V is the meanfield potential, E is the energy eigen value and r is the distance of the nucleon from the centre of the potential.

where $V(r)$ is the potential and $|\varphi\rangle$ is the wave function that provides the energy eigen value E. By considering a potential given by [60].

$$V(r) = \frac{1}{2}m\omega^2r^2\dots\dots\dots(2-24)$$

where $\frac{1}{2}m\omega^2r^2$ is the potential energy of a particle in a harmonic oscillator with frequency ω and mass m. For a three-dimensional harmonic oscillator the solve Eq.(2-23) give the energy eigen values E_{nl} can be written as [61].

$$E_{nl} = \left(N + \frac{3}{2}\right)\hbar\omega = \left(2n + l + \frac{3}{2}\right)\hbar\omega\dots\dots\dots(2-25)$$

where the harmonic oscillator quantum number is defined by N, the principal quantum number is $n(= 1,2,3, \dots)$ and the orbital angular momentum l is labelled with s, p, d, f, g, h, \dots for values $l = 0,1,2,3,4, \dots$

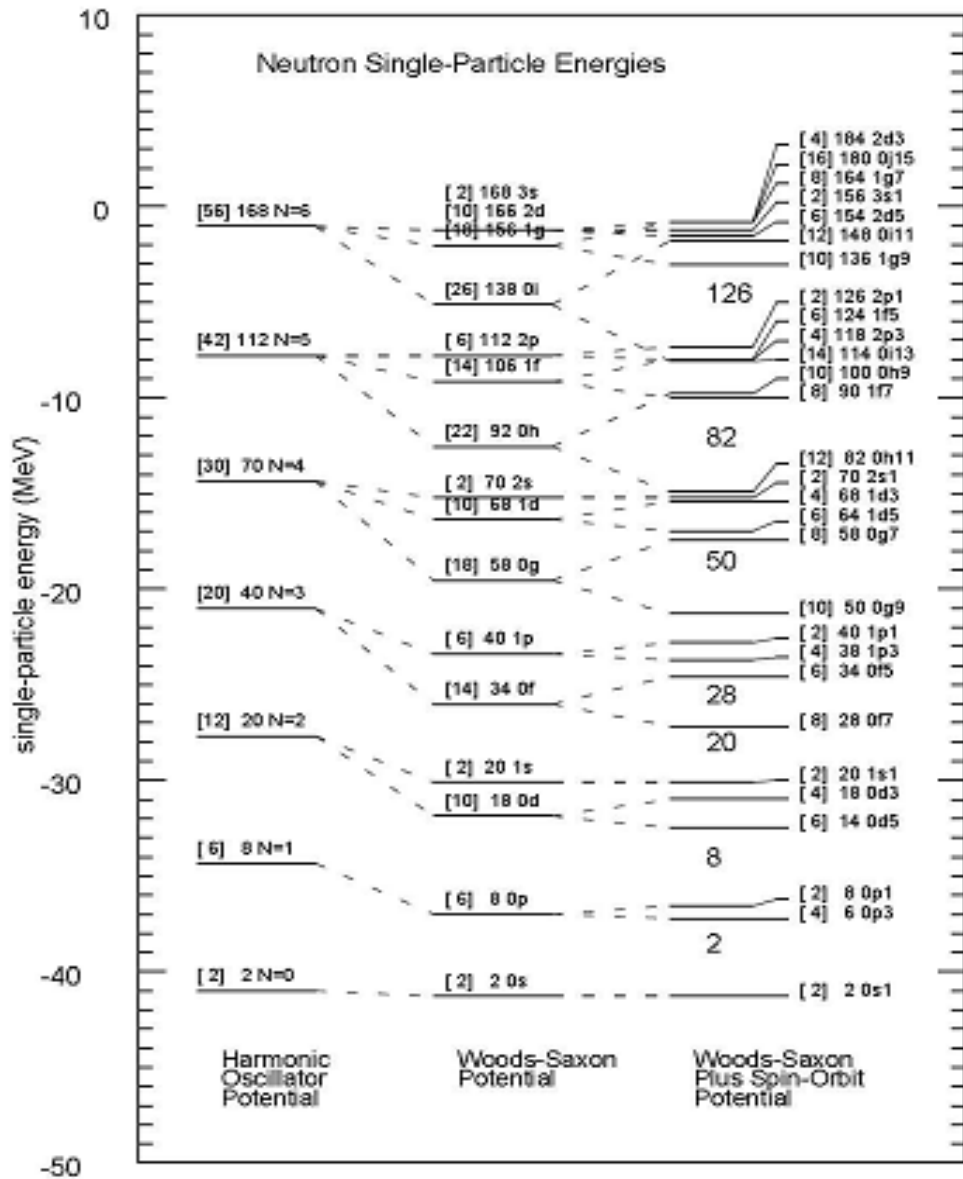


Figure (2-12): Neutron single-particle states in with three different potential for nuclear: harmonic oscillator (left), Woods-Saxon (centre) and Woods-Saxon plus spin-orbit interaction (right) [59].

The left side of figure(2-12), shows the energy of the harmonic oscillator states with a level degeneracy of [61] .

$$D(N) = \frac{1}{2} (N + 1)(N + 2). \dots\dots\dots(2-26)$$

It is clear that the nuclear potential is not accurately represented by the harmonic oscillator since the oscillator levels do not represent the empirically observed magic numbers above N or $Z = 20$. The average nuclear potential arises from the short-range attractive nucleon-nucleon interaction. The nuclear potential can therefore be represented by a function that approximates the nucleon-density distribution which is close to the Woods-Saxon shape [62].

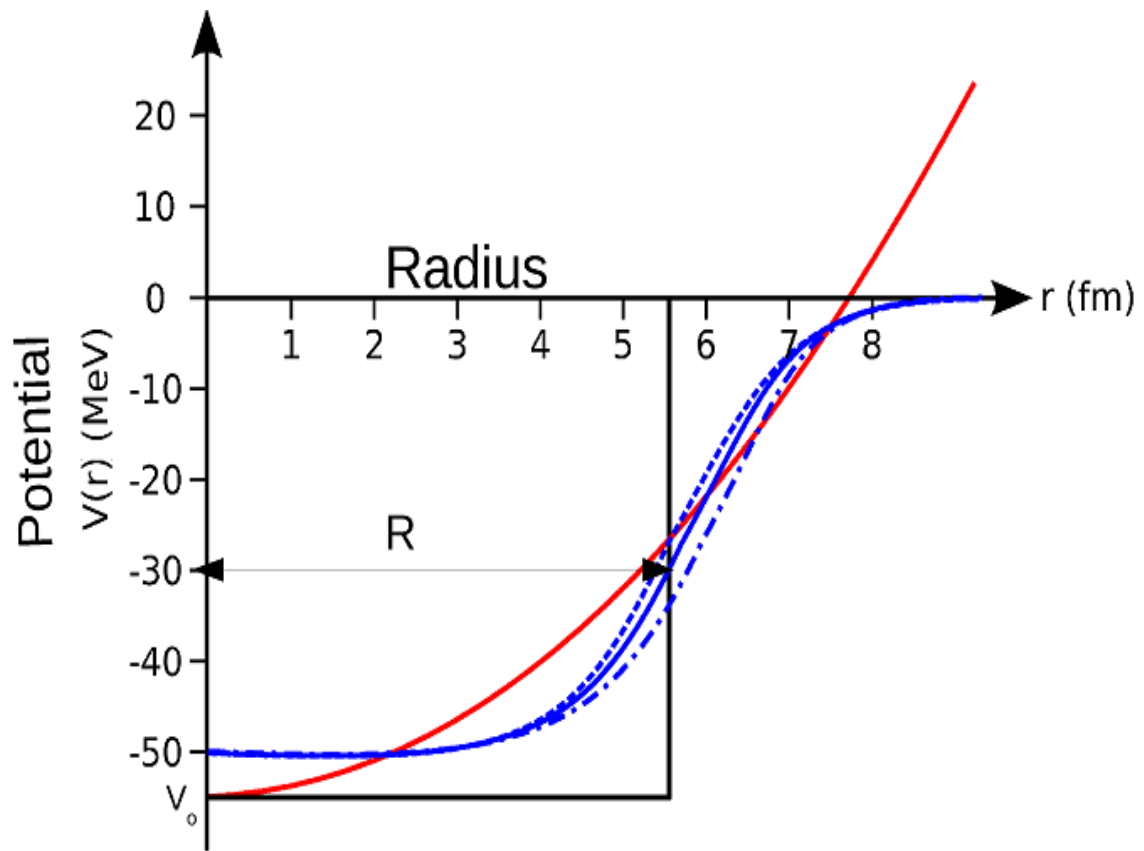


Figure (2-13): A schematic diagram presenting the differences in the shapes of three nuclear potentials. (Red) harmonic oscillator, (black) the finite square well and (blue) the Woods-Saxon potential[46].

A commonly used central potential is the Woods-Saxon potential that given by[63] .

$$V(r) = -V_0 \left[1 + \exp\left(\frac{r-R}{a}\right) \right]^{-1} \dots\dots\dots(2-27)$$

where V_0 is the depth of the potential well, R is the nuclear radius, and a is the skin diffuseness parameter. Typically the depth of the well, V_0 , is 50 MeV and a is 0.55 fm. The size of the well is based on the nuclear radius derived from the Rutherford model of the atom[63].

$$R = r_0 A^{\frac{1}{3}} \dots\dots\dots(2-28)$$

Where A is the mass number of the nucleus and where r is the radial distance from the centre of the potential, a is the parameter that determines how sharply the potential decreases to zero (typically $a \approx 0.55 \text{ fm}$) and R is the radius at which $V(r) = -V_0/2$ where V_0 defines the depth of the potential .

The shape of the Woods-Saxon potential is similar to that formed by the addition of an attractive l^2 term to the harmonic oscillator potential which is occasionally used for analytical simplicity. The middle of figure(2-12) shows the energy of the states calculated with the Woods-Saxon potential such that states with larger angular momentum are lowered. One can see from the middle of figure(2-12) that the degeneracy of levels in the harmonic oscillator is broken. However despite the use of a more physical nuclear potential the empirically observed shell closures are still not reproduced. The successful replication of the magic numbers was achieved with the inclusion of spin-orbit coupling to a square-well potential. This was published simultaneously by Mayer and O. Haxel.

(2-13) The Spin-Orbit Coupling Interaction

Eventually, Mayer in the U.S., and independently Jensen and his co-workers in Germany, concluded that spin had to be involved in explaining the magic numbers above 20. To understand why consider the six 4p and fourteen 4f energy

states at the fourth energy level of the harmonic oscillator model. Clearly the six 4p states cannot produce the eight states of the energy shell needed to explain the next magic number 28. And neither can the fourteen 4f states unless for some reason they split into two different groups whose energy is no longer equal. In nonquantum terms, all fourteen states have orbital and spin angular momentum vectors of exactly the same lengths. One can reproduce the magic numbers, however by introducing spin-orbit coupling term into the single particle Hamiltonian in the form

$$\Delta H \propto -\hat{L} \cdot \hat{S} \dots \dots \dots (2-29)$$

The idea is analogous to atomic spin-orbit coupling where the magnetic moment of an electron interacts with the magnetic field generated by its motion around the nucleus. The strong nuclear spin-orbit interaction term is given by [7].

$$V_{l.s} = f(r)l \cdot s \dots \dots \dots (2-30)$$

Where

$$f(r) = -V_{ls} \frac{\partial V(r)}{\partial r} \dots \dots \dots (2-31)$$

where l and s are the orbital angular momentum and the intrinsic spin vectors of the particle respectively. $V(r)$ is the realistic nuclear potential chosen for the central potential (such as the Woods-Saxon potential) and V_{ls} is a strength constant.

From the spin-orbit coupling theorem one can obtain

$$-l \cdot s |\varphi_j\rangle = -\frac{1}{2} [j(j+1) - l(l+1) - s(s+1)] |\varphi_j\rangle \dots \dots \dots (2-32)$$

where j ; l and s are quantum numbers for the total angular momentum, orbital angular momentum and intrinsic spin. It follows that and the contribution of the spin-orbit term to the energy of the single particle state $|\varphi_{j=l \mp 1/2}\rangle$ is given by the expectation values.

$$\langle \varphi_{j=l+1/2} | -l \cdot s | \varphi_{j=l+1/2} \rangle = -\frac{l}{2} \dots \dots \dots (2-33)$$

$$\langle \varphi_{j=l-1/2} | -l \cdot s | \varphi_{j=l-1/2} \rangle = +\frac{l+1}{2} \dots \dots \dots (2-34)$$

So that orbitals with $j = l + 1/2$ are lower in energy than those with $j = l - 1/2$. This is the converse of the atomic spin-orbit interaction where high- j electron states are increased in energy. The right-hand side of figure(2-12) shows the further lifting of degeneracy by including the spin-orbit interaction with the Woods-Saxon potential. The large energy gaps at N or $Z = 2, 8, 20, 28, 50, 82$ and 126 exactly match the empirically observed magic numbers. The total degeneracy of the single particle levels on the right side of figure (2-12) is given by $2(j + 1)$,

According to the Pauli principle as neutrons or protons are added they go to the lowest unoccupied level. Classically one would expect collisions between nucleons in the nuclear potential but this process is highly suppressed for low-lying states where the nucleons would be scattered into occupied states which is forbidden by the Pauli principle. For even numbers of like nucleons, pairing effect couple nucleons to of angular momentum $J = |J| = \sum_i j_i = 0$, and so for even-even nuclei the spherical shell model predicts nuclear ground states with spin and parity $J^\pi = 0^+$ This is consistent through out all empirical observations. Since even numbers of nucleons contribute $J = 0$, the ground-state angular momentum of an odd mass (spherical) nucleus with a particle (hole) in a shell nlj is equal to j with parity

$$\pi_{tot} = (-1)^{L_{tot}} \dots\dots\dots(2-35)$$

(2-14) Nuclear Energy Levels

The nucleons in the nucleus of an atom like the electrons that circle the nucleus exist in shells that correspond to energy states. The energy shells of the nucleus are less defined and less understood than those of the electrons. There is a state of lowest energy (the ground state) and discrete possible excited states for a nucleus. Where the discrete energy states for the electrons of an atom are measured in eV or keV the energy levels of the nucleus are considerably greater and typically measured in MeV[64].

The shell model works only very well for nuclei with a magic number of protons and neutrons or a valence configuration with only one particle outside the core. But the shell structure of the majority of nuclei in the nuclide chart differ considerable from the theoretical predictions of the shell model. As soon as at least

two particles are outside a closed shell the residual interaction of the Hamiltonian has to be taken into account and will lead to significant changes in the single particle energies. The residual interaction has a short-range character and can therefore be well approximated. It can lead to a further splitting of the single particle energies depending on the structure of the interaction. Figure (2-12) (left) shows the situation for the resulting mixing in the case of two states separated by an energy. The resulting energy shift due to the residual interaction [65]. If residual shell model interactions are neglected each individual nucleon moves independently in a field produced by the other nucleons. However the nuclear shell model includes an attractive potential arising from the short-range interaction between neighbouring nucleons which is directly dependent on the shape of the nuclear distribution [66]. Therefore the shell model is able to treat each nucleon as an independent particle that acts within a mean field of all the rest thus allowing nucleons to occupy the various orbitals within the shells. These fundamental ideas form the basis for the description of nuclear structure within the shell model as well as characterizing the formalism for single-nucleon transfer reactions. To find the eigen values of the Hamiltonian i.e. the energy levels of the nucleus and corresponding eigenvectors one must express the Hamiltonian in matrix form and diagonalize it. More formally the shell model is predicated on the notion that the full nuclear Hamiltonian can be expressed as [66].

$$H = H_i + V \dots \dots \dots (2-36)$$

where V is a residual interaction and H_i is the independent-particle Hamiltonian that is a sum of the single particle Hamiltonians [66].

$$H_i = \sum_i^A h_i \dots \dots \dots (2-37)$$

This concept relies on being able to model the nuclear state is described by a total wave function $\psi(r)$ the solution of the eigenvalue equation can be the product of the eigen functions $\phi(r)$ of the single-particle Schrodinger equation [61].

$$H_i \phi_{ni}(r) = \varepsilon_{ni} \phi_{ni}(r) \dots \dots \dots (2-38)$$

Solving the Schrodinger equation gives wave functions (eigen functions) and the energy eigen values (eigen states) of possible nuclear states that are available for a

system of nucleons. In the shell model the eigen states are obtained by filling the single-particle energy levels while obeying the Pauli principle. Thus the wave function must be antisymmetric with respect to the exchange of coordinates of any pair of nucleons. This can not be fulfilled by a simple product of single particle wave functions. An antisymmetric wave function was given by John Slater and is known as the Slater determinant which is expressed as follows[7].

$$\psi(r) = \frac{1}{\sqrt{N!}} \begin{vmatrix} \phi_{11}(r) & \phi_{12}(r) & \dots & \dots & \dots & \phi_{1m}(r) \\ \phi_{21}(r) & \phi_{22}(r) & \dots & \dots & \dots & \phi_{2m}(r) \\ \phi_{m1}(r) & \phi_{m2}(r) & \dots & \dots & \dots & \phi_{mm}(r) \end{vmatrix} \dots\dots\dots(2-39)$$

where N is the number of nucleons. From here follows that if one tries to put two nucleons in the same quantum state the resulting wave function is zero. The main challenge when using a shell model description is the choice of the one-body potential V(r). Since the nucleons generate the potential, it should have a radial dependence corresponding to the nuclear density. The average potential $U_i(r)$ can be calculated from the nucleon-nucleon interaction [65].

$$U_i(r) = \int V_{if}(r_i - r_f) \rho(r) dr = \sum_f \int \psi_f^*(r) V_{if}(r_i - r_f) \psi_f(r) dr \dots(2-40)$$

Unfortunately to calculate the single particle wave functions for nucleons, one has to know the potential $U_i(r)$ in which they move. But this potential is generated by the same particles. To solve this problem in general a self-consistent variational method like the Hartree-Fock method is used. The shell model potential U, which has to some simple properties:

1. A nucleon close to the center of the nucleus should feel no resulting net force, because all other nucleons are uniformly distributed around this nucleon[57]

$$\left(\frac{\partial U}{\partial r}\right) = 0 \quad \text{at } r = 0 \dots\dots\dots(2-41)$$

2. The nuclear force is short range, which can be for example seen by the fact that nuclei are rather small. So the nuclear binding force has to get stronger going from the surface ($r = R_0$) to the interior of the nucleus:

$$\left(\frac{\partial U}{\partial r}\right) > 0 \quad \text{at } r < R_0 \dots\dots\dots(2-42)$$

3. Because of this short range character of the nuclear force the potential also has to satisfied :

$$U \cong 0 \quad \text{for } r > R_0 \dots \dots \dots (2-43)$$

The values within the level gaps are the calculated magic numbers for the two cases. It should be noted that once the spin-orbit interaction is included the experimentally observed magic numbers are exactly reproduced [67].

(2-15) Single particle energies

The single-particle energies are calculated according to [68].

$$e_{nlj} = \left(2n + l - \frac{1}{2}\right) \hbar\omega + \begin{cases} -\frac{1}{2}(l+1)\langle f(r) \rangle_{nl} \text{ for } j = l - \frac{1}{2} \\ \frac{1}{2}l\langle f(r) \rangle_{nl} \text{ for } j = l + \frac{1}{2} \end{cases} \dots (2-44)$$

With[27] :

$$\langle f(r) \rangle_{nl} \approx 20A^{-\frac{2}{3}} \text{MeV} \dots \dots \dots (2-45)$$

$$\hbar\omega = 45A^{-\frac{1}{3}} - 25A^{-\frac{2}{3}} \dots \dots \dots (2-46)$$

(2-16) Binding and Excitation energies

Binding energy is defined as the amount of energy that must be supplied to a nucleus to completely separate its nuclear particles (nucleons). It can also be understood as the amount of energy that would be released if the nucleus was formed from the separate particles. Binding energy is the energy equivalent of the mass defect. Since the mass defect was converted to binding energy (BE) when the nucleus was formed it is possible to calculate the binding energy using a conversion factor derived by the mass-energy relationship from Einstein's theory of relativity. Einstein's famous equation relating mass and energy is $E = mc^2$

where c is the speed of light ($c = 2.998 \times 10^8$ m/sec). The energy equivalent of 1 amu can be determined by inserting this quantity of mass into Einstein's equation and applying conversion factors. This binding energy depends on the internal structure of the specific nuclei and includes the net effect of all different forces

acting inside. Thus it is possible to investigate the result of the nuclear forces in a many body system by studying the evolution of the mass surface [52].

The discovery of isotopes cleared up the problem of fractional atomic weights and showed that the mass of each atom is close to an integral multiple of a basic atomic mass unit, which is the approximate mass of a nucleon. By international agreement the atomic mass unit is defined as 1/12 of the mass of ^{12}C . The energy equivalent is 931.481 MeV. The atomic mass unit is about 0.8% smaller than the average mass of a nucleon. This means that an energy equivalent to 0.8% of their mass is needed to free nucleons from the nucleus. The energy needed to split up a nucleus completely into free protons and neutrons is called its binding energy.

The binding energy (EB) is given by:

$$E_B = c^2(Zm_H + Nm_n - M)$$

where m_H and m_n are the masses of proton and a neutron respectively.

$$N = A - Z.$$

Nuclear mass data are obtained mainly by mass spectrometry including measurement of mass differences between species with equal mass number.

The relationship $E = mc^2$ has been tested exhaustively in terms of such measurements and its validity confirmed experimentally. Many tabulations of mass excess (ME) and binding energy of nuclides fail to emphasize that nuclear binding energy must be calculated from mass excess on the ^1H rather than ^{12}C mass scale. The conversion of ME on ^{12}C scale to binding energy therefore consists of

$$E_B = -ME + (Zm_p + Nm_n) \text{ -----(2-47)}$$

with $m_p = 7288.696 \text{ keV}$, $m_n = 8071.596 \text{ keV}$ [63] .

The mass is one of the fundamental properties of nuclei and is unique for each of the nearly 3000 known isotopes in the nuclide chart see fig (2-8). More than 90 % of these nuclei are unstable and decay via particle emission. For light nuclei the

stable isotopes are arranged near the $N = Z$ line, whereas a preference for a neutron excess exists for heavier ones.

In all techniques for measuring masses which are used today, the achievable precision is directly connected to the observation time, which is limited by the half-life of the nuclide of interest [69]. Nowadays the most precise measurements of nuclear masses are achieved with penning ion traps [70]. Where the cyclotron frequency of a charged particle inside a magnetic field is determined. One has to distinguish between measurements on stable and on short-lived, radioactive species. For the first ones uncertainties down to a few electron volts or

$\frac{\delta m}{m} < 10^{-10}$ have been obtained [71]. For short-lived nuclei uncertainties in the order of $\frac{\delta m}{m} = 10^{-7} - 10^{-9}$ are achieved. The limiting factors for these measurements are in general the half-life of the ion of interest the yield with which it is produced and possible isobaric contaminations which cannot be separated. Masses of isotopes with half-lives down to a few ms and production rates down to a few ions per second [72] could have been determined. Trap mass spectrometers are placed at many radioactive ion beam facilities [73].

Since Einstein we know of the equivalence of mass and energy in 1905. The mass of a nuclei with N neutrons and Z protons is not only the sum of the masses of the constituent neutrons m_n and protons m_p , it also includes the binding energy EB between them in equation (2-47) :

A nucleus that is in the excited state will not remain at that energy level for an indefinite period. Like the electrons in an excited atom the nucleons in an excited nucleus will transition towards their lowest energy configuration and in doing so emit a discrete bundle of electromagnetic radiation called a gamma ray (γ -ray). The only differences between x-rays and γ -rays are their energy levels and whether they are emitted from the electron shell or from the nucleus.

The ground state and the excited states of a nucleus can be depicted in a nuclear energy-level diagram. The nuclear energy-level diagram consists of a stack of horizontal bars, one bar for each of the excited states of the nucleus. The vertical distance between the bar representing an excited state and the bar representing the ground state is proportional to the energy level of the excited state with respect to

the ground state. This difference in energy between the ground state and the excited state is called the excitation energy of the excited state. The ground state of a nuclide has zero excitation energy. The bars for the excited states are labeled with their respective energy levels [27].

(2-17) Isospin and Isobaric Analogue States

The concept of isospin may be used to distinguish between nuclei which have the same nucleon number A but differ in their proton and neutron numbers Z and N respectively. Within the isospin formalism the proton and the neutron are treated as two states of the same particle the nucleon[74]. The charge independence of the strong nuclear force allows for the general treatment of protons and neutrons as the same particle (the nucleon). However the β -decay process is an electroweak interaction, and does distinguish between these two particles leading to a projection treatment of the nucleon. This two-state degeneracy is analogous to spin and is referred to as isospin. The concept is based on the observation that the strong interaction between nucleons is approximately charge-symmetric and charge-independent. The nucleon is assigned an isospin quantum number t , an isospin t of $\frac{1}{2}$ is defined for each the proton and neutron with the z projection for the neutron $+\frac{1}{2}$ and the proton $-\frac{1}{2}$ effectively treating the neutron and proton as two different states of the same particle with a projection quantum number $T_z = +\frac{1}{2}$ for the neutron state and $T_z = -\frac{1}{2}$ for the proton state [60]. Using this concept the neutron and proton isospin wave functions are [29] :

$$|n\rangle = \left| t = \frac{1}{2}, t_z = +\frac{1}{2} \right\rangle \dots \dots \dots (2-48)$$

$$|p\rangle = \left| t = \frac{1}{2}, t_z = -\frac{1}{2} \right\rangle \dots \dots \dots (2-49)$$

This treatment can be expanded to include systems of several nucleons as well where the isospin coupling follows the same usual rules as ordinary angular momentum [17]. For example, a two-nucleon system can have a total isospin $T = 0$ or 1 , which corresponds to the classical notion of aligned or anti-aligned $t = 1/2$ vectors. For an A -nucleon system the projection of the total isospin is given by [29].

$$T = (N - Z) \dots \dots \dots (2-50)$$

where N and Z are the number of neutrons and protons in the nucleus, respectively. This implies that mirror nuclei i.e. nuclei a and b with $N_a = Z_b$ and $N_b = Z_a$ have opposite signs of T_z ; $T_{z,a} = -T_{z,b}$. The possible values of T depend on the configuration of the system [60]. In nearly all situations the nuclear ground state of any given nucleus has isospin

$$T = |T_z| \dots \dots \dots (2-51)$$

The only exceptions are some odd-odd $N = Z$ nuclei where the pairing energy is large enough to overcome the symmetry energy [76].

CHAPTER

Three

The Mathematical

Model

(3-1) Binding and Excitation Energies

In general the starting point for a theoretical model to describe nuclei in microscopic calculations is always solve the many-body Schrödinger equation with a two -body interaction V_{ik} (a possible 3-body interaction should be neglected) is given by .

$$\frac{-\hbar^2}{2m} \nabla_i^2 \psi(1,2, \dots, A) + V_{ik}(r_i - r_k) \psi(1,2, \dots, A) = E \psi(1,2, \dots, A) \dots (3-1)$$

The nuclear Hamiltonian can invariant to many body system [30].

$$H = T + V = \sum_{i=1}^A \frac{p_i^2}{2m_i} + \sum_{i>k=1}^A V_{ik}(r_i - r_k) \dots (3-2)$$

where m_i is the mass of the nucleon and A is the number of nucleons present (i.e., the mass number) and p_i is the momentum of nucleon .The first term of the Hamiltonian represents the relative the kinetic energy of the nucleons. A two body interaction between the nucleons is described by the second term. As the

nucleon-nucleon interaction is illustrated in figure(3-1) and compare with one body approximation.

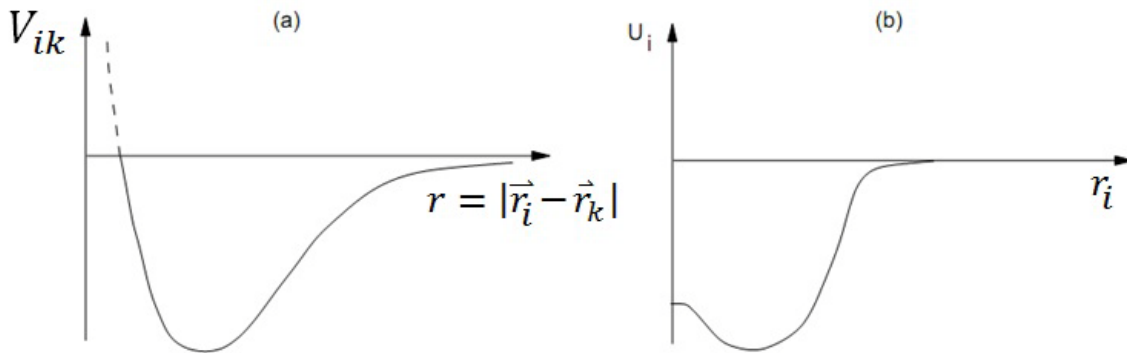


Figure (3-1): (a) The two-body interaction $V_{ik}(r_i - r_k)$ in a nucleus, is repulsive (attractive) at short (long) distances between the nucleons. (b) The average one body potential $U_i(r)$ is used to approximate of the two body interaction[30].

In figure (3-1) the difference between the two potentials is schematically shown. The $V_{ik}(r_i - r_k)$ potential is repulsive at short distances between the two particles, reflecting the behaviour of the strong force. The $U_i(r_i - r_k)$ potential on the other hand is attractive for all distances, inside the nucleus. It also utilizes the short range of the strong force in that the central potential is proportional to the density distribution of the nucleus. The interaction V_{ik} is not known and has to be constructed from theoretical considerations. But even with a known interaction V_{ik} equation (3-2) would have $3A$ position coordinates and would be therefore very difficult to solve especially for larger systems. To compensate for this one can transform the nucleon-nucleon interaction V_{ik} into a nuclear mean field potential $U_i(r_i - r_k)$. It is only an effective potential created by all nucleons inside the core. Equation (3-2) can thus be modified to [30].

$$H = \sum_{i=1}^A \left[\frac{p_i^2}{2m_i} + U_i(r_i - r_k) \right] + \sum_{i>k=1}^A V_{ik}(r_i - r_k) - \sum_{i=1}^A U_i(r_i - r_k) \dots (3-3)$$

where $U_i(r_i - r_k)$ has to be chosen such that residual is only a small perturbation. The average potential $U_i(r_i - r_k)$ can be calculated from the nucleon-nucleon interaction V_{ik} [30]:

$$U_i(r_i - r_k) = \int V_{ik}(r_i - r_k) \rho(r) dr = \sum_k \int \varphi_k^*(r) V_{ik}(r_i - r_k) \varphi_k(r) dr \dots (3-4)$$

Unfortunately to calculate the single particle wave functions $\varphi_k(r)$ one has to know the potential $U_i(r_i - r_k)$ in which they move. But this potential is generated by the same particles. To solve this problem in general a self-consistent variational method like the Hartree-Fock method is used. The basic assumption of the nuclear shell model is that to a first approximation each nucleon moves independently in a potential that represents the average interaction with the other nucleons in a

Chapter Three

nucleus. This independent motion can be understood qualitatively from a combination of the weakness of the long-range nuclear attraction and the Pauli exclusion principle. The complete Schrödinger equation eigen values for A nucleons is given by [46].

$$\hat{H}\psi(1,2,3, \dots, A) = E\psi(1,2,3, \dots, A) \dots \dots \dots (3-5)$$

where \hat{H} is the non relativistic Hamiltonian operator contains single nucleon kinetic energies and two-body interactions[76].

In contrast to the atom no central potential exists a priori in the nucleus. Within the framework of the shell model, it is assumed that such a central potential is created by the nucleons themselves, i.e. the Hamiltonian is split into two parts,

$$\begin{aligned} \hat{H} &= \sum_{i=1}^A \left[\frac{-\hbar^2}{2m} \nabla_i^2 + U(i) \right] + \sum_{i < j = 1}^A W(i, j) - \sum_{i=1}^A U(i) \\ &= \hat{H}^{(o)} + \hat{H}_{res}^{(1)} \dots \dots \dots (3-6) \end{aligned}$$

where $\hat{H}^{(o)}$ is the Hamiltonian of one body potential describes the motion of A nucleons independent of each other in the same average field, $U(i)$ and $\hat{H}_{res}^{(1)}$ are the residual interaction , the smaller the effect of it, the better the assumption of an average independent potential field .

The $W(i, j)$ potential is repulsive at short distances between the two particles, reflecting the behaviour of the strong force. The $U(i)$ potential is attractive for all distances inside the nucleus. It also utilises the short range of the strong force in that the central potential is proportional to the density distribution of the nucleus.

Chapter Three

The residual interactions can be small if a suitable mean field $U(i)$ is chosen and are therefore neglected in the independent particle shell model. In this model the nucleons interact only indirectly via the mean field. In addition they have to obey the Pauli principle. The central potential is usually approximated by a square well, harmonic oscillator or Woods-Saxon potential (see figure 2.1 1). The breakthrough for the shell model was the observation by Goeppert-Mayer and Haxel, Jensen and Suess in 1949 that the interaction between the angular momentum l and the spins s of the nucleons is much more important in the nucleus than for the electrons in an atom. The magnitude of this interaction is of the same order as the shell gaps so it strongly affects the shell structure and must be included in $\widehat{H}^{(o)}$ with an additional term [77].

Inserting of Eq. (3-6) in Eq. (3-5) results.

$$(\widehat{H}^{(o)} + \widehat{H}_{res}^{(1)}) \psi (1,2..A) = \widehat{H}^{(o)} \psi (1,2,..A) + \widehat{H}_{res}^{(1)} \psi (1,2,3, ... A).....(3-7)$$

Under the first order perturbation theory the wave function have been made in

$$\psi(1,2 ..., A) = |\psi^0(1,2 ..., A)\rangle + |\psi^{res}(1,2 ..., A)\rangle.....(3-8)$$

Results to energies .

$$E = E^0 + E^{res}(3-9)$$

Substituting Eq.(3-8) in Eq.(3-7) give zeroth and first order quantity one obtain [78].

$$(\widehat{H}^{(o)} + \widehat{H}_{res}^{(1)})(|\psi^0(1,2 ..., A)\rangle + |\psi^{res}(1,2 ..., A)\rangle) = (E^0 + E^{res})(|\psi^0(1,2 ..., A)\rangle + |\psi^{res}(1,2 ..., A)\rangle)..... (3-10)$$

Then simply to .

Chapter Three

$$\widehat{H}^{(o)}|\psi^0(1,2 \dots, A)\rangle = E^0|\psi^0(1,2 \dots, A)\rangle \dots \dots \dots (3-11)$$

$$\widehat{H}^{(o)}|\psi^{res}(1,2 \dots, A)\rangle + \widehat{H}_{res}^{(1)}|\psi^0(1,2 \dots, A)\rangle = E^0|\psi^{res}(1,2 \dots, A)\rangle + E^{res}|\psi^0(1,2 \dots, A)\rangle \dots \dots \dots (3-12)$$

Multiply Eq.(3-12) by $|\psi^0(1,2 \dots, A)\rangle$ and reformation the result equation , we can get.

$$E^{res} \langle \psi^0(1,2 \dots, A)|\psi^0(1,2 \dots, A)\rangle = \langle \psi^0(1,2 \dots, A)|\widehat{H}_{res}^{(1)}|\psi^0(1,2 \dots, A)\rangle + \langle \psi^0(1,2 \dots, A)|\widehat{H}^{(o)} - E^0|\psi^{res}(1,2 \dots, A)\rangle \dots \dots (3-13)$$

Depending on Eq.(3-10) the second term of Eq.(3-13) vanishes:

$$\langle E^{res} \rangle = \langle \psi^0(1,2 \dots, A)|\widehat{H}_{res}^{(1)}|\psi^0(1,2 \dots, A)\rangle \dots \dots \dots (3-14)$$

when $\widehat{H}^{(o)}$ is Hermitian operator, The energy of state in Eq.(3-9)

$$E = E^0 + E^{res} = \langle \psi^0(1,2 \dots, A)|\widehat{H}^{(o)}|\psi^0(1,2 \dots, A)\rangle + \langle \psi^0(1,2 \dots, A)|\widehat{H}_{res}^{(1)}|\psi^0(1,2 \dots, A)\rangle \dots \dots (3-15)$$

And results

$$E = \sum_{j=1}^A e_{ij} + \langle \psi^0(1,2 \dots, A)|\widehat{H}_{res}^{(1)}|\psi^0(1,2 \dots, A)\rangle \dots \dots \dots (3-16)$$

Here $\sum_{j=1}^A e_{ij}$ is the single particle energies and

$\langle \psi^0(1,2 \dots, A)|\widehat{H}_{res}^{(1)}|\psi^0(1,2 \dots, A)\rangle$ is the residual interaction.

Chapter Three

Due to shell model calculation one assume that a nuclei most be made in term of an inert core of closed shell and extra nucleons in the orbit not occupied by core nucleus. Then the total binding energies are given by[79].

$$E^B(\text{core} + \delta^2) = E_{JT} + E^{B.E}(\text{core}) \dots \dots \dots (3-17)$$

Where E_{JT} is the energy of the residual interaction that given by [80].

$$E_{JT} = \sum_i \varepsilon_i + \sum_{a \leq b, c \leq d} \sum_{JT} V_{JT}(ab; cd) \hat{T}_{JT}(ab; cd) \dots \dots \dots (3-18)$$

here ε_i are the single-particle energies with quantum number i , $V_{JT}(ab; cd)$ is a two-body matrix element, and $\hat{T}_{JT}(ab; cd)$ is the scalar two-body transition density for nucleon pairs (a, b) and (c, d) , each pair coupled to spin quantum numbers JM , and $E^{B.E}(\text{core})$ is the energy of the core that assume and given by[81].

$$E^{B.E}(\text{core}) = 931.5[Zm_H + Nm_n - M(A, Z)] \dots \dots \dots (3-19)$$

Then the total energies is written by

$$E^B(\text{core} + \delta^2) = \sum_i \varepsilon_i + \sum_{a \leq b, c \leq d} \sum_{JT} V_{JT}(ab; cd) \hat{T}_{JT}(ab; cd) + E^{B.E}(\text{core}) \dots (3-20)$$

is employed to account the two body, the residual interaction energy with USD, and the universal potential energies (USDA ,and USDB)

are qualitatively for the mass dependence expected from the evaluation of a medium-range interaction with harmonic oscillator radial wave functions as was done for the original USD. The mass dependence is of the form[82].

$$V_{JT}(j_a j_b; j_c j_d)^A = \left(\frac{18}{A}\right)^{0.3} \left(\langle j_a j_b | V_{1,2}^{Int} | j_c j_d \rangle_{JT=1}\right)^{A=18} \dots \dots \dots (3-21)$$

The excitation energy $E_{Ext}(k)$ of k^{th} excited state follows from the binding energy of the nucleus in that state taken with results respect to the ground state binding energy given by [68].

$$E_{Ext}(k) = E^{B.E}(k) - E^{B.E}(0) \dots\dots\dots(3-22)$$

(3-2) Addition of two Angular Momentums

We concentrate on the coupling of two distinct angular momenta .Specified by suppose one has two particles in one orbit ,which is spin s and isospin T are coupled to $J = j_1 + j_2$ And $T = t_1 + t_2$ With $T = 0$ $T = 1$ since $t_1 = \frac{1}{2}$ a two particale wave function for particles numbered $\psi^0_{j_1 m_1}$ and $\psi^0_{j_2 m_2}$ can be written as aproduct of total angular momentum -dependent part as[46].

$$\Psi_{JM}(j_1, j_2) = \sum_{m_1 m_2} \langle j_1 m_1 j_2 m_2 | JM \rangle \psi^0_{j_1 m_1} \psi^0_{j_2 m_2} \dots\dots\dots(3-23)$$

Such that , we observe that a Clebsch-Gordan coefficient $\langle j_1 m_1 j_2 m_2 | JM \rangle$ vanishes unless[83].

$$M = m_1 + m_2 \dots\dots\dots(3-24)$$

The overlap coefficient going from one basis to the other are called the Clebsch –Gordan coefficient or called Wigner –coefficient (see in Appendix (A))are well-known from angular momentum where they normally are introduced as the overlap between states in a orthonormal basis $\{|j_1 m_1; j_2 m_2\rangle\}$ or $\{|jm\rangle\}$ can then be expanded in the form[84].

$$|jm\rangle = \sum_{m_1 m_2} \langle j_1 m_1; j_2 m_2 | jm \rangle |j_1 m_1; j_2 m_2\rangle \dots\dots\dots(3-25)$$

However, this notation is equivalent to the multiplication by the matrix C written

Chapter Three

element-wise. On the other hand ,we can write Eq.(3-23) using the Clebsch-Gordan coefficients properties in the form[68].

$$\Psi^0_{j_1 m_1} \Psi^0_{j_2 m_2} = \sum_{JM} \langle j_1 m_1 j_2 m_2 | JM \rangle \Psi_{JM}(j_1, j_2) \dots (3-26)$$

The Clebsch-Gordan coefficients are reduce to form relations[85].

$$\langle j_1 m_1 j_2 m_2 | JM \rangle = \left[\frac{(2J+1)(j_1+j_2-J)!(j_1-j_2+J)!(j_2-j_1+J)!}{(j_1+j_2+J+1)!} \right]^{\frac{1}{2}} \times [(j_1 + m_1)! (j_1 - m_1)! (j_2 + m_2)! (j_2 - m_2)! (J + M)! (J - M)!]^{\frac{1}{2}} \times \sum_k (-1)^k k! (j_1 + j_2 - J - k)! (j_1 - m_1 - k)! (j_2 + m_2 - k)! (J + j_2 + m_2 + k)! (J - j_1 - m_2 + k)! \dots (3-27)$$

Where k is the number of nucleons.

From Eq.(3-27)we can find three principle symmetric properties that's mean

$$\begin{aligned} \langle j_1 m_1 j_2 m_2 | JM \rangle &= (-1)^{j_1+j_2-J} \langle j_1 m_2 j_2 m_1 | JM \rangle = \\ &(-1)^{j_1+j_2-J} \langle j_1 -m_1 j_2 - m_2 | J - M \rangle = \\ &(-1)^{j_1-m_1} \left[\frac{(2J+1)}{(2j_2+1)} \right]^{\frac{1}{2}} \langle j_1 m_1 J - M | j_2 -m_2 \rangle \dots (3-28) \end{aligned}$$

This is for single particle state, while for many particle state the wave function may be written as a modified formula shorthand notation that's express by $\Psi_{JM}(j_1, j_2)$ to do Clebsch Gordon coefficient then to construct the state JM from add j_1 and j_2 then we can write .

$$\Psi_{JM}(j(1), j(2)) = \sum_{m \acute{m}} \langle jm \acute{j}m | JM \rangle \Psi^0_{jm}(1) \Psi^0_{\acute{j}m}(2) \dots (3-29)$$

Such that .

$$|j(1) - j(2)| \leq J \leq |j(1) + j(2)| \dots \dots \dots (3-30)$$

That's means J , $j(1)$, and $j(2)$ are coupled to a total diagram defined as [68]

$$\psi_{JM}(j(1), j(2)) = \sum_{m \ m'} \langle jm \ jm' | JM \rangle \psi_{jm}^0(1) \psi_{jm'}^0(2) = j(1) \triangle_{JM} j(2) \dots (3-31)$$

And .

$$\psi_{JM}(j(2), j(1)) = \sum_{m \ m'} \langle jm \ jm' | JM \rangle \psi_{jm}^0(2) \psi_{jm'}^0(1) = j(2) \triangle_{JM} j(1) \dots (3-32)$$

And from Eq.(3-28) we get a results .

$$\psi_{JM}(j(2), j(1)) = (-1)^{j(1)+j(2)-J} \psi_{JM}(j(1), j(2)) \dots (3-33)$$

(3-3) Addition of many Angular Momentum

For a system concentrate on the coupling of three distinct angular momentum, $j_1 m_1$, $j_2 m_2$, and $j_3 m_3$ then the total angular momentum JM is made at many methods one of this we can make a wave function ψ_{JM} refer state from adding $(j_1 + j_2) + j_3$ the describe by [86].

$$\psi_{JM} = [(\psi_{j_1 m_1}^0 \times \psi_{j_2 m_2}^0)_{j_{1,2}} \times \psi_{j_3 m_3}^0]_{JM} \dots \dots \dots (3-34)$$

While if the a wave function ϕ_{JM} refer to state from adding $j_1 + (j_2 + j_3)$ then ϕ_{JM} may be written as

$$\phi_{JM} = [\psi_{j_1 m_1}^0 \times (\psi_{j_2 m_2}^0 \times \psi_{j_3 m_3}^0)_{j_{2,3}}]_{JM} \dots \dots \dots (3-35)$$

Chapter Three

When the $\varphi_{j_i m_i}$ are orthonormal wave function the coupling with angular momentum by Clebach Gordon coefficient by realation .

$$\langle \Psi_{JM} | \varphi_{JM} \rangle = \sum_{m_1 m_2 M_{2,3}} \Psi_{JM} \langle j_1 m_1 j_2 m_2 | J_{1,2} M_{1,2} \rangle \langle J_{1,2} M_{1,2} j_3 m_3 | JM \rangle \times \langle j_2 m_2 j_3 m_3 | J_{2,3} M_{2,3} \rangle \langle j_1 m_1 J_{2,3} M_{2,3} | JM \rangle \varphi_{JM} \dots\dots\dots(3-36)$$

At this point we must inter new coefficient called Racah coefficient that's conection with Clebach Gordan coefficient by [68].

$$R(j_{1,2} j_{2,3}) = [(2j_{1,2} + 1)(2j_{2,3} + 1)]^{\frac{1}{2}} U(j_1 j_2 J j_3; j_{1,2} j_{2,3}) \dots\dots\dots(3-37)$$

Racah coefficient are coupled with 6-j symbols by .

$$\left\{ \begin{matrix} j_1 & j_2 & j_{1,2} \\ j_3 & J & j_{2,3} \end{matrix} \right\} = (-1)^{j_1+j_2+j_3+J} U(j_1 j_2 J j_3; j_{1,2} j_{2,3}) \dots\dots\dots(3-38)$$

On the other hand for adding fourth angular momentum $j_1 m_1, j_2 m_2, j_3 m_3, j_4 m_4$ then we can write the adding by same method .

$$\langle \Psi_{JM} | \varphi_{JM} \rangle = [(2j_{1,2} + 1)(2j_{3,4} + 1)(2j_{1,3} + 1)(2j_{2,4} + 1)]^{\frac{1}{2}} \times \left\{ \begin{matrix} j_1 & j_2 & j_{1,2} \\ j_3 & j_4 & j_{3,4} \\ j_{1,3} & j_{2,4} & J \end{matrix} \right\} \dots\dots\dots(3-39)$$

From above we can knowing evaluation the all posiple of angular momentum state that's results of nucleons out of core. To evaluate the total results of angular momentum to system we can applied that's condation:

- 1- when find same nucleon protons or neutrons at same orbit of single particle state then the angular momentum may be evaluation by.

Chapter Three

$$J = 0, 2, \dots, (2j - 1) \dots \dots \dots (3-40)$$

2-when found same nucleons at different orbit one find in j_1 , and other found in state j_2 , then results of total angular is satisfied selection rule[87].

$$|\hat{j}_1 - \hat{j}_2| \leq J \leq |\hat{j}_1 + \hat{j}_2| \dots \dots \dots (3-41)$$

CHAPTER

Four

Results and

Discussion

(4-1) Introduction

A theoretical study of nuclear structure based on shell model for the binding and excitation energies for the $^{18}_8\text{Ne}_{10}$, $^{30}_{16}\text{S}_{14}$ and $^{30}_{14}\text{Si}_{16}$ nuclei. According to quantum system we derive an expression of binding and excitation energies between two localized quantum states of the nucleons move in configuration model space that describe nucleons move out of the closed shell .

The nuclear structure of low lying is basically defined as a relative to the binding energies and excitation energies for nuclei. It was calculated the expectation values of energies using quantum treatment according to perturbation theory as a results in expressione in Eq. (3-20) and Eq.(3-22) due to the binding energy of closed core and single particles energy and two body matrix element for USD,USDA and USDB potential .

Nuclear shell model calculation have been applied to known the energy level of $^{18}_8\text{Ne}_{10}$, $^{30}_{16}\text{S}_{14}$ and $^{30}_{14}\text{Si}_{16}$ nuclei according to evaluated the binding and excitation energy that more important parameters for nuclear structure studies . Total angular momentum , single particle energies ,two body matrix element potential that associated with the binding energy and excitation energy of nuclei are calculated using a MATLAB program.

(4-2) Closed-Shell Cores

The elementary basis of the nuclear shell model calculation have been assume a closed shell and the other nucleon move in configuration space out of closed shell by building individual nucleons on the cumulative interaction of all of the others which occupy the levels up to the closest shell-closure below. These cumulative states which are magic for protons and neutrons are referred to as cores. Thus the core can be approximated as a closed system which is not open to

interactions with external nucleons. As a theoretical calculation of binding and excitation energies for $^{18}\text{Ne}_{10}$, $^{30}\text{S}_{16}$, and $^{30}\text{Si}_{14}$, we can assume a closed core $^{16}\text{O}_8$ for $^{18}\text{Ne}_{10}$ with 8 neutrons and 8 protons, and $^{28}\text{Si}_{14}$ for $^{30}\text{S}_{16}$, and $^{30}\text{Si}_{14}$ with 14 protons and 14 neutrons alternatively. There are represents the lightest doubly-magic shell-model core as shown in figure (4-1).

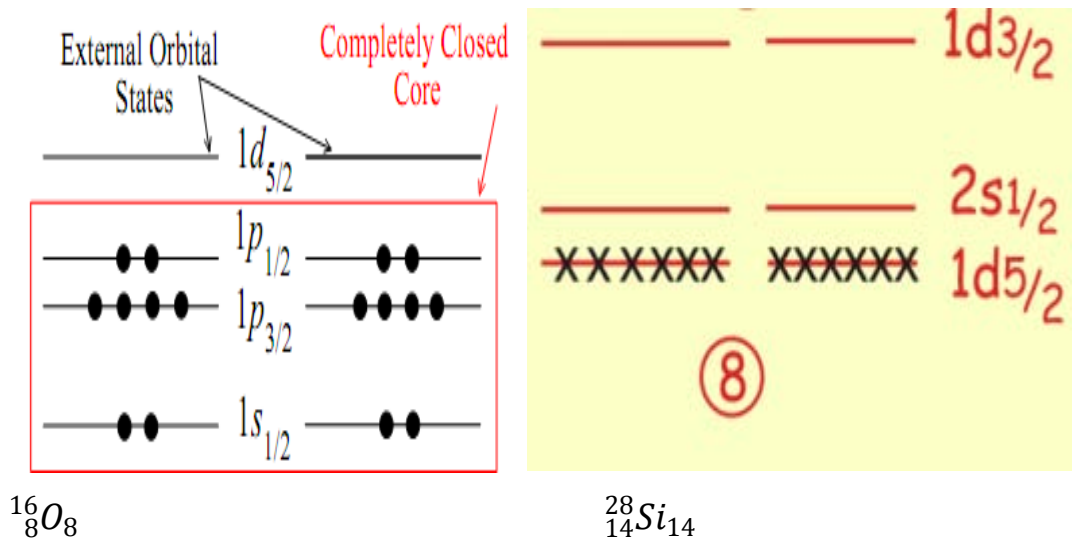


Figure (4-1): The neutron and proton particle configurations for the doubly - magic nucleus $^{16}\text{O}_8$ and $^{28}\text{Si}_{14}$ [29].

Although this is a seemingly gross approximation of what occurs within a realistic nuclear system, there is good evidence to support the theory of nuclear cores. If an additional neutron is introduced into the $^{16}\text{O}_8$ or $^{28}\text{Si}_{14}$ system the structure of the resulting nucleus should thus be determined by the one particle outside of the doubly-magic core. Since the additional neutron is located in the $d_{5/2}$ orbital for $^{17}\text{O}_9$, and $s_{1/2}$ for $^{29}\text{Si}_{14}$ the model predicts a ground state for $^{17}\text{O}_9$ of $\frac{5}{2}+$ (since parity is determined by $(-1)^l$, and $\frac{1}{2}+$ for $^{29}\text{Si}_{14}$ and indeed this is what is observed experimentally.

The states which occur as a result of adding a nucleon above a closed shell are referred to as particle states and similarly states below the closed core which are introduced are known as hole states. Using these two forms of interactions with the closed cores can describe nearly all structure related information within the nuclear-shell model. To first order these reactions can be approximated as one-body interactions that induce changes in the final-state nuclear structure[29].

(4-3) Calculation of The Single Particle Energy

For the shell model calculation, one of the most important parameter for theoretical evaluation and investigation of the binding and excitation energies of nuclei are depending on many important parameters. One of these important parameters is the single particle energies $\epsilon_{1d_{\frac{5}{2}}}$, $\epsilon_{2s_{\frac{1}{2}}}$ and $\epsilon_{1d_{\frac{3}{2}}}$ for s-d shell respectively. In general the term “single-particle” model is used when referring to nuclei whose properties are determined solely by a single neutron or proton. Simple review of the single-particle shell model as detailed down is quite useful in making first-order approximations especially for ground-state spins and parities.

Scenario of shell-model descriptions of the ordering spins and parities of nuclear excited states require sophisticated calculations and have used a variety of available nuclear potentials that include effective interactions. Nevertheless a number of nuclides close to closed shells have been studied and are well described by the single-particle shell model. Unfortunately the term “single particle energy” is used throughout the nuclear structure community to describe several concepts. As a result a division into two categories effective and uncorrelated SPE is necessary. Uncorrelated SPE are defined as the solution to the mean field Hamiltonian in Eq. (3-6). Uncorrelated SPE do not correspond to an experimental

quantity because the single particle picture is only an approximate representation of physical nuclei.

(4-3-1) Calculation of The Single Particle Energies for $^{18}\text{Ne}_{10}$ Nuclei

To the calculated the values of the single particle energies ε_i (MeV) theoretically for the configuration system $1d_{5/2}^2 2s_{1/2}^2 1d_{3/2}^3$, it can be using the spectrum of ^{16}O and ^{17}O with expression of binding energy (3-19). One can illustrated the configuration space of closed core ^{16}O that's showing in figure(4-2).

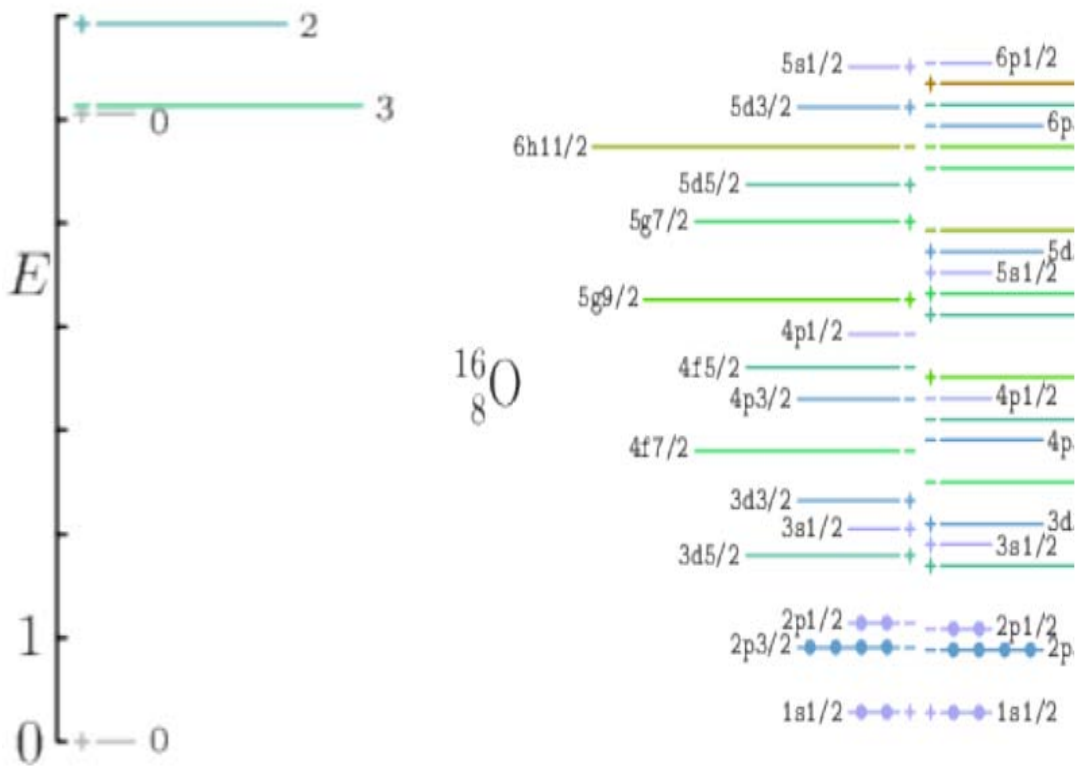


Figure (4-2): Energy levels for doubly-magic oxygen-16

When the nucleus is treated as a core, the Pauli principle prevents particles from moving within the closed system and the $1d_{5/2}$ state is closed to interaction since it is external to the ^{16}O core model space.

Once the fundamental parameters of nuclear structure turn to the arrangement and properties of nuclear excited states. In fact the nuclear shell model calculation have been provides a principle explanation for the origin of nuclear excited states. In a first approximation for perturbation theory methods the nuclear excited states arise from the properties of a few valence nucleons , i.e., those nucleons that lie in unfilled shells. The valence-nucleon concept is illustrated in figure (4-3), which shows the ground and first five excited -state spins and parities of $^{17}_8\text{O}_9$. This nuclide has one neutron outside the doubly-magic $^{16}_8\text{O}_8$ core.

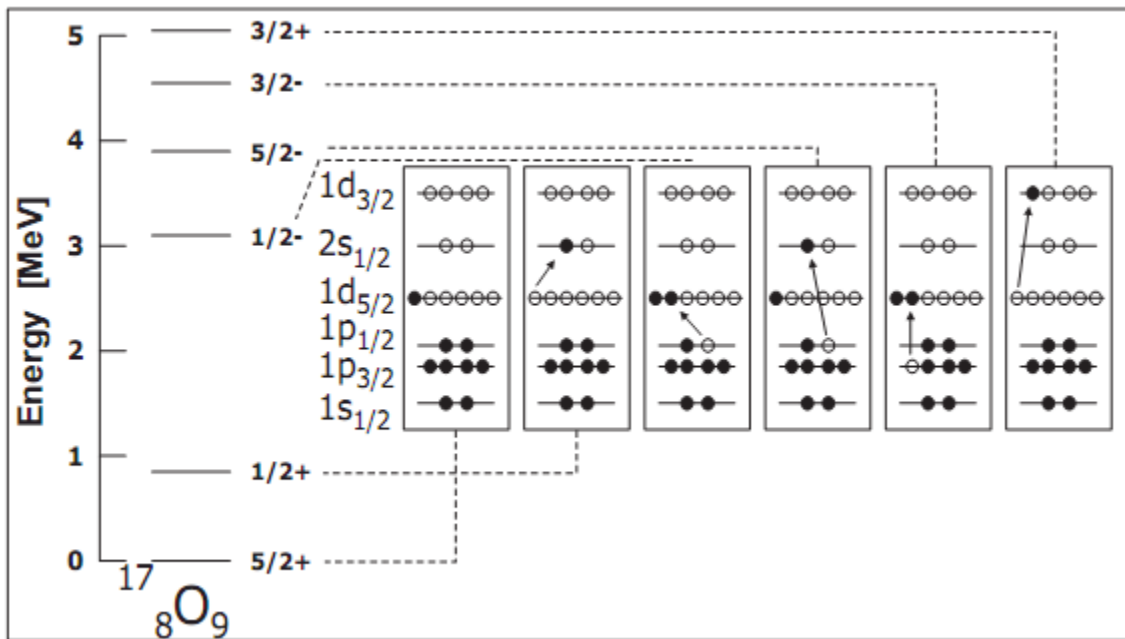


Figure (4-3): Within the shell model the first several excited states in $^{17}_8\text{O}_9$ are explained by the valence neutron configurations.

The spin and parity of $\frac{5}{2}^+$ for the ground state is due entirely to the $1d\frac{5}{2}$ neutron since all other neutrons and all protons in this nucleus are inside closed shells. The ground-state spin comes directly from the total angular momentum of the odd neutron ($J = \frac{5}{2}$); the positive parity is given by $(-1)^\ell$ where the orbital angular momentum value, ℓ , is 2. The first excited state is explained by the promotion of this odd neutron to the $2s\frac{1}{2}$ orbital, and the spin and parity are explained in the same manner as the ground-state spin and parity. Beyond the extreme single-particle picture the third and fourth excited states of $^{17}_8\text{O}_9$ are each produced by the coupling of two unpaired neutrons in separate orbitals ; however these odd-parity states actually result from the mixing of several of these configurations and are more complicated than suggested by the extreme single-particle model .The energies of single particle can be extracted as difference in binding energies between $^{17}_8\text{O}_9$ and $^{16}_8\text{O}_8$ as shown in figure(4-4) .

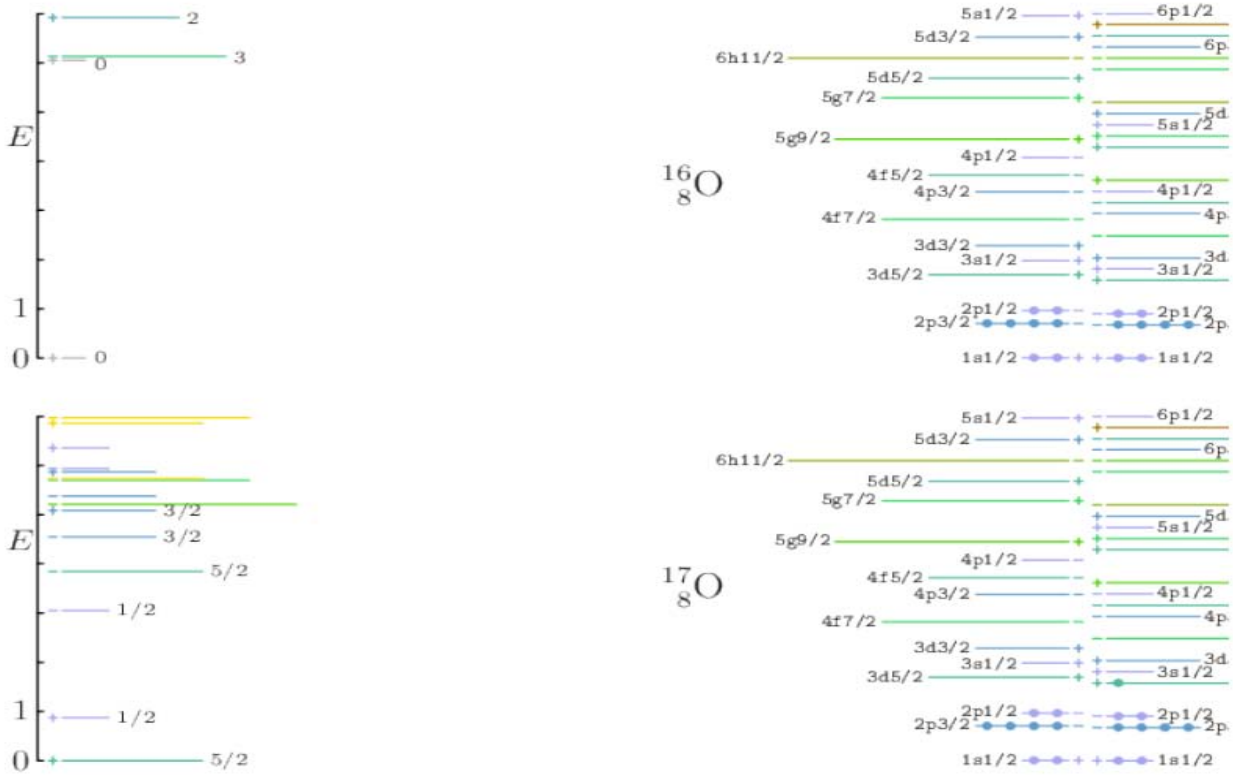


Figure (4-4) : Energy levels for doubly-magic oxygen- $^{16}_8\text{O}_8$ and oxygen- $^{17}_8\text{O}_9$

The ground state of $^{17}_8\text{O}_9$ is supposed to correspond to $0d_{5/2}^5$ configuration while the first two excited states $\frac{1}{2}^+$ and $\frac{3}{2}^+$ can be assumed to contain dominant $1s_{1/2}$ and $0d_{3/2}$ single-particle states respectively.

Thus we have

$$\begin{aligned} \varepsilon_{0d_{5/2}} &= E^{B.E} (^{17}_8\text{O}_9) - E^{B.E} (^{16}_8\text{O}_8) = (-131.762 + 127.619)\text{MeV} \\ &= -4.143\text{MeV} \dots\dots\dots(4-1) \end{aligned}$$

$$\varepsilon_{1s_{1/2}} = \varepsilon_{0d_{5/2}} + E^{B.E} \left(^{17}_8\text{O}_9 \left(\frac{1}{2}^+ \right) \right) = - 3.273\text{MeV} \dots\dots\dots(4-2)$$

$$\varepsilon_{0d_{3/2}} = \varepsilon_{0d_{5/2}} + E^{B.E} \left(^{17}_8\text{O}_9 \left(\frac{3}{2}^+ \right) \right) = - 0.942\text{MeV} \dots\dots\dots(4-3)$$

(4-3-2) Calculation of The Single Particle Energies for ${}^{30}_{16}\text{S}_{14}$ and ${}^{30}_{14}\text{Si}_{16}$ Nuclei

For the binding and excitation energies calculation we can evaluate the values of the single particle energies $\varepsilon_i(\text{MeV})$ by theoretical for the $2s_{\frac{1}{2}}1d_{\frac{3}{2}}$ configuration system. It can be calculated depending on the spectrum of ${}^{28}_{14}\text{Si}_{14}$ and ${}^{29}_{14}\text{Si}_{15}$ according to the binding energy Eq (3-19).

We can derive schematically the configuration space of closed core ${}^{28}_{14}\text{Si}_{14}$ that's shown in figure (4-5).

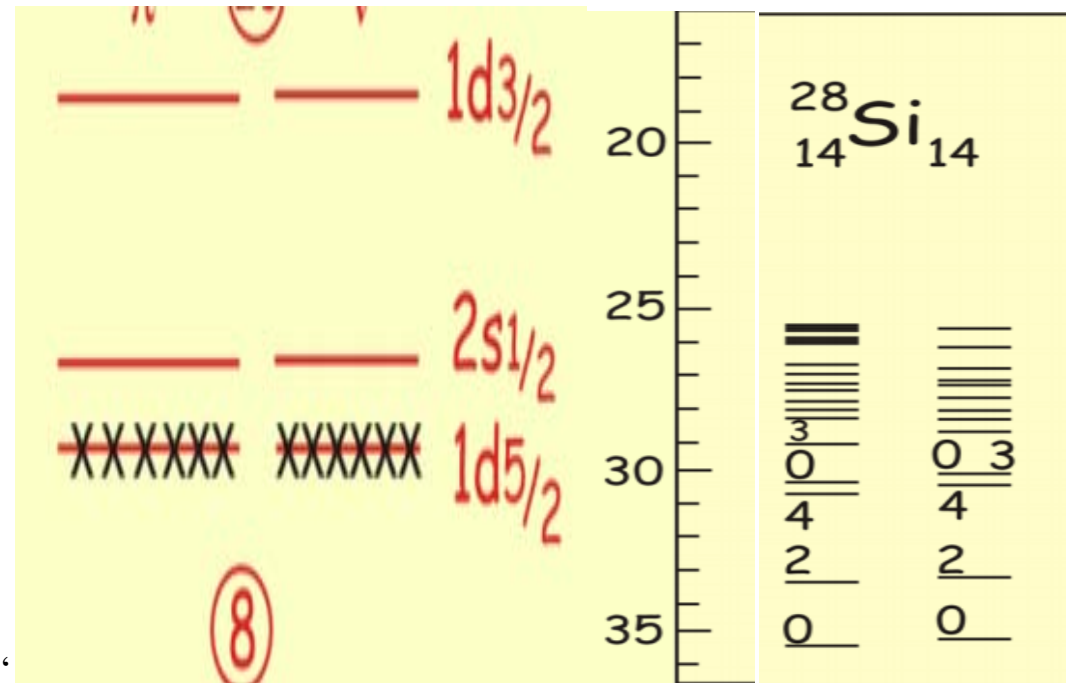


Figure (4-5): Energy levels for doubly-magic ${}^{28}_{14}\text{Si}_{14}$.

The ${}^{28}_{14}\text{Si}_{14}$ nucleus is treated as a core for both ${}^{30}_{16}\text{S}_{14}$ and ${}^{30}_{14}\text{Si}_{16}$, then Pauli principle prevents particles from moving within the closed system and the $1d_{\frac{5}{2}}$ state is closed for 6 nucleons to interaction since it is external to the ${}^{28}_{14}\text{Si}_{14}$ core model space.

For instance, the nuclear shell model calculation have been indicate that the excited states for ${}^{30}_{16}\text{S}_{14}$ and ${}^{30}_{14}\text{Si}_{16}$ arise from a few valence nucleons lie in unfilled shells as shown in the figure (4-6), which shows the ground and excited-state spins and parities of ${}^{29}_{14}\text{Si}_{15}$. This nuclide has two nucleon outside the doubly-magic ${}^{28}_{14}\text{Si}_{14}$ core.

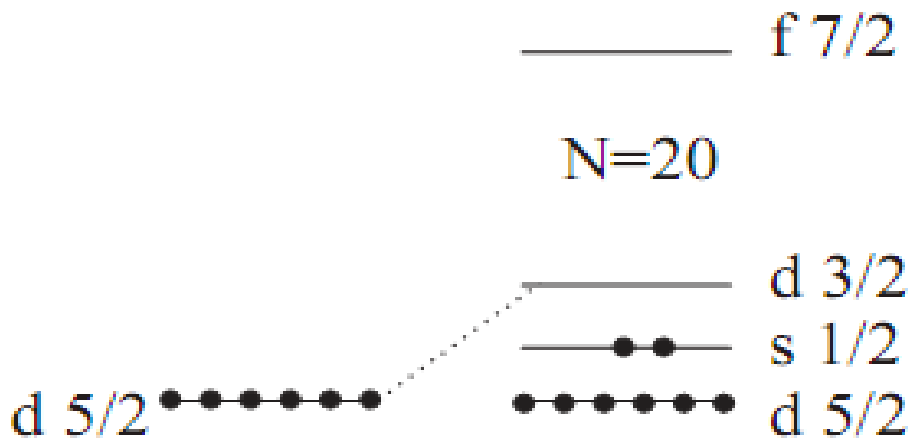


Figure (4-6): The effective single energies for ${}^{30}_{14}\text{Si}_{16}$ [88]

Parity and spin of $\frac{1}{2}^+$ for the ground state is due to the $2s \frac{1}{2}$ nucleon while all the other nucleons (neutrons and all protons) in this nucleus are inside closed shells. The ground-state spin comes directly from the total angular momentum of the odd neutron ($J = 1/2$); the positive parity is given by $(-1)^\ell$ where the orbital angular momentum value ℓ is 0. The first excited state is explained by the promotion of this odd neutron to the $1d \frac{3}{2}$ orbital and the spin and parity are explained in the same manner as the ground-state spin and parity. The upper excited states of ${}^{29}_{14}\text{Si}_{15}$ can be produced by the coupling of two unpaired nucleons in separate orbitals.

On the other addition the odd-parity states produced as a results from the mixing of several of these. The ground state of $^{29}_{14}\text{Si}_{15}$ is supposed to correspond to $0d_{\frac{5}{2}}$ configuration while the first two excited states $\frac{1}{2}+$ and $\frac{3}{2}+$ can be assumed to contain dominant $1s_{\frac{1}{2}}$ and $0d_{\frac{3}{2}}$ single-particle states respectively. The energies of single particle can be extracted as difference in binding energies between $^{29}_{14}\text{Si}_{15}$ and $^{28}_{14}\text{Si}_{14}$ thus we have [68].

$$\begin{aligned} \varepsilon_{2s_{\frac{1}{2}}} &= E^{B.E}(^{29}_{14}\text{Si}_{15}) - E^{B.E}(^{28}_{14}\text{Si}_{14}) = (-245.02 + 236.54)\text{MeV} \\ &= -8.48\text{MeV} \dots\dots\dots(4-4) \end{aligned}$$

And[4].

$$\varepsilon_{1d_{\frac{3}{2}}} - \varepsilon_{2s_{\frac{1}{2}}} = 1.27 \text{ MeV} \dots\dots\dots(4-5)$$

$$\varepsilon_{1d_{\frac{3}{2}}} = \varepsilon_{2s_{\frac{1}{2}}} + 1.27 \text{ MeV} \dots\dots\dots(4-6)$$

Results

$$\varepsilon_{1d_{\frac{3}{2}}} = - 7.21 \text{ MeV} \dots\dots\dots(4-7)$$

(4-4)Calculation of the Binding Energy

The binding energy are very important parameter to the nuclear astrophysicists to determine Q-values reaction and decays. The perturbation theory approximation method has been used to employed the binding energies in the present work to study the energy levels. The binding energies are calculated depending on the formalism in Eq.(3-20)due to the two body matrix element and single particle energies for nuclei that assume to be described by an inert closed shell core and two nucleons in S-D shell model.

(4-4-1) Calculation of the Binding Energy for $^{18}\text{Ne}_{10}$ Nuclei

Theoretical calculation and investigation of the binding energy for $^{18}\text{Ne}_{10}$ nuclei is depending on many important parameters :core binding energy, single particle energy and two body matrix element .However $^{18}\text{Ne}_{10}$ nuclei is describe by the closed inert core $^{16}\text{O}_8$ and two protons move at $1d_{\frac{5}{2}}2S_{\frac{1}{2}}1d_{\frac{3}{2}}$ cotionfiguration space . The binding energies of the core $^{16}\text{O}_8$ is calculated from Eq.(3-19) with mass number are $M(^{16}\text{O}_8) = (15.9949146221) \text{amu}$, $M(^1_0n^1)=(1.008665)\text{amu}$ and $M(p)=(1.007825) \text{amu}$ for neutron and proton respectively[88] .The binding energies is(-127.62017MeV). The configuration model space $\langle 1d_{\frac{5}{2}}2S_{\frac{1}{2}}1d_{\frac{3}{2}} \rangle$ can be describe in the representation (J^π, T) combination $(5^+,0)$,(4⁺,1), $(3^+,0)$, $(2^+,1)$, $(1^+,0)$ and $(0^+,1)$ for $|1d_{\frac{5}{2}}\rangle$, $(1^+,0)$ and $(0^+,1)$ for $|2S_{1/2}\rangle$, $(3^+,0)$, $(2^+,1)$, $(1^+,0)$ and $(0^+,1)$ for $|1d_{\frac{3}{2}}\rangle$. $(3^+,1)$, $(3^+,0)$, $(2^+,1)$, and $(2^+,0)$ for $|1d_{\frac{5}{2}}2S_{\frac{1}{2}}\rangle$, $(4^+,0)$,(4⁺,1), $(3^+,1)$, $(3^+,0)$, $(2^+,1)$, $(2^+,0)$, $(1^+,0)$ and $(1^+,1)$ for $|1d_{\frac{5}{2}}1d_{\frac{3}{2}}\rangle$ and $(2^+,1)$, $(2^+,0)$, $(1^+,0)$, and $(1^+,1)$ for $|2S_{1/2}1d_{3/2}\rangle$ and allowed for the two neutrons moving in configuration space.

Next the another important parameters used in shell-model calculation is two body effective interaction matrix element at $1d_{\frac{5}{2}}2S_{\frac{1}{2}}1d_{\frac{3}{2}}$ configuration space and derived microscopically that's shown in table(4-1) for the USD ,USDA and USDB potential .

Table (4-1): The two body matrix element interactions by using USD, USDA and USDB potential (are given in MeV) . The shell-model orbits are labeled $1 \cong 1 d_{\frac{3}{2}}$, $2 \cong 1 d_{\frac{5}{2}}$ and $3 \cong 2 s_{\frac{1}{2}}$ [82].

j_1	j_2	j_3	j_4	2J	2T	USDA	USDB	USD
2	2	3	3	1	0	-0.8900	-0.5344	-1.1756
2	1	2	1	1	0	-6.5106	-6.0099	-6.5058
2	1	1	1	1	0	0.0136	0.1922	0.5647
2	1	1	3	1	0	1.5511	1.6231	-1.7080
2	1	3	3	1	0	1.9021	2.0226	2.1042
1	1	1	1	1	0	-1.4927	-1.6582	-1.4151
1	1	1	3	1	0	-1.0014	-0.8493	0.3983
1	1	3	3	1	0	0.0949	0.1574	0.0275
1	3	1	3	1	0	-3.8051	-4.0460	-4.2930
1	3	3	3	1	0	-0.6655	-0.9210	1.2501
3	3	3	3	1	0	-3.8693	-3.7093	-3.2628
2	1	2	1	2	0	-4.5452	-4.2117	-3.8253
2	1	2	3	2	0	-1.0254	-0.6464	0.0968
2	1	1	3	2	0	-1.2803	-0.4429	0.2832
2	3	2	3	2	0	-0.4874	-0.3154	-1.4474

Table (4-1): (Continued)

j_1	j_2	j_3	j_4	2J	2T	USDA	USDB	USD
2	3	1	3	2	0	-2.5947	-2.5110	-1.9410
1	3	1	3	2	0	-1.753	-1.8504	-1.8194
2	2	2	2	3	0	-1.4018	-1.6651	-1.5012
2	2	2	1	3	0	2.2427	2.3102	2.2216
2	2	2	3	3	0	-1.7954	-1.2167	-0.8616
2	2	1	1	3	0	0.9812	1.1792	1.8949
2	1	2	1	3	0	-1.2963	-1.2124	-0.5377
2	1	2	3	3	0	0.8962	1.2526	1.2032
2	1	1	1	3	0	1.8985	1.4300	2.0334
2	3	2	3	3	0	-3.9337	-4.1823	-3.8598
2	3	1	1	3	0	0.4599	0.0968	0.1887
1	1	1	1	3	0	-2.9800	-2.9660	-2.8842
2	1	2	1	4	0	-4.4652	-4.6189	-4.5062
2	2	2	2	5	0	-4.3811	-4.3205	-4.2256
2	2	2	2	0	1	-2.4796	-2.5598	-2.8197
2	2	1	1	0	1	-3.5693	-3.1025	-3.1856
2	2	3	3	0	1	-1.1572	-1.5602	-1.3247
1	1	1	1	0	1	-1.505	-1.8992	-2.1845
1	1	3	3	0	1	-0.9834	-1.0150	-1.0835
3	3	3	3	0	1	-1.8461	-1.6913	-2.1246
2	1	2	1	1	1	0.2510	0.6556	1.0334
2	1	1	3	1	1	0.0736	-0.0456	0.1874
1	3	1	3	1	1	0.3105	0.5158	0.6066
2	2	2	2	2	1	-0.9899	-1.0007	-1.0020
2	2	2	1	2	1	-0.3092	-0.2137	-0.2828
2	2	2	3	2	1	-0.7746	-0.9317	-0.8616
2	2	1	1	2	1	-1.1335	-1.2187	-1.6221

Table (4-1): (Continued)

j_1	j_2	j_3	j_4	2J	2T	USDA	USDB	USD
2	2	1	3	2	1	0.8901	0.8866	-0.6198
2	1	2	1	2	1	0.2248	-0.1545	-0.3248
2	1	2	3	2	1	0.1022	-0.3147	-0.4770
2	1	1	1	2	1	-0.5208	-0.5032	-0.6149
2	1	1	3	2	1	0.2811	0.3713	-0.5247
2	3	2	3	2	1	-0.9039	-0.9405	-0.8183
2	3	1	1	2	1	-0.5542	-0.3173	-0.4041
2	3	1	3	2	1	1.7072	1.6131	-1.9410
1	1	1	1	2	1	-0.1570	-0.0974	-0.0665
1	1	1	3	2	1	0.1368	0.3494	-0.5154
1	3	1	3	2	1	-0.2533	-0.3034	-0.4064
2	1	2	1	3	1	0.4777	0.7673	0.5894
2	1	2	3	3	1	-0.4507	-0.5525	0.6741
2	3	2	3	3	1	0.6470	0.6841	0.7626
2	2	2	2	4	1	-0.2136	-0.2069	-0.1641
2	2	2	1	4	1	-1.3155	-1.3349	-1.2363
2	1	2	1	4	1	-1.2509	-1.4447	-1.4497

The two body effective interaction matrix element is the energy required to interaction at the configuration space system . It is important to evaluate the binding energies . It can be calculated theoretically using Eq.(3-21),results are shown in table(4-2) .

Table(4-2):Results of the two body matrix element for $^{18}\text{Ne}_{10}$ using USD,USDAand USDB interaction.

J_a	J_b	J_c	J_d	J^π	T	$\langle j_a j_b V^{USDA} j_c j_d \rangle$	$\langle j_a j_b V^{USDB} j_c j_d \rangle$	$\langle j_a j_b V^{USD} j_c j_d \rangle$
5/2	5/2	5/2	5/2	5+	0	-4.3811	-4.3205	-4.2256
5/2	5/2	5/2	5/2	4+	1	-0.2136	-0.2069	-0.1641
5/2	5/2	5/2	5/2	3+	0	-1.4018	-1.6651	-1.5012
5/2	5/2	5/2	5/2	2+	1	-0.9899	-1.0007	-1.0020
5/2	5/2	5/2	5/2	1+	0			
5/2	5/2	5/2	5/2	0	1	-2.4796	-2.5598	-2.8197
1/2	1/2	1/2	1/2	0	1	-1.8461	-1.6913	-2.1246
1/2	1/2	1/2	1/2	1	0	-3.8693	-3.7093	-3.2628
3/2	3/2	3/2	3/2	3	0	-2.9800	-2.9660	-2.8842
3/2	3/2	3/2	3/2	2	1	-0.1570	-0.0974	-0.0885
3/2	3/2	3/2	3/2	1	0	-1.4927	-1.6582	-1.4151
3/2	3/2	3/2	3/2	0	1	-1.505	-1.8992	-2.1845
5/2	1/2	5/2	1/2	3	1	0.6470	0.6841	0.7626
5/2	1/2	5/2	1/2	3	0	0.4599	0.0968	0.1884
5/2	1/2	5/2	1/2	2	0	-0.4874	-0.3154	-1.4474
5/2	1/2	5/2	1/2	2	1	-0.9039	-0.9405	-0.8183
5/2	3/2	5/2	3/2	4	0	-4.4652	-4.6189	-4.5062
5/2	3/2	5/2	3/2	4	1	-1.2509	-1.4447	-1.4497
5/2	3/2	5/2	3/2	3	0	-1.2963	-1.2124	-0.5377
5/2	3/2	5/2	3/2	3	1	0.4777	0.7693	0.5894

5/2	3/2	5/2	3/2	2+	0	-4.5452	-4.2117	-3.8253
5/2	3/2	5/2	3/2	2+	1	0.2248	-0.1545	-0.3248
5/2	3/2	5/2	3/2	1+	0	-6.5106	-6.0099	-6.5058
5/2	3/2	5/2	3/2	1+	1	0.2510	0.6556	1.0334
1/2	3/2	1/2	3/2	2+	1	-0.2533	-0.3034	-0.4046
1/2	3/2	1/2	3/2	2+	0	-1.753	-1.8504	-1.8194
1/2	3/2	1/2	3/2	1+	0	-3.8051	-4.0460	-4.2930
1/2	3/2	1/2	3/2	1+	1	0.3105	0.5158	0.6066

Depending on the evaluation of single particle energy from Eqs(4-1) to (4-3) according to experimental results of binding energies of nucleus $^{16}_8\text{O}_8$ and $^{17}_8\text{O}_9$ respectively, we can be calculate the binding energy for $^{18}_8\text{Ne}_{10}$ nuclei by using Eq.(3-20) with a Matlab program and substituting the values of single particles energies $\varepsilon_{0d_{\frac{5}{2}}} = -4.143\text{MeV}$, $\varepsilon_{1s_{\frac{1}{2}}} = -3.273\text{MeV}$, and $\varepsilon_{0d_{\frac{3}{2}}} = -0.942\text{MeV}$ from Eqs.(4-1 to 4-3), and two body effective interaction from table(4-2) with core binding energies -127.62017MeV , results of data for binding energies have been summarized in table (4-3) for $^{18}_8\text{Ne}_{10}$.

Table(4-3):Results of the binding energy B.E(MeV) for $^{18}\text{Ne}_{10}$ that calculated with USD,USDA,and USDB potential .

Configuration	J^π T	Binding Energy (B.E)(Mev)		
		USDA	USDB	USD
$(1d\ 5/2)^2$	5+ 0	-140.3012	-140.2406	-140.1457
$(1d\ 5/2)^2$	4+ 1	-136.1337	-136.1270	-136.0842
$(1d\ 5/2)^2$	3+ 0	-137.3219	-137.5852	-137.4213
$(1d\ 5/2)^2$	2+ 1	-136.9100	-136.9208	-136.9221
$(1d\ 5/2)^2$	1+ 0	-137.0124	-137.2468	-137.5522
$(1d\ 5/2)^2$	0+ 1	-138.3997	-138.4799	-138.7398
$(2S1/2)^2$	0+ 1	-136.0262	-135.8714	-136.3047
$(2S1/2)^2$	1+ 0	-138.0494	-137.8894	-137.4429
$(1d\ 3/2)^2$	3+ 0	-128.7201	-128.7061	-128.6243
$(1d\ 3/2)^2$	2+ 1	-125.8971	-125.8375	-125.8066
$(1d\ 3/2)^2$	1+ 0	-127.2328	-127.3983	-127.1553
$(1d\ 3/2)^2$	0+ 1	-127.2451	-127.6393	-127.9247
$1d_{5/2}2S_{1/2}$	3+ 1	-141.8331	-141.7960	-141.7175
$1d_{5/2}2S_{1/2}$	3+ 0	-142.0202	-142.3833	-142.2917
$1d_{5/2}2S_{1/2}$	2+ 0	-142.9675	-142.7955	-143.9275
$1d_{5/2}2S_{1/2}$	2+ 1	-143.3840	-143.4206	-143.2984
$1d_{5/2}\ 1d\ 3/2$	4+ 0	-138.5053	-138.6590	-138.5463
$1d_{5/2}\ 1d\ 3/2$	4+ 1	-135.2910	-135.4848	-135.4898
$1d_{5/2}\ 1d\ 3/2$	3+ 1	-133.5624	-133.2728	-133.4507
$1d_{5/2}\ 1d\ 3/2$	3+ 0	-135.3304	-135.2525	-134.5778
$1d_{5/2}\ 1d\ 3/2$	2+ 1	-133.8153	-134.1946	-134.3649

$1d_{5/2} 1d_{3/2}$	2+ 0	-138.5853	-138.2618	-137.8654
$1d_{5/2} 1d_{3/2}$	1+ 0	-140.5507	-140.0500	-140.5459
$1d_{5/2} 1d_{3/2}$	1+ 1	-133.7891	-133.3845	-133,0067
$2S_{1/2} 1d_{3/2}$	2+ 1	- 134.0531	- 134.1505	- 134.1195
$2S_{1/2} 1d_{3/2}$	2+ 0	- 132.5534	- 132.6035	- 132.7065
$2S_{1/2} 1d_{3/2}$	1+ 0	- 136.1052	- 136.3461	- 136.5931
$2S_{1/2} 1d_{3/2}$	1+ 1	- 131.9896	- 131.7843	- 131.6935

(4-4-2) Calculation of the Binding Energy for $^{30}_{16}\text{S}_{14}$ Nuclei

For configuration space $\langle 2S_{1/2} 1d_{3/2} \rangle$ with a stable closed core $^{28}_{14}\text{Si}_{14}$, the binding energy at the low -lying states for $^{30}_{16}\text{S}_{14}$ nuclei can be calculated using Eq.(3-20). The two nucleon have been move at the configuration model space $\langle 2S_{1/2} 1d_{3/2} \rangle$ that's allow us illustrated at larger representation (J^π, T) for the Sd-shell nuclei. The configuration model space $\langle 2S_{1/2} 1d_{3/2} \rangle$ had been represented by (J^π, T) combination, results $(0^+, 1)$ and $(1^+, 0)$ for pure state $| 2S_{1/2} \rangle$, $(2^+, 1)$, $(2^+, 0)$, $(1^+, 0)$, $(1^+, 1)$ and $(0^+, 1)$ for mixed state $| 2S_{1/2} 1d_{3/2} \rangle$ and $(3^+, 0)$, $(2^+, 1)$, $(1^+, 0)$ and $(0^+, 1)$ for pure $| 1d_{3/2} \rangle$ state .

At first to calculation the binding energies at low lying level state we can evaluation the two body matrix element effective interaction for configuration system that indication in the Eq.(3-21)

Two-body matrix elements of two particles effective interaction at the configuration space system $\langle 2S_{1/2} 1d_{3/2} \rangle$ as derived from a microscopic nucleon-nucleon interaction by the USD ,USDA,and USDB potential and has been

calculation according Eq(3-21)with a MATLAB program , and result of our calculation are listed in table(4-5).

Table(4-4):Results of the matrix element for ${}_{16}^{30}\text{S}_{14}$ using USD,USDA,and USDB interaction.

J_a	J_b	J_c	J_d	J^π	T	$\langle j_a j_b V^{USDA} j_c j_d \rangle$	$\langle j_a j_b V^{USDB} j_c j_d \rangle$	$\langle j_a j_b V^{USD} j_c j_d \rangle$
1/2	1/2	1/2	1/2	1+	0	-3.8693	-3.7093	-3.2628
1/2	1/2	1/2	1/2	0+	1	-1.8461	-1.6913	-2.1246
3/2	3/2	3/2	3/2	3+	0	-2.9800	-2.9660	-2.8842
3/2	3/2	3/2	3/2	2+	1	-0.1570	-0.0974	-0.0665
3/2	3/2	3/2	3/2	1+	0	-1.4927	-1.6582	-1.4151
3/2	3/2	3/2	3/2	0+	1	-1.505	-1.8992	-2.1845
1/2	3/2	1/2	3/2	2+	1	-0.2533	-0.3034	-0.4064
1/2	3/2	1/2	3/2	2+	0	-1.753	-1.8504	-1.8194
1/2	3/2	1/2	3/2	1+	1	0.3105	0.5158	0.6066
1/2	3/2	1/2	3/2	1+	0	-3.8051	-4.0460	-4.2930

In addition to matrix element of two body effective interaction calculation the shell model calculation for ${}_{16}^{30}\text{S}_{14}$ we must calculation the binding energies of the core ${}_{14}^{28}\text{Si}_{14}$ is calculated from Eq(3-19). with mass number are $M({}_{14}^{28}\text{Si}_{14}) = (28.976494700) \text{amu}$, $M({}_0n^1) = (1.008665) \text{amu}$ and $M(p) = (1.007825) \text{amu}$ for neutron and proton respectively[88] .The binding energy is -236.54MeV.

The binding energy for ${}_{16}^{30}\text{Si}$ levels nuclei can be calculation by inserting the values of single particles energy $\varepsilon_{2s_{1/2}} = -8.48\text{MeV}$ and $\varepsilon_{1d_{3/2}} = -7.21\text{MeV}$ and core binding energy -236.54MeV in the Eqs.(4-4 to 4-7) using a Matlab program, results are shown in table (4-5).

Table(4-5):Results of the binding energy B.E(MeV) for ${}_{16}^{30}\text{Si}$ that calculated with USD,USDA,and USDB.

Configuration	J^π T	Binding Energy (B.E)(Mev)		
		USDA	USDB	USD
$(2s_{1/2})^2$	1+ 0	-256.8179	-256.6807	-256.2976
$(2s_{1/2})^2$	0+ 1	-255.0833	-254.9494	-255.3211
$(1d_{3/2})^2$	3+ 0	-253.5165	-253.5045	-253.4344
$(1d_{3/2})^2$	2+ 1	-251.0946	-251.0435	-251.0170
$(1d_{3/2})^2$	1+ 0	-252.2406	-252.3825	-252.1740
$(1d_{3/2})^2$	0+ 1	-252.2511	-252.5893	-252.8341
$2s_{1/2} 1d_{3/2}$	2+ 1	-252.4473	-252.4902	-252.5786
$2s_{1/2} 1d_{3/2}$	2+ 0	-253.7339	-253.8174	-253.7908
$2s_{1/2} 1d_{3/2}$	1+ 1	-252.4963	-252.6725	-252.7504
$2s_{1/2} 1d_{3/2}$	1+ 0	-255.4944	-255.7011	-255.9130

(4-4-3)Calculation of the Binding Energy for ${}_{14}^{30}\text{Si}_{16}$ Nuclei

The binding energies for ${}_{14}^{30}\text{Si}_{16}$ are calculated at the low -lying states depending on the $\langle 2s_{1/2} 1d_{3/2} \rangle$ configuration model space for the shell model that allow us to perform larger calculations, for the Sd-shell nuclei. One of the shell model calculation for ${}_{14}^{30}\text{Si}_{16}$ nuclei we can assume the closed inert core ${}_{14}^{28}\text{Si}_{14}$

and two protons move at $2S_{\frac{1}{2}}1d_{\frac{3}{2}}$ configuration space . The binding energies of the core ${}^{28}_{14}\text{Si}_{14}$ is calculated from Eq(3-20) with mass number are $M({}^{28}_{14}\text{Si}_{14}) = (28.976494700) \text{amu}$, $M({}_0n^1) = (1.008665) \text{amu}$ and $M(p) = (1.007825) \text{amu}$ for neutron and proton respectively[88] .The binding energy is -236.54MeV . We take experimental single particles energy that find from different experimental energies levels in Eqs.(4-4 to 4-7) $\varepsilon_{2S_{\frac{1}{2}}} = -8.48 \text{MeV}$ and $\varepsilon_{1d_{\frac{3}{2}}} = -7.21 \text{MeV}$.The model space $\langle 2S_{1/2}1d_{3/2} \rangle$ describe in the representation (J^π, T) combination $(0^+, 1)$ and $(1^+, 0)$ for $|2S_{1/2}\rangle$, $(2^+, 1)$, $(2^+, 0)$, $(1^+, 0)$, $(1^+, 1)$ and $(0^+, 1)$ for $|2S_{1/2} 1d_{3/2}\rangle$ and $(3^+, 0)$, $(2^+, 1)$, $(1^+, 0)$ and $(0^+, 1)$ for $|1d_{3/2}\rangle$ and allowed for the two neutrons in configuration space. The matrix element of two particles effective interaction energy required to interaction at the configuration space system $\langle 2S_{1/2}1d_{3/2} \rangle$ are calculated using Eq.(3-19) with the USD ,USDA and USDB potential using a MATLAB program , and result listed in table(4-6).

Table(4-6):Results of the matrix element for $^{30}_{14}\text{Si}_{16}$ using USD,USDA,and USDB interaction.

J_a	J_b	J_c	J_d	J^π	T	$\langle j_a j_b V^{USD} j_c j_d \rangle$ [82]	$\langle j_a j_b V^{USDA} j_c j_d \rangle$ [82]	$\langle j_a j_b V^{USDB} j_c j_d \rangle$ [82]
1/2	1/2	1/2	1/2	0+	1	-2.1246	-1.8461	-1.6913
1/2	1/2	1/2	1/2	1+	0	-3.2628	-3.8693	-3.7093
1/2	3/2	1/2	3/2	2+	1	-0.4064	-0.2533	-0.3034
1/2	3/2	1/2	3/2	2+	0	-1.8194	-1.753	-1.8504
1/2	3/2	1/2	3/2	1+	0	-4.2930	-3.8051	-4.0460
1/2	3/2	1/2	3/2	1+	1	0.6066	0.3105	0.5158
1/2	3/2	1/2	3/2	0+	1	-1.0835	-0.9834	-1.0150
3/2	3/2	3/2	3/2	3+	0	-0.4000	-2.9800	-2.9660
3/2	3/2	3/2	3/2	2+	1	-0.0665	-0.1570	-0.0974
3/2	3/2	3/2	3/2	1	0	-1.4151	-1.4927	-1.6582
3/2	3/2	3/2	3/2	0	1	-2.1845	-1.505	-1.8992

The binding energies of the $^{30}_{14}\text{Si}_{16}$ nucleus for each term for configuration (J^π , T) values can be evaluated from Eq(3-20) depending on the evaluation of single particle energy, two body effective interaction from table(4-8) for USD ,USDA and USDB and binding energy core $^{28}_{14}\text{Si}_{14} = -236.54\text{MeV}$,the result are sammarized in table (4-7).

Table(4-7):Results of the binding energy B.E(MeV) for $^{30}_{14}\text{Si}_{16}$ that calculated with USD,USDA,and USDB.

Configuration	J^π T	Binding Energy (B.E)(Mev)		
		USD	USDA	USDB
$(2S_{1/2})^2$	0+ 1	-255.3227309	-255.0838009	-254.9509900
$(2S_{1/2})^2$	1+ 0	-256.2992122	-256.8195390	-256.6822723
$2S_{1/2} 1d_{3/2}$	2+ 1	-252.5786576	-252.4473104	-252.4902921
$2S_{1/2} 1d_{3/2}$	2+ 0	-253.7908946	-253.7339289	-253.8174900
$2S_{1/2} 1d_{3/2}$	1+ 1	-255.9130385	-255.4944607	-255.7011330
$2S_{1/2} 1d_{3/2}$	1+ 0	-251.7095874	-251.9636167	-251.7874863
$2S_{1/2} 1d_{3/2}$	0+ 1	-253.1595533	-253.0736758	-253.1007860
$(1d_{3/2})^2$	3+ 0	-251.3031669	-253.5165933	-253.5045824
$(1d_{3/2})^2$	2+ 1	-251.0170515	-251.0946930	-251.0435611
$(1d_{3/2})^2$	1+ 0	-252.1740386	-252.2406130	-252.3825983
$(1d_{3/2})^2$	0+ 1	-252.8341201	-252.2511654	-252.5893563

(4-5)Calculation of Excitation Energies for $^{18}_8\text{Ne}_{10}$, $^{30}_{16}\text{S}_{14}$, and $^{30}_{14}\text{Si}_{16}$ Nucleus

One of the most important parameters for the investigation and studied of the nuclear structure is the excitation energy . Study of low-lying excited states of nuclei using shell model provide information about the specific nuclear orbital nucleus .This is because few nuclear orbits dominate the contribution to their wave functions. Therefore the excitation energies follow directly from the different values can be calculated theoretically using Eq. (3-22) as a function of the binding energy of nuclei at ground state and excited state .

The excitation energy due to closed core and two nucleon move at configuration space have been calculated by substituting the results of the binding energies from

tables (4-3) , (4-5) and (4-7) for $^{18}_8\text{Ne}_{10}$, $^{30}_{16}\text{S}_{14}$, and $^{30}_{14}\text{Si}_{16}$ nuclei respectively into Eq. (3-22). One immediately obtains the values of the excitation energies for three nuclei. Results of calculation of the excited energy are listed in tables (4-8) , (4-9) and (4-10) for $^{18}_8\text{Ne}_{10}$, $^{30}_{16}\text{S}_{14}$, and $^{30}_{14}\text{Si}_{16}$ nuclei system .

Table(4-8):Results of the excitation energy (MeV) for $^{18}_8\text{Ne}_{10}$ that calculated with USD,USDA,and USDB.

Configuration	J^π T	Excitation Energy (Ex_1)(Mev)		
		USDA	USDB	USD
$(1d\ 5/2)^2$	5+ 0	0	0	0
$(1d\ 5/2)^2$	4+ 1	4.1675	4.1136	4.0615
$(1d\ 5/2)^2$	3+ 0	2.9793	2.6554	2.7244
$(1d\ 5/2)^2$	2+ 1	3.3912	3.3198	3.2236
$(1d\ 5/2)^2$	1+ 0	3.2888	2.9937	2.5935
$(1d\ 5/2)^2$	0+ 1	1.9015	1.7607	1.4059
$(2s\ 1/2)^2$	0+ 1	2.2518	2.3512	2.7028
$(2s\ 1/2)^2$	1+ 0	4.2750	4.3692	3.8410
$(1d\ 3/2)^2$	3+ 0	11.5811	11.5345	11.5214
$(1d\ 3/2)^2$	2+ 1	14.4041	14.4031	14.3391
$(1d\ 3/2)^2$	1+ 0	13.0684	12.8423	12.9905
$(1d\ 3/2)^2$	0+ 1	13.0561	12.6013	12.2211
$1d_{5/2}2s_{1/2}$	3+ 1	-1.5319	-1.5554	1.5718
$1d_{5/2}2s_{1/2}$	3+ 0	-1.719	-2.1427	2.1460
$1d_{5/2}2s_{1/2}$	2+ 0	-2.6663	-2.5549	3.7818
$1d_{5/2}2s_{1/2}$	2+ 1	-3.0828	-3.1800	3.1527

1d_{5/2} 1d_{3/2}	4+ 0	1.7959	1.5816	1.5997
1d_{5/2} 1d_{3/2}	4+ 1	5.0102	4.7558	4.6559
1d_{5/2} 1d_{3/2}	3+ 1	6.7388	6.9678	6.6950
1d_{5/2} 1d_{3/2}	3+ 0	4.9708	4.9881	5.5679
1d_{5/2} 1d_{3/2}	2+ 1	6.4859	6.0460	5.9363
1d_{5/2} 1d_{3/2}	2+ 0	1.7159	1.9888	2.4358
1d_{5/2} 1d_{3/2}	1+ 0	-0.2495	0.1906	-0.2447
1d_{5/2} 1d_{3/2}	1+ 1	6.5121	6.8561	7.2945
2S_{1/2} 1d_{3/2}	2+ 1	6.2481	6.0901	6.1817
2S_{1/2} 1d_{3/2}	2+ 0	7.7478	7.6371	7.5947
2S_{1/2} 1d_{3/2}	1+ 0	4.1960	3.8945	3.7081
2S_{1/2} 1d_{3/2}	1+ 1	8.3116	8.4563	8.6077

Table(4-9):Results of the excitation energy (MeV) for $^{30}_{16}\text{S}_{14}$ that calculated with USD,USDA and USDB.

Configuration	J^π T	Excitation Energy (Ex)(Mev)		
		USDA	USDB	USD
$(2S_{1/2})^2$	1+ 0	0	0	0
$(2S_{1/2})^2$	0+ 1	1.7346	1.7313	0.9765
$(1d_{3/2})^2$	3+ 0	3.3014	3.1762	2.8632
$(1d_{3/2})^2$	2+ 1	5.7233	5.6372	5.2806
$(1d_{3/2})^2$	1+ 0	4.5773	4.2982	4.1236
$(1d_{3/2})^2$	0+ 1	4.5668	4.0914	3.4635
$2S_{1/2} 1d_{3/2}$	2+ 1	4.3706	4.1905	3.7190
$2S_{1/2} 1d_{3/2}$	2+ 0	3.0840	2.8633	2.5068
$2S_{1/2} 1d_{3/2}$	1+ 1	4.3216	4.0082	3.5472
$2S_{1/2} 1d_{3/2}$	1+ 0	1.3235	0.9796	0.3846

Table(4-10):Results of the excitation energies (MeV) for $^{30}_{14}\text{Si}_{16}$ that calculated with USD,USDA,and USDB interaction.

Configuration	J^π T	Excitation Energy E_{x1} (Mev)		
		USD	USDA	USDB
$(2S_{1/2})^2$	0+ 1	0.00000000	0.00000000	0.00000000
$(2S_{1/2})^2$	1+ 0	-0.97648713	-1.7357381	-1.7312769
$2S_{1/2} 1d_{3/2}$	2+ 1	2.7440737	2.6364905	2.4607033
$2S_{1/2} 1d_{3/2}$	2+ 0	1.5318363	1.3498720	1.1335054
$2S_{1/2} 1d_{3/2}$	1+ 1	0.5903076	-0.4106598	-0.7501376
$2S_{1/2} 1d_{3/2}$	1+ 0	3.6131435	3.1201842	3.1635091
$2S_{1/2} 1d_{3/2}$	0+ 1	2.1631776	2.0101251	1.8502094
$(1d_{3/2})^2$	3+ 0	4.0195640	1.5672077	1.4464130
$(1d_{3/2})^2$	2+ 1	4.3056794	3.9891079	3.9074343
$(1d_{3/2})^2$	1+ 0	3.1486923	2.8431879	2.5683971
$(1d_{3/2})^2$	0+ 1	2.4886108	2.8326355	2.3616391

(4-6) Discussion

(4-6-1) Introduction

Shell model calculation have been permission to understand many things about the nucleus structure which is primarily based on the experimentally deduced of properties nuclides close to decay stability. The shell model is a first-principles nuclear structure technique with which one can calculate the observable properties of nuclei. However nuclear shell structure has been seen to evolve in regions away from stability, and the characteristics of stable and nearly stable nuclides should not be blindly extrapolated to nuclides with N/Z ratios that deviate significantly from unity. With the advent of experimental facilities in recent years more Neutron / Proton rich nuclides have been studied experimentally allowing for more stringent tests of the nuclear shell model.

In the present work the $^{18}_8\text{Ne}_{10}$, $^{30}_{16}\text{S}_{14}$ and $^{30}_{14}\text{Si}_{16}$ nuclei were investigated by studying low-lying quantum states depending on the perturbation theory approximation method. Inferences regarding the binding and excitation energy spin-parity, and ordering of nuclear excited states were evaluation based on the theory of shell model and compared with experimental. We will model it by two nucleons beyond a closed core $^{16}_8\text{O}_8$ in $1d_{5/2} 2S_{1/2} 1d_{3/2}$ shell-model space for $^{18}_8\text{Ne}_{10}$, and two nucleons beyond a closed core $^{28}_{14}\text{Si}_{14}$ in $2S_{1/2} 1d_{3/2}$ shell-model space for $^{30}_{14}\text{Si}_{16}$, and $^{30}_{16}\text{Si}_{14}$ nuclei respectively.

(4-6-2) Theoretical calculation of shell model

Theoretical calculation of shell mode have been used for describing and investigation of the nuclear structure depending on the calculated the expectation values of binding energy and excitation energy at low lying state level according on the quantum consideration theory. Depending on this model we have been assuming the configuration space model of nucleon state describe the space of interaction . The simple approximation shell model calculation of binding and excitation energies are proposed in which the low energy excitation spectra corresponds to the identical nucleons occupying the same single particle states where they preferred to form pairs for the ground states.

The configuration space model interaction in the nuclear shell model are simplifies by selecting an inert core of occupied single particle levels with mass number A with ground state energy. The entire description of occupied particles is contained in a model space of valence orbits outside the core . One effect of this reduction in the allowed configuration space requires the modification of the Hamiltonian. The interactions between nucleons in the configuration model space for nucleon out of the core must take into account effects outside of the model space both from the core and from higher energy orbits which are not included in the valence space.

The utility of the configuration model space interaction depends upon a single particle energy . In this model the A nucleons produce a mean field that bind s them in the nucleus and a one-body potential can be used to represent the complicated effects of the nuclear interaction that's view in Eq.(3-6). The mean field Hamiltonian in Eq.(3-6) is usually selected so that the many-body system is reasonably approximated by the exact solution to the Schrödinger equation . It follows from Eq. (3-6), that one can simplify the H_{res} calculation by choosing a nucleus with closed shells as a reference core and only study the configurations

with a two particles relative to it. The established shell model calculation of the binding energies have been depending on many parameters such that: configuration space model, the single particle energy, two body matrix element effective interaction potential, inert closed core binding energy.

The two nucleon for $^{18}_8\text{Ne}_{10}$, $^{30}_{16}\text{S}_{14}$ and $^{30}_{14}\text{Si}_{16}$ nuclei were describe by $1d\frac{5}{2}2S\frac{1}{2}1d\frac{3}{2}$ configuration space model for $^{18}_8\text{Ne}_{10}$, and $2S\frac{1}{2}1d\frac{3}{2}$ for $^{30}_{14}\text{Si}_{16}$, and $^{30}_{16}\text{Si}_{14}$ nuclei respectively. The two nucleons must be satisfy the rule $|j(1) - j(2)| \leq |j_1 + j_2|$ for the probability of excited at configuration space. The total angular momentum J and isospin T of the coupled nucleons must be calculation to find the configuration space model. We call this approximation as nonzero angular momentum pairing shell model. It not only reduces the dimensionality of the shell model but also matches the number of low energy levels in experimental spectra for few cases where exact shell model predicts many more states. The single particle energy can be determination for standard model spaces with a stable core depending on the experimental energy difference between the core with mass number A particles and states in mass number $A+1$ nuclei provide reasonable SPE since the lowest-energy experimental states can be approximated as single particle states.

As regards to the two body effective interaction it should be realistic in nature which is derived from free nucleon-nucleon scattering data using USD, USDA, and USDB. But when these types of interactions are used in binding energies calculation the results are usually unsatisfactory. It does not mean that fault lies in realistic interactions but rather it lies in energy state levels methodology where many unnecessary components in wave functions produces extra states and also lowers the low energy states.

In addition to the symmetry of isospin is quite good in nuclei. That's because isospin is broken by the Coulomb long-range interaction and by small charge-dependent parts of the strong interaction. Thus the structure of a given proton-rich nucleus $^{18}_8\text{Ne}_{10}$ is similar to its isospin mirror in which the roles of protons and neutrons are interchanged $^{18}_{10}\text{O}_8$. However the isospin are associated multiplets $T=1$ triplets in $^{18}_8\text{Ne}_{10}$ and $^{18}_{10}\text{O}_8$.

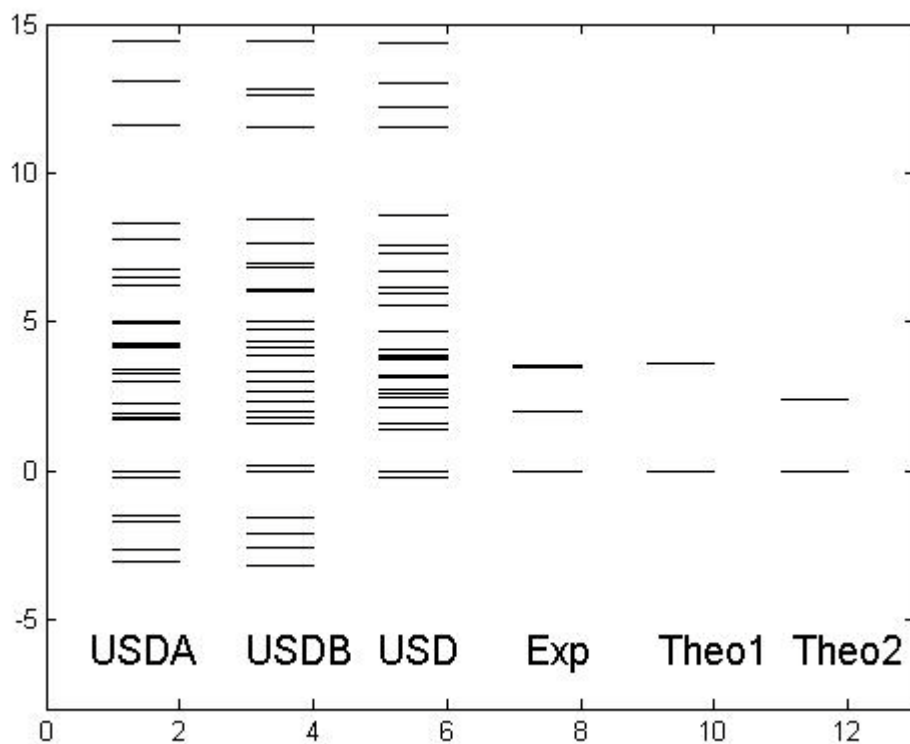
(4-6-3)The Energy Level of $^{18}_8\text{Ne}_{10}$ Nuclei

The main objectives for using shell model was to calculate the binding and excitation energies and observable nuclear structure properties on the S-d shell for the nuclei of the mass range ($A = 18$ and 30) using the three USD,USDA and USDB potential model interactions. The results of the calculations of binding and excitation energies are listed in tables (4-3)and(4-8). A summary calculation of binding and excitation energy for all of the configuration space $1d_{\frac{5}{2}}2S_{\frac{1}{2}}1d_{\frac{3}{2}}$ for $^{18}_8\text{Ne}_{10}$ nuclei that were compared with available experimental data that is provided in table (4-11) and figure(4-1).

From figure (4-1),we can show the theoretical calculation of binding energy for ground state of $^{18}_8\text{Ne}_{10}$ is -132.1543MeV that's agreement with experimental data results -132.1430MeV and theoretical result -131.244 MeV [90]. On the other hand the results of energy level of excited state for $^{18}_8\text{Ne}_{10}$ nuclei is agreement with experimental results .A summary compared of the theoretical results data for the excitation energies and experimental and other theory results is:

1-The $E(2^+, 1)$ value was found agreement with the other theory but found less agreement with experimental results (1.98). On the other hand we found the USD was agreement with experimental compared with USDB and USDA.

2-Also the $E(4^+ 1)$ values for isotopes that calculated with USD(4.061) was agreement with result of experimental (3.55) and other theory(3.60-3.79) compare with USDA and USDB(4.1675 , -4.1136) respectively .



figure(4-7):Our theoretical data of level energy for $^{18}\text{Ne}_{10}$ using USD, USDA, and USDB potential compare with the experimental data.

Generally a good agreement with experiment was observed for the observables calculated with the wave functions from the effective interactions (USD, USDA, and USDB).. No obvious differences between the three interactions could be discerned. However, the agreement was fine-tuned at upper levels by using three effective matrix element determined from (USD, USDA, and USDB) and the resulting calculated showed general good agreement with experiment compare with result at lower levels .

Table(4-11): Compared results data of the excitation energy E.X(MeV) for $^{18}\text{Ne}_{10}$ that calculated with USD,USDA,and USDB with expermental and other theory .

Configuration	J^π T	Calculated Excitation Energy (Ex)(Mev)			Exp[68]	Theo[68]	Theo[68]
		USDA	USDB	USD			
$(1d\ 5/2)^2$	5+ 0	0	0	0			
$(1d\ 5/2)^2$	4+ 1	4.1675	4.1136	4.0615	3.55	3.60	3.79
$(1d\ 5/2)^2$	3+ 0	2.9793	2.6554	2.7244			
$(1d\ 5/2)^2$	2+ 1	3.3912	3.3198	3.2236	1.98	2.41	3.23
$(1d\ 5/2)^2$	1+ 0	3.2888	2.9937	2.5935			
$(1d\ 5/2)^2$	0+ 1	1.9015	1.7607	1.4059	3.50		
$(2S1/2)^2$	0+ 1	2.2518	2.3512	2.7028			
$(2S1/2)^2$	1+ 0	4.2750	4.3692	3.8410			
$(1d\ 3/2)^2$	3+ 0	11.5811	11.5345	11.5214			
$(1d\ 3/2)^2$	2+ 1	14.4041	14.4031	14.3391			
$(1d\ 3/2)^2$	1+ 0	13.0684	12.8423	12.9905			
$(1d\ 3/2)^2$	0+ 1	13.0561	12.6013	12.2211			
$1d_{5/2}\ 2S_{1/2}$	3+ 1	-1.5319	-1.5554	1.5718			
$1d_{5/2}\ 2S_{1/2}$	3+ 0	-1.719	-2.1427	2.1460			
$1d_{5/2}\ 2S_{1/2}$	2+ 0	-2.6663	-2.5549	3.7818			
$1d_{5/2}\ 2S_{1/2}$	2+ 1	-3.0828	-3.1800	3.1527			
$1d_{5/2}\ 1d\ 3/2$	4+ 0	1.7959	1.5816	1.5997			
$1d_{5/2}\ 1d\ 3/2$	4+ 1	5.0102	4.7558	4.6559			

1d_{5/2} 1d_{3/2}	3+ 1	6.7388	6.9678	6.6950			
1d_{5/2} 1d_{3/2}	3+ 0	4.9708	4.9881	5.5679			
1d_{5/2} 1d_{3/2}	2+ 1	6.4859	6.0460	5.9363			
1d_{5/2} 1d_{3/2}	2+ 0	1.7159	1.9888	2.4358			
1d_{5/2} 1d_{3/2}	1+ 0	-0.2495	0.1906	-0.2447			
1d_{5/2} 1d_{3/2}	1+ 1	6.5121	6.8561	7.2945			
2S_{1/2} 1d_{3/2}	2+ 1	6.2481	6.0901	6.1817			
2S_{1/2} 1d_{3/2}	2+ 0	7.7478	7.6371	7.5947			
2S_{1/2} 1d_{3/2}	1+ 0	4.1960	3.8945	3.7081			
2S_{1/2} 1d_{3/2}	1+ 1	8.3116	8.4563	8.6077			

(4-6-4)Energy Levels of $^{30}_{16}\text{S}_{14}$ Nuclei

As mentioned that the calculation of the binding and excitation energies depending on shell model need the choice of valence space and single particale energy of the states involved in valence space and finally the appropriate effective two body interactions. From figure (4- 2),we can show the theoretical calculation of binding energy for ground state of $^{30}_{16}\text{S}_{14}$ nuclei is -243.6861MeV that's agreement with experimental data results -243.8861MeV.

The results of the calculations were compared with available experimental data from[68] .According on the results data of theoretical calculation we can discussion the results with experiment data :

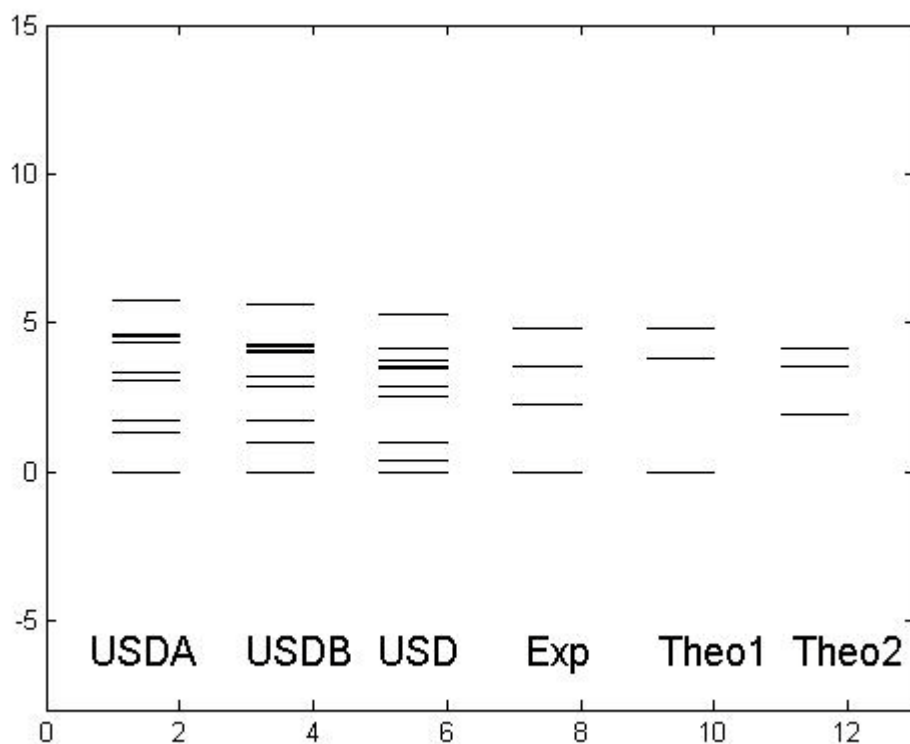


Figure (4-8): our theoretical data of level energy for $^{30}_{16}\text{S}_{14}$ using USD, USDA and USDB potential compare with experiment data.

1- The excitation energy level $E(2^+, 1)$ value that calculated with USD potential (5.2806) was found in agreement with the experimental result(4.83) and other theory(4.82) compare with result calculated with USDA and USDB potential (5.723 and 5.63).

2-The excitation energy level $E(0^+, 1)$ value that calculated with USD potential (3.4635) was found in agreement with the experimental result(2.23) and less agreement with other theory(1.94) compare with result calculated with USDA and USDB potential (4.5668 and 4.0914).

Chapter Four

3-The second excitation energy level $E(2^+, 1)$ value that calculated with USD potential (3.7190) was found good in agreement with the experimental result(3.52) and other theory(3.52 and 2.302) compare with result calculated with USDA and USDB potential (4.3706 and 4.1905)

4-The excitation energy level $E(1^+, 1)$ value that calculated with USDB potential (4.0082) was found in agreement with the experimental result(3.80) and other theory(4.12) compare with result calculated with USDA and USD potential (4.3216 and 3.5472)

We can summary as a conclusion the USD potential used in theoretical calculation which gives the best agreement between the calculated energy levels in the present result and their corresponding experimental data taken from ref. [92] is shown in table (4-12).

Table(4-12):Results of the excitation energy Ex_1 (MeV) for $^{30}_{16}S_{14}$ that calculated with USD,USDA,and USDB.

Configuration	J^π T	Excitation energy Ex.(Mev)			[92]		
		USDA	USDB	USD	Exp	Theo	Theo
$(2S_{1/2})^2$	1+ 0	0	0	0	0	0	0
$(2S_{1/2})^2$	0+ 1	1.7346	1.7313	0.9765			
$(1d_{3/2})^2$	3+ 0	3.3014	3.1762	2.8632			
$(1d_{3/2})^2$	2+ 1	5.7233	5.6372	5.2806	4.83	4.82	4.82
$(1d_{3/2})^2$	1+ 0	4.5773	4.2982	4.1236			
$(1d_{3/2})^2$	0+ 1	4.5668	4.0914	3.4635	2.23	1.94	1.94
$2S_{1/2} 1d_{3/2}$	2+ 1	4.3706	4.1905	3.7190	3.52	3.52	2.302
$2S_{1/2} 1d_{3/2}$	2+ 0	3.0840	2.8633	2.5068			
$2S_{1/2} 1d_{3/2}$	1+ 1	4.3216	4.0082	3.5472	3.8	4.12	
$2S_{1/2} 1d_{3/2}$	1+ 0	1.3235	0.9796	0.3846			

(4-6-5) Energy Levels of $^{30}_{14}\text{Si}_{16}$ Nuclei

The approximation of the shell model calculation has been applied to calculate the energy spectra of $^{30}_{14}\text{Si}_{16}$ nuclei where only two neutrons occupy the valence states outside the core $^{28}_{14}\text{Si}_{14}$. The shell model based on the wave functions of the configuration model was applied to analyze the theoretical data of the low-lying level structure at Sd-shell nuclei $^{28,30}\text{Si}$ and nucleon interaction with them a unified way. It is shown that the sequence of the lower levels is well but that the level spacing is somewhat too the effect of variation of the strength parameter for calculation in USDA and USDB compare with less in USD.

Depending on result in figure (4-3) we can show:

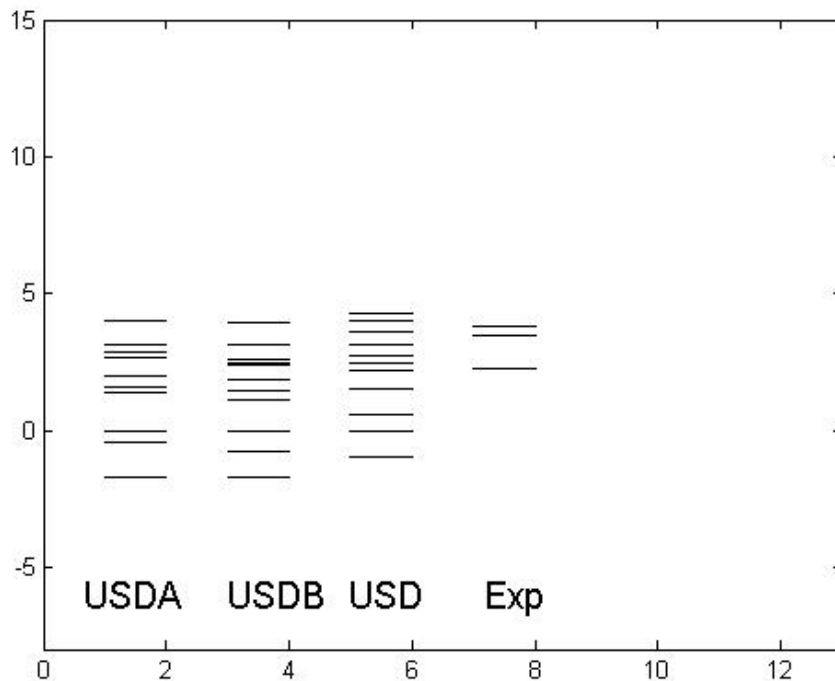


Figure (4-9): our theoretical data of level energy for $^{30}_{14}\text{Si}_{16}$ using USD, USDA and USDB potential compare with experiment data.

1-The theoretical calculation of binding energy for ground state of $^{30}_{14}\text{Si}_{16}$ is -255.6213MeV that's agreement with experimental data results -255.6000MeV and theoretical result -253.5000 MeV and -254.1000MeV[68].

2-The excitation energy level $E(2^+, 1)$ value that calculated with USDB potential (2.4607) was found agreement with the experimental result(2.24) compare with result calculated with USD and USDA potential (2.7440 and 2.6364).

3-The excitation energy level $E(1^+, 0)$ value that calculated with USD potential (3.6131) was found agreement with the experimental result(3.77) and less agreement with other theory result calculated with USDA and USDB potential (3.1201 and 3.1635).

4-The second excitation energy level $E(2^+, 1)$ value that calculated with USDB potential (3.9074) was found in good agreement with the experimental result(3.5000) compare with result calculated with USD and USDA potential (4.3056 and 3.9891) compare with result calculated with USD and USDB potential (2.4886 and 2.3616).

When compared with the experimental data, the results are found to be encouraging. It is expected that results will be more pronounced if the even-even nuclei with higher number of valence nucleons are considered. Furthermore the excitation energies that calculations theoretically are quite for first or second excited state but its become very complicated for higher spectral because several nucleons can be excited simultaneously into superposition of many different configuration to produce a given nuclear spin and parity. The ground state configuration indicate that all the proton sub shell filled and all the neutron is effect on the excitation .The examination of the experimental energy levels for the nuclei shows that they are more agreement with theoretical result calculation .

Table(4-13): Compared our results of the binding and excitation energies (MeV) for $^{30}_{14}\text{Si}_{16}$ that calculated with Wildenthal ,USDA,and USDB with experimental data.

Configuration	J^π T	Binding Energy (B.E)(Mev)			Expermental
		255.3227309	-255.0838009	-254.9509900	
		Excitation Energy (Ex)(Mev)			
		USD	USDA	USDB	
$(2S_{1/2})^2$	0+ 1	0.00000000	0.00000000	0.00000000	
$(2S_{1/2})^2$	1+ 0	-0.97648713	-1.7357381	-1.7312769	
$2S_{1/2} 1d_{3/2}$	2+ 1	2.7440737	2.6364905	2.4607033	2.24
$2S_{1/2} 1d_{3/2}$	2+ 0	1.5318363	1.3498720	1.1335054	
$2S_{1/2} 1d_{3/2}$	1+ 1	0.5903076	-0.4106598	-0.7501376	
$2S_{1/2} 1d_{3/2}$	1+ 0	3.6131435	3.1201842	3.1635091	3.77
$2S_{1/2} 1d_{3/2}$	0+ 1	2.1631776	2.0101251	1.8502094	
$(1d_{3/2})^2$	3+ 0	4.0195640	1.5672077	1.4464130	
$(1d_{3/2})^2$	2+ 1	4.3056794	3.9891079	3.9074343	3.5
$(1d_{3/2})^2$	1+ 0	3.1486923	2.8431879	2.5683971	
$(1d_{3/2})^2$	0+ 1	2.4886108	2.8326355	2.3616391	3.79

The calculation of binding energies for the single-particle energy factors show agreement with experiment was found for all three interactions, with little to choose between the interactions. Generally, a good agreement with experiment was observed for the observables calculated with the wave functions from the effective interactions (USD, USDA, and USDB).

No obvious differences between the three interactions could be discerned. However the agreement was fine-tuned at upper levels by using three effective matrix element determined from (USD, USDA, and USDB), and the resulting calculated moments showed general good agreement with experiment compare with result at lower levels

CHAPTER

Five

Conclusions

And future work

(5-1) Conclusions

According to the present data that have been discussed in the previous chapter; several conclusions can be mentioned. Anyway, the most important conclusions one may summarize them as follows:

1- The theoretical calculation depending on quantum theory and quantum consideration succeeded to describe and study the low-lying excited states of near-closed shell provide information about specific nuclear orbital nuclei and the behavior of interaction and enabled us to study the nuclear structure and provided a knowledge about nuclei characteristic

2-The present study demonstrated the binding energy of the ground state, low excited energy levels values for $^{18}_{10}\text{Ne}$, $^{30}_{16}\text{S}$, and $^{30}_{14}\text{Si}$ nuclei with mass number $A=18$ and 30 . Good agreements were obtained by comparing these calculations with the recently available experimental data for binding energy. The theoretical level spectra are in agreement with experimental data.

3- Generally, the USD, USDA, and USDB with experimental single energies for S and d shell enable us to describe the nuclear structure for light nuclei in S-D shell. In our results, the effect of residual interaction force emerges evidently when we compare the calculated for three potential with experimental data

4- The shell model calculation results has enabled us to elaborate and describe the interaction between two body in the configuration model space and has its advantage to use in study of nuclear structure through calculations of the energy levels.

5- Single particle energies are an important component of the shell model calculation, that's determined from experiment result of energy levels. The single

particle energy in the effective interaction can be parameterized to improve upon the levels state of nuclei description

6- Results data of binding and excitation energy levels that calculation depends on the USD at lower level energy are a good agreement with experimental results compare with USDA and USDB

7-Generally, a good agreement with experiment was observed for the observables calculated with the wave functions from the effective interactions (USD, USDA, and USDB). In terms of energies, USD provided a superior agreement for three nuclei compare with another USDA and USDB .

(5-2) Suggested Future work

Depending on the present work results, discussions and conclusions, several ideas could be adopted to be future theoretical projects that describe the shell model should be addressed on the following points such as:

- 1- Calculation of the transition rate at $^{18}_{10}\text{Ne}$, $^{30}_{16}\text{S}$, and $^{30}_{14}\text{Si}$ nuclei .
- 2- Modifying the simulation to approach the influence of the two body matrix potential on the energy level .
- 3- Calculation of binding and excitation energy for light nuclei using mixed state levels .

References

- 1- Thomas M. “The Shape of Ancient Thought: Comparative Studies in Greek and Indian Philosophies” . book McEvilley pub, 2002.
- 2- Yong Yng,2013 “Search for a Standard Model Higgs Boson Decaying to Two Photons in CMS at the LHC” PhD Thesis , California Institute of Technology, Pasadena, California.
- 3- Takuma H. oraguchi , 2006 “ Prompt Photon Production in Proton-Proton Collisions at $\sqrt{s} = 200\text{GeV}$ ”Ph D, Tokyo Institute of Technology.
- 4-Alex Buytenhuijs “QCD Gluon Radiation Studies with the L3 Detector” PhD Thesis, Catholic University of Nijmegen.
- 5-Richard Enbeng “Quantum Chromodynamics and Colour Singlet Exchange in High Energy Interactions” PhD Thesis, Uppsala University, Uppsala, Sweden, 2003.
- 6-Kristin Fanebust Hetland “Production of strange particles in lead-lead interactions at $158 \text{ A GeV}/c$ ” PhD Thesis, Institute of Physics and Technology, University of Bergen, Bergen, Norway, 2005.
- 7-Baharak Hadinia “In-beam Study of ^{106}Te and ^{107}Te Using Recoil-Decay Tagging” PhD Thesis in Physics,Stockholm, Sweden, 2006.
- 8- Michal Macek” Classical Chaos in Collective Nuclear Models” Diploma Thesis, Charles University in Prague, Faculty of Mathematics and Physics, 2005.
- 9-Norman D. Cook, "Model of the atomic nucleus; with interactive software" Springer- Verlag Berlin Heidelberg, 2006.
- 10- Deana. D.J, Engelandb. T, Hjorth-Jensenb .M, Kartamyshevb. M.P, and Osnesb. E “Review Effective interactions and the nuclear shell-

model” Progress in Particle and Nuclear Physics Vol53 No14 (2004) ,pp419–500.

11-Gareth Jones “Study of Isomers using Reactions with a 178Hf beam”PhD Thesis, University of Surrey Guildford, Surrey,2006.

12-Sharda H., Bansal R. K. and Ashwani Kumar “Effective Two-body Interactions in the s-d Shell Nuclei Using Sum Rule Equations in Transfer Reactions “Progress of Theoretical Physics, Vol. 100, No.4, PP737-743 , 1998.

13- Liuy Xu. YB. And Liao,J.Z. 1999“ study the deformed nuclei $^{104-116}\text{Cd}$, $^{102-116}\text{Pd}$, $^{102-114}\text{Ru}$ using the modified surface delta interaction for shell model” High Energy Phys.Nucl.Phys.- Chin.Ed,vol.23,No6,1999.

14- Taqi A.H ,Ph.D. Thesis,Nahreen university,2000.

15- Hasan A. K. , Journal Of Babylon. For Pure and Appl. Sci. , 6 (3),2001.

16-Vesselin Gueorguiev “Mixed-Symmetry Shell-Model Calculation in nuclear Physics ”PhD Thesis, Louisiana State University,2002.

17- Jennifer Anne Church “Collectivity in light neutron rich nuclei near N=20:inter mediate energy coulomb excitation of Mg, Al and Si ” PhD Thesis ,Michigan state University, 2003.

18-Samah A.H.Al Ramahy 2005”Applied nuclear shell model on nuclei ^{50}Ti , ^{51}V , ^{52}Cr ‘MsC Thesis,Al Kufa University ,Iraq.

19-Praha Listopad 2006 “Structure and Properties of Exotic Nuclei using Radioactive Nuclear Beams” PhD Thesis, Academic edition v.ed , Ceske Republiky.

- 20-Ali H. TAQI¹, Ra'ad. A. RADHI,2007"Longitudinal Form Factor of Isoscalar Particle-Hole States in ^{16}O , ^{12}C and ^{40}Ca with M3Y Interaction" Turk J Phys Vol.31,pp253 – 258(2007).
- 21-Nicholas J. Thompson "Gamma-Ray Spectroscopy and Shell Model Description of High Spin States in-Stable $^{91,92}\text{Zr}$ "PhD Thesis , University of Surrey, 2008.
- 22- Bertsch G. F. and Johnson C. W. "Model space truncation in shell-model fits" Physical Review C, Vol. 80, (2009).
- 23-Simon Mark Brown,2010" Neutron Shell Breaking in Neutron-Rich Neon Isotopes"PhD Thesis , University of Surrey, Guildford.
- 24- Lei Y₁, Zheng X₁,Zhao YuMin& LU DaHai "SD-pair structure in the pair approximation of the nuclear shell model "Science China Physics, Mechanics & Astronomy, 2010 Vol. 53 No. 8": 1460–1465.
- 25-Angelo Signoracci "Effective Interactions for Nuclear Structure Calculations" PhD Thesis , Michigan State University ,2011 .
- 26- Fiase J. O. and Gbaorun F. 2012"Effects of Tensor Correlations on the Positive Parity States of the Even-Even Nuclei in the sd Shell" Journal of Physics: Conference Series 337 (2012) 012024.
- 27-Khalid S. Jassim, and Hassan ABU Kassim,2013" Core Polarization Effects Of Some Odd Sd-Shell Nuclei Using M3y Effective Nucleon-Nucleon Interaction" Rom. Journ. Phys., Vol. 58, Nos. 3–4, P. 319–329, Bucharest, 2013.
- 28- Brown B. A. and Wildenthal B. H., Ann. Rev. of Nucl. Part. Sci. 38, 29 (1988).

29-Kyle G. Leach “ Neutron Transfer Reactions on ^{64}Zn as a Probe for Testing Shell-Model Isospin-Symmetry-Breaking Theory” PhD Thesis, The University of Guelph . Guelph, Ontario, Canada, 2012.

30-Von Dennis Neidherr “Nuclear structure studies in the xenon and radon region and the discovery of a new radon isotope” PhD Thesis Naturwissenschaften Gutenberg-Universität Mainz , Frankfurt am Main ,Mainz 2010.

31-Das and T. Ferbel “Introduction to Nuclear and Particle Physics” 2003 ,World Scientific Publishing Co. Pte. Ltd.

32- Nader Ghahramany , Shirvan Gharaati and Mohammad Ghanaatian “New approach to nuclear binding energy in integrated nuclear model” Journal of Theoretical and Applied Physics 2012, 6.

33-Evans R. D. Evans, The Atomic Nucleus (McGraw-Hill, New York, 1955 .

34- Meyerhof W. E., Elements of Nuclear Physics (McGraw-Hill, New York, 1967), Chap. 2. P. Marmier and E. Sheldon, Physics of Nuclei and Particles (Academic Press, New York, 1969), Vol. I, Chap. 2.

35- Nilsson S. G. and Ragnarsson I. "Shape and Shells in Nuclear Structure"Book , Cambridge University Press, 1995.

36 - Hilde De Witte,2004”Probing the nuclear structure along the Z=82 closed shell: decay- and laser spectroscopic studies of exotic Pb, Bi and Po nuclei”PhD Thesis, Katholieke University, Wetenschappen .

37- Das and T. Ferbel “Introduction to Nuclear and Particle Physics” 2003 ,World Scientific Publishing Co. Pte. Ltd.

38-Adrian Buzatu, Search for the Standard Model Higgs boson produced in association with a W Boson in the isolated-track charged-lepton channel using the Collider Detector at Fermilab, PhD Thesis, Department of Physics, McGill University, Montreal, 2011.

39-Hwidong Yoo, Top Quark Pair Production Cross Section in the Lepton + Jets Channel Using b-tagging at $DØ$, PhD Thesis, Brown University, 2008.

40-Mathew C Osborn “Kinematic scaling in Quasielastic electron scattering” Master of science, Massachusetts institute of technology, 1995.

41-Eva Dorothy Kuhnle “Strongly Interacting ${}^6\text{Li}$ Fermi Gases with Bragg Spectroscopy” PhD Thesis, Swinburne University of Technology Melbourne, Australia, June 15, 2011.

42-Simon Fraser “Introduction to Nuclear Science” Book, Spring edition, 2011.

43- Aubrecht G.J., The Nuclear Science Wall Chart, The Physics Teacher 35, 544 (1997).

44-Gharam A. Alharshan “The isomeric structure in the $N = 73$ neutron-deficient nuclei ${}^{132}\text{Pr}$ and ${}^{130}\text{La}$ ” PhD Thesis, University of Manchester, 2013.

45-Strong Deformation and Tidal Waves in Nuclei” PhD Thesis, University of Notre Dame, Notre Dame, Indiana, July 2007.

46 - Heyde K. L. G., “Basic ideas and concepts in nuclear physics: An Introductory approach”, First ed. John Wiley & Sons, Inc., Bristol, UK, pp37, 1999.

- 47-Robert L.V.”A parametrization of the nucleon –nucleon optical model potential” Ph D Thesis ,University of North Carolina ,1986 .
- 48- Koning A.J. , Delaroche J.P. “Local and global nucleon optical models from 1 keV to 200 MeV” Nuclear Physics A 713 ,231–310(2003).
- 49-Randal I S. Caswel I “Nuclear Optical Model Analysis of Neutron Elastic Scattering for Calcium” Journal Of Research of the National Bureau of Standards—A. Physics and Chemistry, Vol. 66A, No. 5, 1962 .
- 50-XIE Wenfang and Chen Chuanyu. “A generalized talmi-moshinsky trans. Communications in Theoretical Physics”, page 419, 1998.
- 51-Jake Bouma “Elastic scattering and cluster-transfer reactions of ^{98}Rb on ^7Li at REX-ISOLDE” Master of Science, KU Leuven ,2013.
- 52- Krane K. S., "Introductory Nuclear Physics", John Willey & Sons (1988) .
- 53- Moshinsky M. and Smirnov Y. F., “The Harmonic Oscillator in Modern Physics”, Contemporary Concepts in Physics Volume 9, ed. H. Feshbach, Amsterdam, Harwood Academic Publishing (1996).
- 54-Kue T.T.S.”shell model effective interaction and the free nucleon interaction”1972.
- 55- Blaum K., High-Accuracy Mass Spectrometry with Stored Ions, Phys. Rep. 425 (2006) 1.
- 56- Wapstra A.H., Audi G., and Thibault C., The AME2003 atomic mass evaluation, Nucl. Phys. A 729 129(2003).
- 57- Suhonen J., From Nucleons to Nucleus. Springer-Verlag Berlin Heidelberg, 2007.
- 58-Alexander Belyaev “Nuclear and particales”Book,2014.
- 59- Brown B. A., Lecture Notes, JINA Workshop: Tools and Toys of Nuclear Astro-physics School on Nuclear Shell Model Applications (2006).

- 60- Casten R. F., Nuclear Structure From a Simple Perspective, Oxford University Press, 2nd ed., (2000).
- 61- Ring P. and Schuck P., The Nuclear Many-Body Problem, Springer, (1980).
- 62- Woods R. D. and Saxon D. S., Phys. Rev., 95, 577 (1954) .
- 63-Jan C.A. Boeyens ,and Demetrius C. Levendis “Number Theory and the Periodicity of Matter” Springer Science, Busch R.V.2008.
- 64-“Nuclear Physics and Reactor Theory”Book,Volume 1 of 2,1993
- 65-Dennis Neidherr “Nuclear structure studies in the xenon and radon region and the discovery of a new radon isotope by Penning trap mass spectrometry “PhD Thesis,Gutenberg-University of Frankfurt Mainz 2010.
- 66-David J Rowe and John L Wood. Fundamentals of Nuclear Models. World Scientific Publishing, first edition, 2010.
- 67-Kenneth Krane. “Introductory Nuclear Physics”. Book John Wiley and Sons, second edition, 1988 .
- 68- Brussard P. J. and Glademans P. W. M., “Shell-model Application in Nuclear Spectroscopy”, Book North-Holland Publishing Company Amsterdam (1977).
- 69- Blaum K., “ High-Accuracy Mass Spectrometry with Stored Ions”, Phys. Rep. 425 (2006).
- 70- Brown L., and Gabrielse G., “ Geonium Theory - Physics of a single Electron or Ion in a Penning Trap”, Rev. Mod. Phys. 58 , 233(1986).
- 71- Rainville S., Thompson J.K., and Pritchard D.E., “ An Ion Balance for Ultra-HighPrecision Atomic Mass Measurements”, Science 303 , 334 (2003).
- 72- Block M., “ Direct mass measurements beyond uranium”, Nature in print (2010).
- 73- Mukherjee M., Isoltrap: “An on-line Penning trap for mass spectrometry on short-lived nuclides”, Eur. Phys. J. A 35 (2008).

- 74- Bentley M. A. and S. M. Lenzi: “Coulomb energy differences between high-spin states in isobaric multiplets”. *Progr. Nucl. Part. Phys.* 2006.
- 75- Svensson. C.E. “advanced nuclear physics”, course notes *Phys A7150*,2009.
- 76-Kris L. G. “the nuclear shell model” , Book, Springer Verlag pub study edition 1994 .
- 77-Alexander Bürger “Nuclear Structure of Light Ca and Heavy Cr Isotopes “PhD Thesis ,Wilhelms -Universität Bonn,Bonn,2007 .
- 78-Trun ,B, 1999“Quantum Mechanics Concept and application ” Book , phys. Dep.State University New York.
- 79 - Hadi J. M.Al-Agealy, Naz T.J., Samera and Rajaa F. Al-Rabeea" Theoretical calculation of the Binding and Excitation Energies for ${}_{28}^{58}\text{Ni}_{30}$ using shell model and perturbation Theory"" *Ibn AL-Hatham Journal for Pure and Applied Science*, Vol.26,No21,PP160-169 .2014.
- 80- Amos K., Richter W. A., Karataglidis S., and Brown B. A. “Proton Reaction Cross Sections as Measures of the Spatial Distributions of Neutrons in Exotic Nuclei “*Phys. Rev. Lett.* 96, 032503 – Published 27 January 2006 .
- 81-Paola Cappellaro,2012 “Introduction to Applied Nuclear Physics” Book, Massachusetts Institute of Technology, Nuclear Science and Engineering Department.
- 82-Percival S. M. “Calculation Of Observables In The Nuclear $0s_{1d}$ Shell Using New Model -Independent Two-Body Interactions” University of the Western Cape 2007.

- 83- Arne Alex “ Non-Abelian Symmetries in the Numerical Renormalization Group” Diploma Thesis, Ludwig-Maximilians-Universität at München, 2009.
- 84- Sakurai J. J., “ Modern quantum mechanics”. Reading, MA: Addison-Wesley, revised ed, 1994.8, p.208.
- 85- Lawson R.D. “Theory of the nuclear shell model ” Book , Glendon press Ltd., Oxford, 1980.
- 86- Bohr A., and Mottelson B.R. “Nuclear structure” Vol.1 Benjamin New York, PP210, 1969.
- 87- Rose M. E., Elementary Theory of Angular Momentum, John Wiley & Sons, Inc, 1995.
- 88- Otsuka T., Fujimoto R., Utsuno Y., Brown A., Honma M., and Mizusaki T. “Shell model calculation of the Level Mixing and Nuclear Magnetic Resonance techniques” Phys. Rev. Lett. Vol. 87, 2001, PP82502.
- 89- G. Audi, A. H. Wapstra, C. Thibault, J. Blachot and O. Bersillon (2003). “The NUBASE evaluation of nuclear and decay properties” Nuclear Physics A 729: 3–128.
- 90- Sharrad F. I. “Nuclear Structure of 18-30Ne Isotopes Using NuShell” Journal of Natural Sciences. JNS 1(2): 37-43 (2013) ISSN 2308-506 .
- 91- Jiang M F., Machleidt R. , Stout D B and Kue TT “Bonn potential and sd shell nuclei” Physic Rev. C Vo.46 No.3, 1992.
- 92- Akito Arima “ Nuclear Binding Energies and Low-Lying Energy Levels in the 2s_{1/2} and 1d_{3/2} Shells “ Progress of Theoretical Physics, Vol. 19, No.4, April 1958 .



جمهورية العراق
وزارة التعليم العالي والبحث العلمي

جامعة بغداد

كلية التربية للعلوم الصرفة- ابن الهيثم

دراسة نظرية لطيف مستويات الطاقة الواطنة
ولنوى خفيفة بأستعمال أنموذج القشرة النووي
 $^{30}_{16}\text{S}_{14}, ^{30}_{14}\text{Si}_{16}, ^{18}_8\text{Ne}_{10}$

رسالة قدمتها

هدى بطرس بهنام مقادسي

بكلوريوس-الجامعة المستنصرية - (1994)

إلى

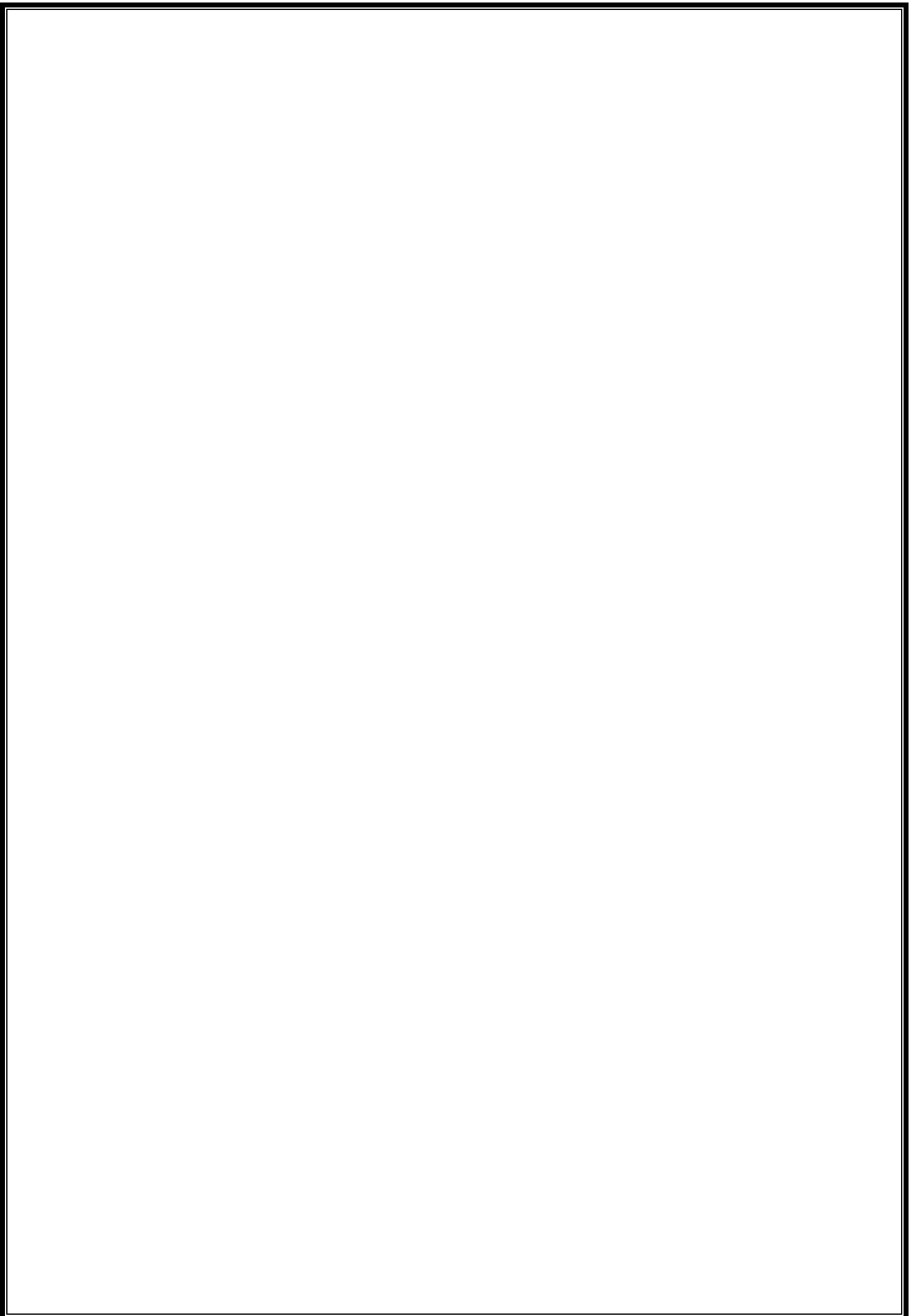
مجلس كلية التربية - للعلوم الصرفة ابن الهيثم - جامعة
بغداد كجزء من متطلبات نيل درجة الماجستير في الفيزياء

بأشراف

أ. م. د. هادي جبار مجبل العكيلي

2015م

1436هـ



الخلاصة

ان طاقات الربط والتهييج حسبت لنوى $^{30}_{14}\text{Si}_{16}$, $^{30}_{16}\text{S}_{14}$, $^{18}_8\text{Ne}_{10}$ وللمستويات الدنيا بأستعمال حسابات أنموذج القشرة النووي ولبروتونين في القشرة S,d لنوى $^{30}_{16}\text{S}_{14}$ بينما لنيوترونين لنواة $^{18}_8\text{Ne}_{10}$, $^{30}_{14}\text{Si}_{16}$ ولمدارات خارج القلب المغلق . عناصر مصفوفة التفاعل تم الحصول عليها من خلال أستخدام جهد تفاعل USD,USDA ,USDB نتائج الحسابات النظرية لطاقات الربط والتهييج والمحسوبة بأستعمال عناصر المصفوفة النظرية اظهرت تطابقاً مع النتائج العملية .

حسابات أنموذج القشرة استعملت لفهم ودراسة خصائص المستويات الدنيا ولعدد الكتلة لنوى $A=18,30$. استعمل القلب المغلق مع التفاعل المتبقي للجسمين ما بين النكليونات الخارجية $^{16}_8\text{O}_8$, $^{28}_{14}\text{Si}_{14}$.

لحالات التماثل الموجبة فأن جميع التشكيلات لقشرة S,d اخذت بالحساب بأعتبار ان هناك قشرة مغلقة مع جسيمين في مستويات القشرة S,d . تفاعل الجسمين الفعال للنوى أختير على أساس جهد USD,USDA,USDB .

اظهرت قيم طاقات الربط والتهييج تطابق جيد مع القيم العملية . واعتبرت الجهود USD,USDA,USDB هي المدخلات الاساسية لحساب الطاقات النووية والتي تتضمن تفاعل نكليون – نكليون .

الحسابات اظهرت لئلا امكانية اكبر لفضاء تفاعل النكليونات كون طاقات الحالات الأرضية متقاربة .